UNIVERSITY OF GENOA
POLYTECHNIC SCHOOL
Department of Civil, Chemical and Environmental Engineering

MASTER DEGREE IN CHEMICAL AND PROCESS ENGINEERING

Biodegradable engineered vascular prostheses: a validation comparative study in bioreactor

Supervisors:

Prof. Patrizia Perego

Prof. Jan Oscar Pralits,

Dr. Pier Francesco Ferrari,

Co-supervisor:

Dr. Maria Bolla

Candidates:

Agnese Gamberini

Chiara Repetto

Academic year 2021-2022

GENERAL INDEX

INDEX OF FIGURES

INDEX OF TABLES

ABSTRACT

Vascular tissue engineering aims to manufacture biodegradable and bioabsorbable small diameter vascular prostheses, trying to overcome the problems that common vascular scaffolds show *in vivo*. For these drawbacks, several studies have been made and before any *in vivo* experimentation a thorough study of the manufactured prostheses is essential. These studies are needed to provide information on the behaviour of vascular substitutes in dynamic conditions, such as predict many parameters (degradation, release of bioactive compounds, etc.) that the biodegradable vascular scaffolds will show *in vivo*. In this work, the scaffolds were made from a blend of poly (caprolactone) and poly(glycerol sebacate), both 20% (m/v), with a ratio of 1:1 (v/v) and in the presence of quercetin (0.05% m/v); this was made possible by using the electrospinning technique on a 2 and 5 mm diameter collector and subsequently coated with a layer of gelatin at 37 ° C for 1 hour, in order to reduce their permeability. Two different bioreactors were used for the simulation: an *ad hoc* home-made bioreactor and a high-performance bioreactor; as regards the first, it consists of a peristaltic pump, a pressure gauge, a chamber containing the scaffold and a tank, used to test the scaffolds in dynamic conditions. The high-performance bioreactor instead, basically consisted of some components like the previous one, but a more complex and sophisticated piping system was present. Three different vessels were installed: a compliance chamber, a pulse dampener, and a room with the possibility of accommodating 3 scaffolds at the same time. A buffered saline solution (PBS) was flowed into the chamber at three different pressures 80, 80-120,120 mmHg. Each day, a portion of the PBS was collected to be analysed in terms of the amount of gelatin and quercetin released. The chemical-physical and mechanical properties of the vascular graft were studied at the end of the experiment. The residence time in the bioreactor, as evidenced by scanning electron microscopy, influenced the random fibrous structure of the scaffold. The release of gelatin and quercetin was significantly different than in studies previously performed under static conditions. The shear stresses to which the walls of the scaffold undergo, as a function of the operating pressures, have been evaluated analytically thanks to the equations that describe the incompressible and time-independent flow. These allow for an in-depth understanding of the relationship between mechanical forces and the release of gelatin and quercetin under dynamic conditions. The mechanical properties were studied in terms of Young's modulus, tensile strength, and percentage of elongation, highlighting that the proposed engineered prostheses could represent a valid tool to

support tissue regeneration. The results obtained demonstrated the importance of studying these electrospun grafts under dynamic conditions, using a bioreactor, with the aim of simulating an *in vivo* implant.

1. INTRODUCTION

1.1 Vascular pathologies

Through blood circulation, the cardiovascular system has the main task of supplying the body's cells with oxygen, nutrients, and, more generally, all the elements necessary for their sustenance.

Given its serious impact on the worldwide population, mainly in western countries, cardiovascular diseases are the leading cause of death for both sexes.

An estimated 17.9 million people died from CVDs in 2019, representing 32% of all global deaths. Of these deaths, 85% were due to heart attack and stroke (https://www.who.int/).

Vascular surgery finds its field of application in the diagnosis and therapy of diseases affecting blood vessels (arteries and veins) and lymphatics. Some diseases belonging to this group are aneurysms of the arteries, peripheral arterial disease, peripheral chronic obstructive arterial disease (AOCP), peripheral arterial embolism, venous insufficiency, lymphomas, and thrombosis (Menzyanova et. al.,2019)

The most common pathology affecting the *arterial system* is atherosclerosis. This disease is not present at birth, but it is revealed with increasing age and it consists in the deposition of plaques inside the arteries, causing a loss of elasticity of the arteries themselves, their progressive closure or, sometimes, their exhaustion (aneurysm).Regarding the *venous system, it* includes the upper caval district, responsible for the outflow of blood from the arms and head, and the lower caval district, responsible for draining the blood from the remaining areas. The superior caval system is mainly affected by compressive pathologies at the subclavian vein level, while the inferior caval system is mainly affected by thrombotic pathologies.

Finally, the *lymphatic system* is made up of very thin vessels, which contain lymph glands. They contain a clear liquid (lymph) which is rich in protein. The most frequent pathology of this system is lymphedema or swelling, that can even reach considerable dimensions (elephantiasis) and can depend on both congenital and acquired causes (Libby, 2021).

1.2 Blood vessels

The cardiovascular system is a closed system that includes the heart and blood vessels. The heart acts as a pump: it distributes the blood flow through an extensive network which acts as a connection with peripheral tissues and organs.

Blood is a liquid connective tissue flowing within the circulatory system. It is essentially made up of two components:

- plasma: it represents about the 55% of the blood volume. It is a liquid matrix with a density slightly greater than water and it is composed of electrolytes, nutrients, organic waste, proteins, and water.
- other suspended elements: erythrocytes, leukocytes, and platelets. These compounds are present in high quantities, and they are highly specialized. Erythrocytes carry around oxygen and carbon dioxide, leukocytes have the task of defending against pathogens, and platelets are important for coagulation.

Blood performs many essential functions: it carries dissolved gases and waste substances, it stabilizes the pH, it regulates the body temperature, and it distributes nutrients, enzymes, and hormones.

The dense network of vessels crossed by blood can be divided into two circles: the pulmonary circulation, which carries blood rich in carbon dioxide from the heart to the lungs, and the systemic circulation, in which the oxygenated flow circulates to the peripheral organs of the body.

The heart is a muscle with four chambers, two atria and two ventricles. The pulmonary circulation begins at the level of the pulmonary semilunar valve, and it ends with the entry of the pulmonary veins into the left atrium. The systemic circulation, instead, begins at the level of the aortic semilunar valve and it ends with the hollow veins in the right atrium.

The cardiac cycle consists of two distinct periods, during which there is a change in the aortic pressure. This appears to be minimal during the diastole (ventricular relaxation), while it reaches the maximum value in correspondence of the systole (ventricular contraction). The mean arterial pressure during the cycle represents the pushing force exerted on blood to go through the systemic cycle.

1.2.1 Types of blood vessels

Native blood vessels in the human body have complex structures with distinct characteristics. Their classification is based on their ability to conduct blood from the heart to the tissues or vice versa, as well as based on their dimension.

In general, they can be gathered into three groups: arteries, veins, and capillaries (Figure 1).

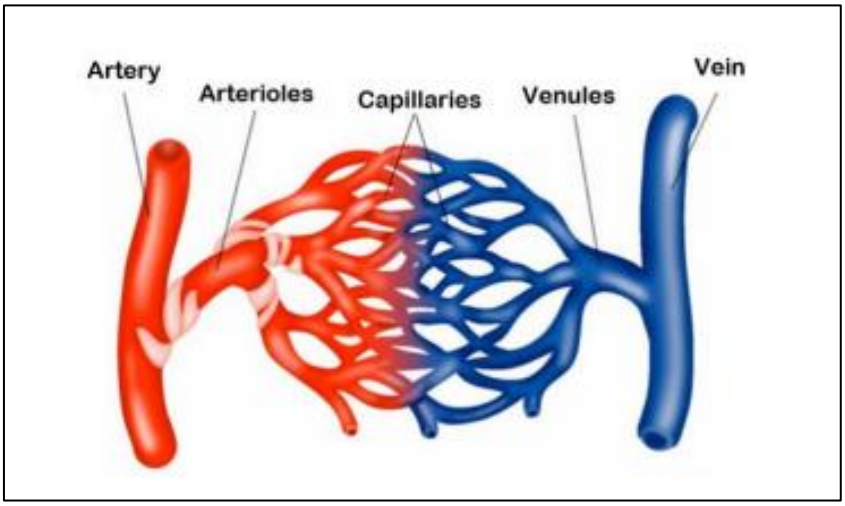

***Figure 1**: Classification of blood vessels*
(https://www.diabete.com/il-danno-dei-piccoli-vasi-periferici/)

Arteries and arterioles transfer blood from the heart to the capillaries, which are drained by venules and veins, capable of returning blood to the heart.

All the vessels have a cavity called "lumen", through which blood flows. Arterioles, venules, and capillaries are small caliber blood vessels and, therefore, they constitute the so-called "microcirculation".

The arterial wall has a unique composition, consisting of three different concentric layers: intima, media, and adventitia.

- *intima* is the innermost layer of a blood vessel. It consists of a continuous monolayer of endothelial cells, adjacent to an underlying connective tissue, which constitutes the basement membrane. This membrane contains a variable number of elastic fibers. In larger arteries, the connective tissue is more extensive, and the inner tunic is thicker than in the smaller ones.
- *media* represents the middle layer, and it contains concentric bundles of smooth muscle tissue immersed in a network of connective tissue. Following the stimulus

from the sympathetic system, the presence of the muscle allows the contraction or relaxation of the fibro-cells, with consequent vasoconstriction or vasodilation (Hasan et. al., 2014).

- *adventitia* is the outermost connective layer of the vessel. It is quite thick, and it is essentially made up of collagen fibers dispersed in elastic fibers.

Collagen fibers are made up of proteins, which connect each layer to the others and confer elastic resistance to the vessel walls. Furthermore, the elastic connective tissue contains fibers formed by elastin, a protein that allows the vessels to expand and contract, following a variation in the pressure inside themselves (Awad et. al.,2018).

Each layer performs a specific function: the endothelial monolayer is essential to prevent blood coagulation, inflammation, and infection of adjacent tissues and it allows the exchange of gases, molecules, and cellular signals. (Hasan et al., 2014). The muscle layer is essential to ensure contractile function, while the outermost layer confers high elasticity.

Arteries and veins are characterized by a particular concentric layered arrangement, which gives them - a considerable resistance. Some of these layers may be less evident or absent in the smaller arterioles and capillaries (Figure 2).

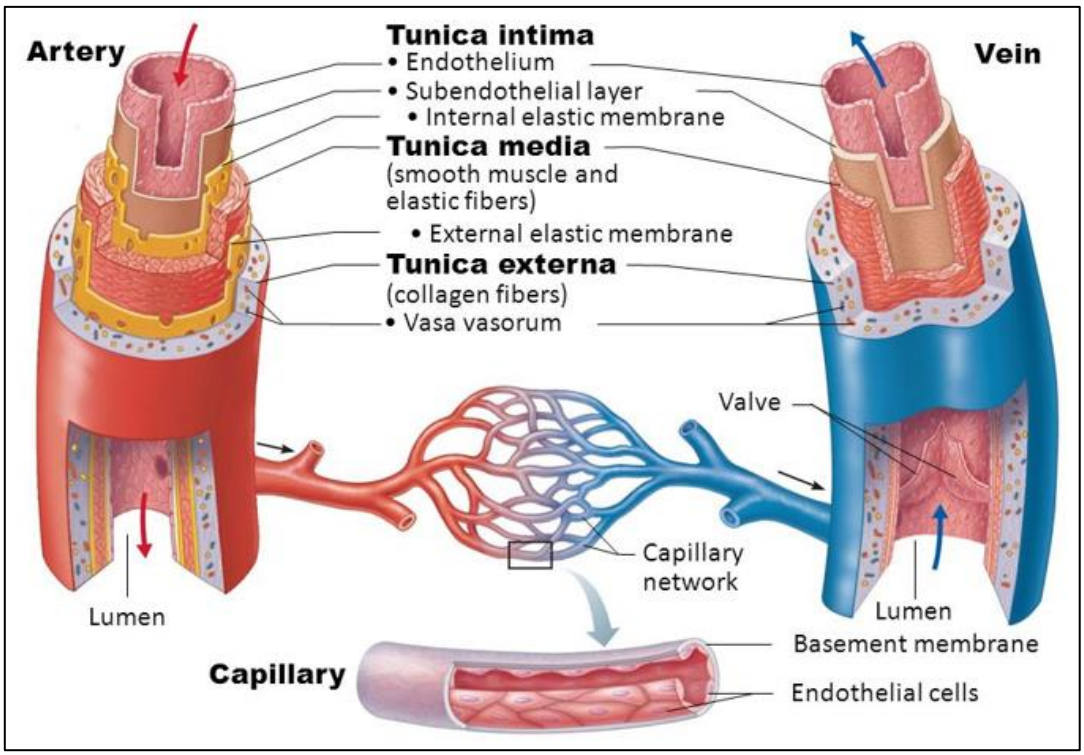

***Figure 2**: Concentric layered arrangement between arteries, veins, and capillaries (http://superagatoide.altervista.org/vasi-sanguigni.html)*

Veins are the blood vessels that collect blood from tissues and organs, and they make it flow towards the heart. They roughly have the same diameter as the arteries, but their wall is about one half in thickness, and they present a lower elasticity. In fact, the pressure of the venous flow is - lower than the arterial pressure. Except for the smaller sized venules, all veins are made up of the same three layers that constitute the arteries. The peculiarity of these vessels lies in the presence of one-way valves, called "swallow's nest", which allow blood rich in carbon dioxide to flow in one direction only. These valves are present in the peripheral veins, but not in the central ones. According to their internal diameter, veins are divided into small, medium, or large caliber venules and veins.

Capillaries, on the other hand, are smaller and more delicate blood vessels: functionally they are particularly important, since they are the only ones, whose wall allows metabolic and respiratory exchanges between blood and the surrounding interstitial fluids.
Thanks to their extensive ramifications, the total cross section of capillaries has a much larger surface area than other's blood vessels. Therefore, blood flows inside them rather slowly, ensuring the necessary time for the diffusion of substances through the thin capillary wall. At this level, the supply of oxygen and nutrients occurs, as well as the removal of waste substances. Three types of capillaries are: continuous, fenestrated and sinusoid capillaries. In the first, the endothelial cells have very closed each other, while the latter present pores in their wall and they are, therefore, highly permeable even to larger molecules. Sinusoids look like fenestrated capillaries, but they have larger pores and a thinner basal lamina.

1.2.2 Vascular tissues

In multicellular organisms, most of the cells belong to organized cooperating cell groups, called tissues. Tissues are composite materials made up of specialized cells and cellular products, suitably organized to carry out specific activities. Tissues found in the vascular system include the endothelial, muscular, and connective tissues (Figure 3). Each layer that makes up the walls of the blood vessels performs a specific function.

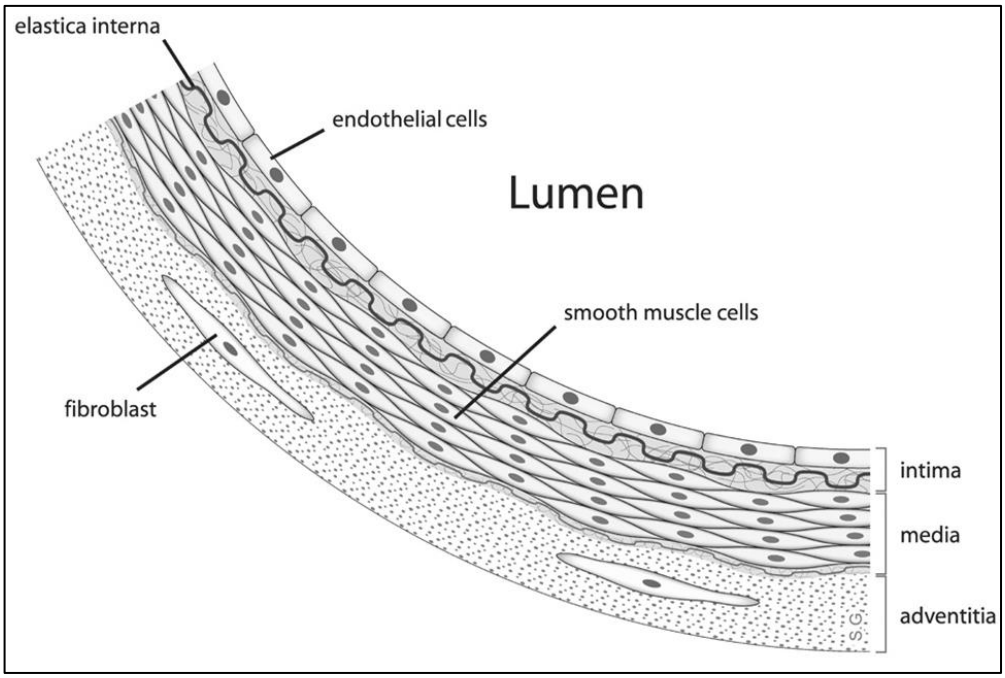

***Figure 3**: Stratification of arteries and veins (https://facellitate.com/it/the-endothelium-an-interface-between-blood-tissue-and-lymph/)*

1.2.2.1 Endothelial tissue

Endothelial tissue is a particular type of not stratified paving epithelial tissue, therefore characterized by a superficial layer of cells with a flattened and polygonal shape. This tissue is the most voluminous in the human body, and it has mesenchymal origin. It internally covers the wall of the heart, veins, arteries, and it forms the capillary wall. It is a single-layer tissue without vascularity, performing several essential functions: it offers physical protection by ensuring homeostasis, it controls permeability and secretion, and it's able to process active substances, if necessary. The epithelial cells come into direct contact with blood in their apical part, and they rest on a basal lamina, which allows the connection with the underlying tissues. These cells are closely linked and typically have

an elongated shape towards the direction of the blood flow. As already mentioned, the functions performed by the endothelium are multiple:

- it is a semipermeable barrier, which controls the passage of substances between blood and the extracellular fluid;
- it checks both coagulation and inflammation;
- it regulates the proliferation of the media smooth muscle cells, as well as the permeability and the structure of the vessels;
- it promotes angiogenesis.

The endothelium can produce active chemicals, distinguished between vasoconstrictor mediators and vasodilating agents. The latter allow the vessel lumen to increase, and they possess antithrombotic and anti-atherogenic action. The result is a modulation of vascular tone, and blood flow in response to nervous, humoral, and mechanical stimuli.

Since the epithelial tissue is a two-dimensional tissue, it is easier to reproduce in the laboratory than other tissues with a more complex structure.

1.2.2.2 Connective tissue

The endothelium of blood vessels is surrounded by a layer of connective tissue. This is one of the four basic types of tissues that make up the human body. The connective is not exclusively constituted of cells; a substantial part of the volume of this tissue consists of the extra-cellular space, largely filled with a variety of macromolecules, making up the extracellular matrix. The connective tissues present multiple functions, including guaranteeing strength and structural support, chemical and physical connection, reserving and exchanging nutrients, immune defense, and transport of fluids and dissolved materials. All the connective tissues own specialized cells, extracellular protein fibers, and essential substances. Depending on their morphological and functional characteristics it is possible to make a distinction into different subgroups. In each of them, a wide variety of cells are identified. They are appointed to carry out different activities (Figure 4):

- Cells for the formation and maintenance of the matrix, such as fibroblasts;
- Cells responsible for the body's defense, such as macrophages and leukocytes;
- Cells that perform special functions, which vary according to the nature of the tissue to which they belong and its position in the body.

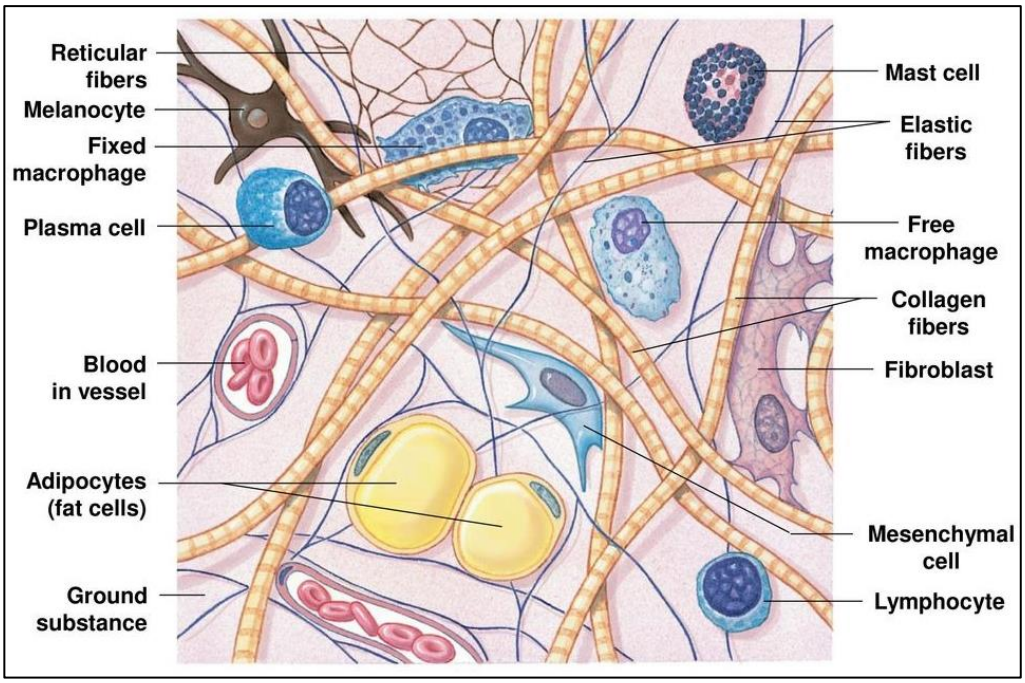

***Figure 4**: Connective tissue*
(https://connective-tissue-proper-cells-diagram/)

1.2.2.3 Muscular tissue

In the blood vessel's structure, around the sub-endothelial connective tissue, there is a circular layer of smooth vascular muscle, particularly developed in the arterial walls (Figure 5). This muscle layer is made up of small, thinned, and mononuclear cells. Smooth muscle has no visible branches or striations, it contains actin and myosin filaments, essential for contraction, while it lacks the troponin protein complex. It therefore appears to be an involuntary type of muscle, whose contraction is triggered by the autonomic nervous system. In fact, the contractile filaments of the smooth fiber cells are arranged in a poorly organized manner and the classic sarcomeres characteristic of the striated muscles are not recognizable.

The cells of smooth muscle tissue can divide themselves and lead to tissue regeneration following damage They act in an essential way for the control of homeostasis and, therefore, for the maintenance of the internal chemical-physical conditions. The regulation of the smooth muscle contractility is modulated by various mechanisms, both electrical and chemical. The main involved neurotransmitters are acetylcholine and norepinephrine.

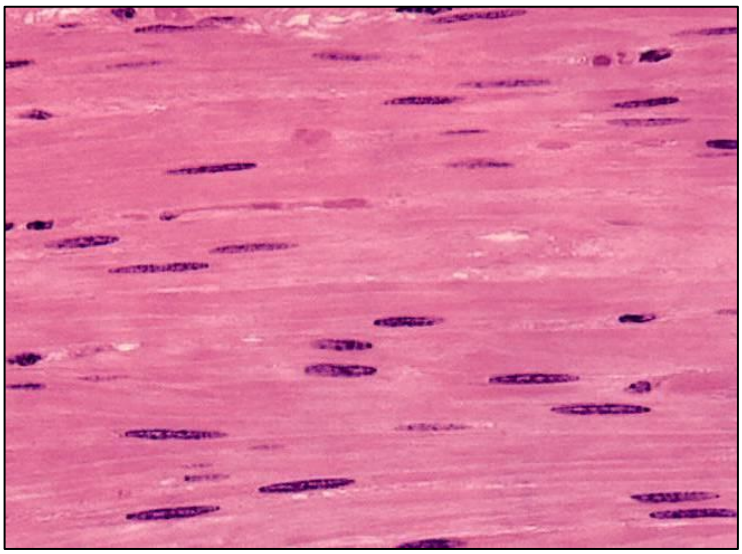

***Figure 5**: Smooth muscle tissue*
(https://www.riccardoquasidoc.it/il-tessuto-muscolare/)

1.3 Atherosclerosis

Atherosclerosis is a pathological condition characterized by an alteration of the arteries, subjected to a thickening, and hardening of their walls. Atherosclerosis is the most common disease, and it is associated with a damage into the endothelial lining of an artery due to the formation of deposits in the tunica media. Several factors can be involved in the development of this disease, and the main is the blood level of lipids. In fact, atherosclerosis tends to develop in people whose blood contains high levels of plasma lipids, especially LDL cholesterol. When blood contains an excess of this compound, foam cells can form. They adhere to the endothelial walls of the blood vessels, where they release growth factors, tending over time to thicken the wall and narrow the vessel lumen. The longer lipoproteins reside in the vessel, the more they tend to undergo chemical changes.

Following these changes, monocytes, muscle, and endothelial cells begin to start an inflammatory response that leads to lipid phagocytosis. The result is the formation of a plaque of fatty mass that cannot be metabolized, with a consequent reduction in the blood flow in the affected artery (Figure 6). Plaques are more likely to form in certain regions of the circulatory system, especially at the bifurcations and at the shrinkage of the vessels (Figure 7).

The behavior of atherosclerotic lesions is not static, but dynamic. Plaques growth can be arrested, but this may lead to permanent structural changes. In their more advanced stages, they can ulcerate, leading to thrombosis.

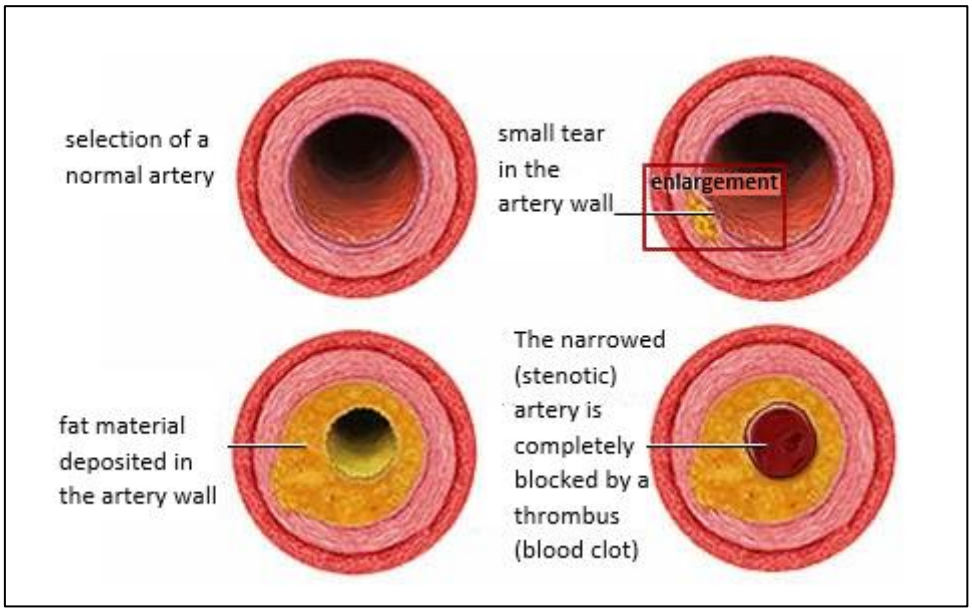

***Figure 6**: Transition from a healthy artery to another one with atherosclerosis plaque (http://www.panvascular.com/pagine/info/pazienti/Varie/aterosclerosi.html)*

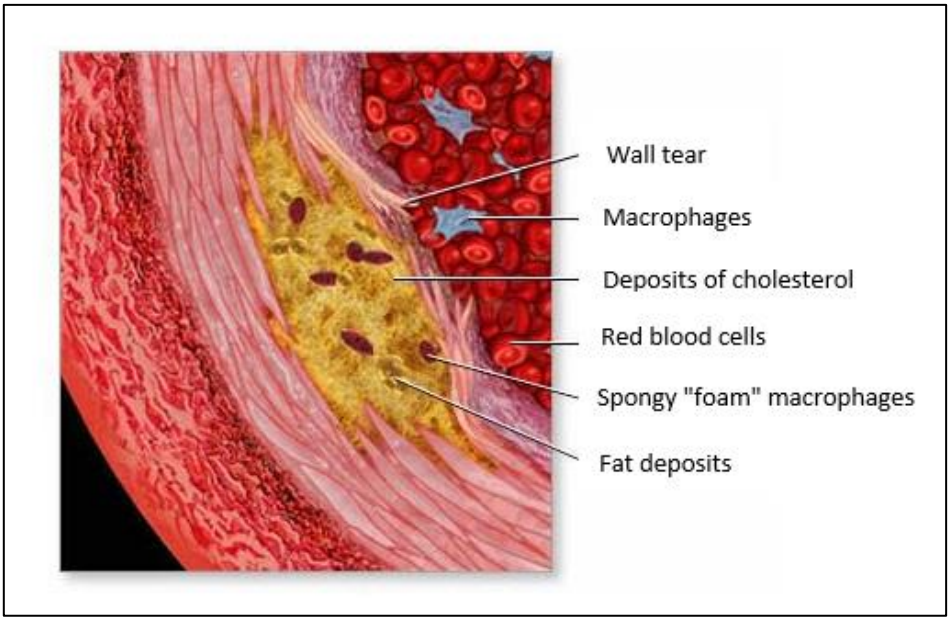

***Figure 7**: Section of a coronary artery with plaque formation. (http://www.panvascular.com/pagine/info/pazienti/Varie/aterosclerosi.html)*

The loss of elasticity of an artery can also be caused by other types of deposits, such as the accumulation of calcium salts, inflammatory cells, and fibrotic material.
Atherosclerosis is commonly associated with aging. However, many factors are involved in its development: hypertension, smoking, diabetes mellitus, and family history. A diet rich in fat, excessive alcohol consumption, insufficient physical activity, pollution, overweight, and stress can also contribute to this.
The atherosclerosis symptoms are different; the typical one is the onset of severe acute or chronic pain. An impaired arterial blood flow can then lead to more grave consequences, such as coronary heart disease, myocardial infarction, stroke, ischemic heart disease and peripheral arterial illness. (Falk, 2006)
The atherosclerotic cardiovascular disease is, therefore, a multifactorial disease that today represents one of the major causes of death in the world. Complications due to atherosclerosis are responsible for about half of deaths in the US, and the probability of recurring related vascular problems is now quite high even in the western countries (Libby, 2021).

In 2016, approximately 17.9 million people died because of cardiovascular diseases, representing the 31% of all deaths worldwide. Among them, the 85% are due to heart attack and stroke. (https://www.emd112.it/blog/news/morti-per-malattie-cardiovascolari-nel-mondo-ed-incidenza-globale/)
Given the global spread of this disease, there is an urgent need to understand the genesis of atherosclerosis and to advance the knowledge necessary for its management. Many risk factors can be reduced or modified by first correcting people's lifestyle. In recent years, a combination of research and clinical investigations has significantly changed the traditional concepts of atherosclerosis, with an increasing inclination towards innovative therapeutic approaches.

1.3.1 Treatment of vascular diseases related to vessel obstruction

In general, atherosclerosis does not cause symptoms itself, until it compromises the flow of blood within the arteries. This occlusion, caused by the presence of plaques, can then generate ischemia and heart attack in the downstream area.
If an artery is blocked by a blood clot, and it is not possible to act through mechanical unblocking, it is possible to use drugs that are administered intravenously to dissolve the thrombus.

Some potential surgical treatments for atherosclerotic plaques include catheterization, balloon angioplasty, and the use of bypass. However, the best approach remains to reduce or eliminate the risk factors.

1) *Catheterization*

This rather simple and widely used procedure allows to remove a single plaque with the aid of a thin catheter. It consists of a long tube of very small diameter, which is inserted into a large artery. Usually, an incision is made in the upper part of the femoral artery and then the metal wire is led to the point where the obstruction occurred, by tracing through imaging. Various tools can be inserted into the catheter to remove the plaque: a laser beam, a pointed blade, or a suitable shredder. The debris obtained is then collected and sucked into the same catheter.

2) Balloon angioplasty

Angioplasty is an endovascular procedure, used in medicine to expand a narrowing of a blood vessel due to small plaques. Being a minimally invasive surgery, it is advantageous compared to traditional surgery due to the lower risk of infections. In fact, it is carried out through smaller incisions, and it allows to achieve a significantly faster healing. In this case, catheter, which has an inflatable balloon at the end, is used. Once the affected artery is reached, the balloon is inflated. The plaque then crushes against the vessel wall, and the internal lumen is restored, with a consequent increase in blood flow. After angioplasty, a stent is often inserted to prevent the plaques from reforming and thus avoid restenosis. This device consists of a network which has the purpose of maintaining the restored diameter over time. The most common stents are metal-based, but continuous research is being carried out to create polymer-based devices that can be reabsorbed over time. In some cases, it is then possible to cover the surface of the mesh with drugs or bioactive materials.

3) Use of bypass

Bypass surgery allows to overcome a partially or totally blocked vessel. The methodology consists in taking a small section from a healthy artery and using it to create a bridge around the area affected by the occlusion, restoring blood flow.

Usually, the fragments are obtained from minor arteries rather than peripheral veins; in recent years, synthetic channels have also been developed.

Compared to the other operations described above, the use of bypass allows to vascularize multiple arteries at the same time. However, it remains reserved for particularly critical cases, in which it would not be possible to carry out less invasive procedures.

1.4 Small caliber vascular substitutes

1.4.1 History of small vessel surgery

Vascular surgery is the branch of surgery that deals with surgical intervention for the resolution of pathologies affecting the blood vessels. Repairing or removing and replacing are two possible intervention types, carried out with open surgeries, minimally invasive surgeries, or endovascular methodologies (Friedman, 2005).

The history of vascular surgery has always gone in parallel with the human history. The first hints regarding the pathologies of this medical branch date back to very ancient times; the first interests in this area can be traced back even in the period B.C., with historical figures such as Sushruta and Hippocrates. However, the first practical treatment was developed in the 16th century A.D. by Ambroise Paré, who used a compressor to repair the damaged arteries of soldiers wounded in battle.

Regarding the twentieth century, it presented countless advances. Among the big names in the vascular surgery, Michael Debakey, Mathieu Jaboulay, and Alexix Carrel should be mentioned.

Michael Debakey is one of the first surgeons to take an in-depth interest in aneurysms and, in 1950, he performed the first removal of a coronary artery block, removing the damaged tract, and replacing it with a healthy one. Debakey was also deeply involved in the problem of rejection. His studies in this area led him to be one of the pioneers of the use of grafts in Dacron for the repairing or replacing of blood vessels. In 1958, he performed the first effective angioplasty using this material, and he carried out the first coronary artery bypass surgery in 1964.

Mathieu Jaboulay was a French surgeon, and it is remembered for having introduced the innovative surgical procedures of arterial anastomosis, a technique that did not involve the use of sutures and took his name.

Another name that emerges is Alexix Carrel, still considered the "father of vascular surgery": he conceived the so-called "triangle suture" of small arteries and anastomoses between vessels of different gauges, also performing bypass operations with autologous veins (Belcaro et. al., 2000).

His career was crowned by the Nobel Prize for medicine in 1912.
The use of vascular prostheses in the joining or replacement of injured blood vessels is the result of a gradual development process that involves many techniques, both surgical and biotechnical. In the first half of the twentieth century, vascular substitutes made with materials tolerable to the blood exposure were proved to be promising alternatives, without, therefore, creating complications such as thrombosis and rejection.
Wars played a significant role in the evolution of vascular surgery. The first non-endogenous materials, such as tubes of glass, ivory, or magnesium, were used by the Germans during the First World War to replace the blood vessels of dying soldiers. The substances used, however, seemed to be poorly tolerated by the body. In fact, several cases of thrombosis and intense scarring reactions emerged. Despite the numerous studies of this period, until the Second World War, the standard treating method of arterial injuries remained the ligation of the artery and the amputation of the limb, During the Korean War a significant progress was achieved in surgery, due to the very high number of victims and injured. The limb amputation rate during this fight was reduced to 19%, from 47% in World War II (Hess, 1985).

In the early 1950s, modern types of plastics and polymeric substances were made available for the creation of prostheses. The use of silk as a suture material, much thinner than the traditional ones, was a fundamental step in the development of microvascular surgery, which deals with the anastomosis of vessels with a diameter of about 1.5 mm. In 1952 A. Voorhees introduced a prosthetic substitute in Vinyon-N tissue, for the experimental replacement of the aorta. During the Vietnam War the treatment with vascular lacerations by synthetic prostheses made of methyl acrylate and polyethylene became a common practice. With the introduction of non-solid, porous, woven, or knitted materials, a new era in the prosthetics has begun.
Continuous research for substances more compatible with blood and optimal production processes led to the creation of constructs of Nylon, Teflon, Orlon, Dacron, and polyurethane. Braided nylon aortic implants started to be used clinically. However,

nylon usually rapidly degenerated after implantation, resulting in the formation of aneurysms. Instead, the grafts of Orlon, Dacron, and Teflon appeared to have more promising properties. Subsequently, expanded polytetrafluorethylene (PTFE) was tested, but it had different application limits, being not flexible, and, therefore, it was considered not suitable for installations in curvilinear areas. (Hess, 1985)
In 1964, Charles Dotter had the idea of treating the damaged arteries from the inside and underwent the first angioplasty of the lower limbs. In the 1970s, Andreas Roland Gruntzig used a prototype of a flexible catheter with satisfactory results in the dilation of the iliac, femoral, renal, and coronary arteries. In 1985, Julio Palmaz realized the balloon expandable stent. In 1992, Juan Carlos Parodi was the first surgeon in the United States to perform minimally invasive aortic aneurysm surgery. Three years later, the first aorto-bifemoral bypass was performed (Belcaro,2000).

1.5 Vascular tissue engineering

1.5.1 Bases and principles

Tissue engineering (TE) is an emerging means of solving the problems of tissue repair and organ replacement in regenerative medicine (MRI) (Wang et. al.,2021).
Tissue engineering and regenerative medicine are terms that refer to multidisciplinary fields, which combine knowledge and technologies from the areas of biology, chemistry, engineering, pharmaceutical medicine, and materials science (Figure 8).

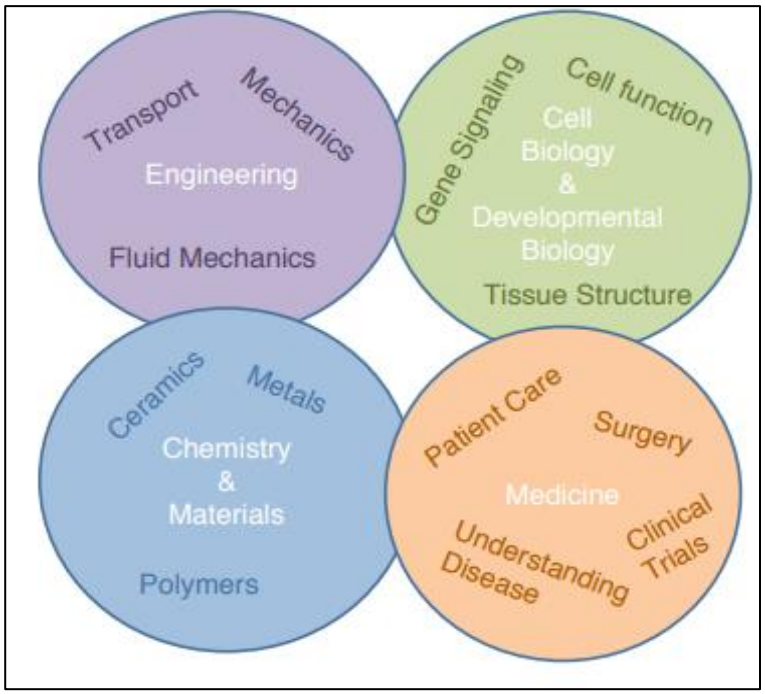

***Figure 8**:Interdisciplinarity needed in the field of tissue engineering and regenerative medicine*

The purpose of TE is to develop products and therapies for the repair or replacement of damaged tissues and organs (Baguneid et al., 2006).

The TE and MRIconcepts are often associated, although they can't be considered equivalent:

- *regenerative medicine* makes an extensive use of stem cells, which are a type of non-specialized cells capable of differentiating themselves into the many different cell types present in the human body;
- *tissue engineering*, on the other hand, is a science that focuses on the research and use of engineering supports, composed by innovative materials.

Some human tissues are unable to self-regenerate, as in the case of the onset of cardiovascular diseases. In this case, some permanent treatment strategies include the use of autologous grafts, allografts, or the application of ducts from other species. The use of materials taken from the patient himself certainly allows to avoid complications related to rejection.

However, the use of autos and allografts is limited due to the reduced availability and the functional and structural inadequacy of the tissue, the previously taken samples or the excessive anatomical variability. (Hasan et al., 2014). Furthermore, there are several concerns related to their long-term functionality. Regarding xenografts, they suffer from

an even shorter lifespan, the possibility of hyperacute rejection, and the possible transfer of pathogens to humans.

As a result, tissue engineering has emerged as a promising approach to address the shortcomings of current therapies. The goal is the development of new methods of intervention, which can be based on the use of synthetic prostheses, to reach, in the future, the transplantation of real artificial organs.

Concerning the cardiovascular surgery, many researchers have explored the use of arterial tissue cells or differentiated stem cells, combined with various types of natural and synthetic scaffolds. The main purpose is creating tubular structures and subjecting them to chemical and mechanical stimulation to develop a functional replacement arterial graft.

The secret of tissue engineering lies in the ability to imitate the functions of the original tissue, since the substitute must have identical structural and functional characteristics to the previous one. All this involves a thorough knowledge of the original biological tissue and its components.

Since tissue is generally a composite material, made up of cells, extracellular matrix, and signal systems, it will be essential to proceed in several stages, combining different elements that can best mimic the desired neo-tissue or organ. In fact, TE involves the use of a combination of biomaterials, cells, and bioactive molecules. The current tendency concerns the fabrication of constructs from biodegradable materials, so that the cells can produce extracellular matrix (ECM) while the polymer is degraded, gradually creating the intended tissue (Hasan et al., 2014). The goal is, therefore, to support or trigger a regeneration reaction that cannot occur spontaneously.

Unfortunately, an approach of this type is complex due to various uncertainties. While numerous successful transplants have been made for grafts larger than 6 mm in diameter, small-gauge synthetic implants are rejected by the body's immune system within a few months. This rejection derives from the associated obstruction problem that recurs subsequently to phenomena of thrombosis, aneurysm, and intimal hyperplasia, usually caused by the mismatch in compliance of the artificial vessel (Isenberg et al., 2014). A further obstacle to TE is represented, for example, by the scepticism developed in the paediatric setting, in which patients are still growing. This leads to an additional requirement for the growth and adaptation of the engineered tissue to the surrounding environment (Keane et.al., 2014).

1.5.2 Scaffold for blood vessel regeneration

The target of tissue engineering is the regeneration of tissues that have been damaged, using special structures called "scaffolds", constructs capable of summarizing biochemical and mechanical signals typical of natural tissues. They consist of well-defined three-dimensional polymeric structures capable of supporting cell growth. The prostheses used in tissue engineering are designed and manufactured to have some specific functions: they can accommodate cells in an optimal manner, and they are able to promote their growth, while maintaining the same mechanical properties of the tissue that has been replaced. Two characteristics that make scaffolds an important engineering and medical innovation are biocompatibility and biodegradability. These types of implants represent a temporary structure, which would be replaced by the newly formed tissue. A well-designed synthetic scaffold should therefore mimic the natural living environment as much as possible. To achieve this goal is necessary to face multiple challenges; among the most important we can list:

- the study of the degradation kinetics, which must be directly proportional to the healing process.
- the guarantee of a good vascularization, so that the inside of the polymeric scaffold receives sufficient nutrients for the cell survival and the chemical signals suitable for their specialization.
- the assurance of a total integration of the scaffold within the implantation site, by evaluating both its physical and chemical properties, to guarantee its best interaction with the surrounding natural tissues.

The techniques and materials usually used to produce these engineered constructs are multiple. Standard preparation processes, such as solvent casting, electrospinning, and self-assembly are now being matched with three-dimensional moulding technologies.
Regarding the substances used, they can be divided into synthetic, natural, composite, and biomimetic matrices.

1.5.2.1 Requirements of a vascular substitute

The cardiovascular disease affects over 71 million people only in the United States and the clinical treatments cost more than 500 billion dollars per year (Kumar et al., 2011).

Vascular substitutes are medical devices that are permanently implanted to restore the effectiveness of a vascular tract that is no longer able to perform its blood transport function.

Transplants are done in most cases to replace arterial vessels. This depends on the fact that pathologies affecting the veins are much less serious as the venous pressure is lower, an aspect that considerably limits vascular damage. Generally, the life expectancy of the implanted prosthetic replacement must be greater than the patient's life expectancy.

One thing to take into consideration is that the size of the blood vessels in the human body varies greatly. The replacement of the large diameter vessels (> 6 mm), such as the aorta, has now been successfully performed using synthetic polymers. However, most of the peripheral veins and arteries, with a diameter of less than 6 mm, have multiple problems related to the vascularity. Several studies have shown that grafts of small-gauge synthetic polymers lead to a rapid thrombus formation and a neo-intimal hyperplasia. A further complication is linked to the fact that synthetic vascular grafts present a continuous risk of bacterial colonization.

Motivated by these limitations, the development of tissue engineered blood vessels (TEBV) has progressed significantly over the past two decades. Ongoing evolutions require combined approaches between biomaterial science, cell biology, and medical translation to develop viable solutions.

The requirements for the design of TEBV can be conceptually divided into two areas: one related to mechanical performance and one that concerns the biological sphere. Biological failure can occur due to several modalities. The adverse response by the body is usually due to interactions between blood and the used synthetic materials. It could lead to the absorption of non-specific proteins and the subsequent blood clotting. This problem caused much debate between the researchers, who have tried to experiment as much as possible hydrophobic synthetic materials. However, to bypass the potential thrombus formation, the new biomaterials aim to combine hydrophilicity and resistance to protein absorption through surface modifications or by using a luminal layer of endothelial cells.

In order successfully implant a synthetic vascular prosthesis, the manufacturer should consider some prerequisites that the construct must necessarily possess. The mechanical properties of the scaffold should be adequate, as well as the chemical characteristics of the materials used. The manufacturing process is another aspect to keep in mind since the structural properties of the inner and outer walls will be closely linked to the weaving of the prosthesis.

An "ideal" prosthesis should meet different types of specifications (Hess, 1985).
Firstly, the material used for their manufacturing should be biocompatible, biodegradable, inert, non-toxic, and non-carcinogenic. This can prevent tissue reactions and avoid rejection situations. Several scientific groups made some functional tissue replacements to prevent acute and chronic rejection. The incorporation of bioactive materials could represent a solution: for example, quercetin is a possible candidate, since it is able to avoid immune responses.
Regarding the prosthesis manufacturing, it should carry out to obtain a final product with a high degree of flexibility, and optimal adaptability to the natural vessel. For this purpose, the constructs should also be feasible with a high range of internal diameters, so that they can be used for replacing different size vessels.
A further relevant requirement can be expressed by the concept of bioactivity, that is the ability of a material to form a direct bond with the surrounding tissue. The matrix making up the scaffold should allow proper anchoring of the cells to promote the tissue growth and the development of the neointima, without deformation and consequent loss of strength and properties. The neointima consists of the scar tissue that develops within tubular anatomical structures such as blood vessels, the intima being the tissue that covers them internally. The neointima that forms in vascular prostheses mainly consists of several layers of smooth muscle cells and fibroblasts, covered with a flat endothelium. The thickness of the walls should also be highly compatible with that of the damaged vessel, especially in terms of elasticity (compliance).
An additional key feature is the porosity, which must be sufficient to ensure the cell proliferation within the matrix.
About the surgical phase, the prosthesis must be easy to handle, and they must have good resistance to traction and suture. Finally, the material must be non-thrombophilic, to avoid vascular problems after the implantation. In fact, the total integration with the adjacent blood vessels is pursued, as well as the optimal support of blood pressure, and, consequently, a leak-free blood flow.
Finally, it is also necessary to obtain the approval of the Food and Drug Administration (FDA), needed to proceed with the placing on the market and the subsequent clinical use of the tissue engineering product.

Compliance must be included among the requirements; A blood vessel tends to expand as the pressure inside increases and to contract as the pressure decreases. This mechanism

is not determined by the internal pressure of the vessel, but by the difference in pressure established between the inside and the outside, called *distension pressure*.

The *compliance* is defined as the change in volume per unit of change in the release pressure, and it can be mathematically expressed by the following formula (Equation 1):

$$Compliance = \frac{\Delta V}{\Delta(P_{internal} - P_{external})} \quad (1)$$

where:

ΔV is the change in the blood volume (mL);

$P_{internal}$ is the pressure inside the vessel (mmHg);

$P_{aternal}$ is the pressure outside the vessel (mmHg).

The different between the pressure inside and outside the vessel (ΔP), represents the distension pressure. For positive values of ΔP a net force directed towards the outside acts on the vessel wall, favouring its distension. The opposite occurs for negative values of ΔP, with a consequent contraction.

Compliance therefore represents the ability of certain organs to tolerate a change in their volume. This property reflects the presence of elastic fibres and muscle cells.

From a physical point of view, vessels with greater compliance deform more easily. This is the case of the veins, which have a compliance of about 30 times greater than the arterial one.

1.5.2.2 Current prostheses in vascular surgery

Currently, the most used polymers for the construction of vascular prostheses are polyethylene terephthalate (PET), commonly known as Dacron, expanded polytetrafluoroethylene (ePTFE) or Teflon, polyurethanes, and a mixture of poly-ε-caprolactone (PCL) and polyglycerol sebacate (PGS) with a precise stoichiometric ratio.

The great availability and ease of use of these materials allowed them to be employed in a wide range of applications, including aneurysms of the large vessels and atherosclerosis of the peripheral districts.

Dacron refers to the trade name of PET, a thermoelastic polymer belonging to the family of polyesters (Figure 9). It consists of a synthetic textile material that has an accordion

structure due to the undulations, obtained by condensation of terephthalic acid and ethylene glycol.

Dacron is popular thanks to its higher biocompatibility and low rejection rate than other materials (Tremblay et al., 2009).

It is also strong, flexible, and durable. In fact, Dacron prostheses age very slowly: they are practically considered eternal. However, the synthetic tissue mechanical response can be different from that of the human aorta. This negative aspect can cause suboptimal conditions and affect cardiac functions (Nour et. al.,2020).

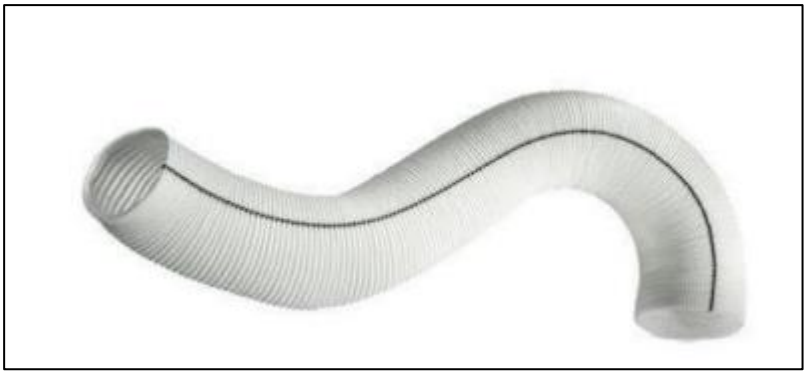

Figure 9*: Vascular prosthesis in Dacron*
(https://www.medicalexpo.it/fabbricante-medico/protesi-vascolare-13924.html)

The production of PET fibers takes place through several steps. First, individual grains of material are heated and melted, and they are pumped into a supply chain. This first step allows to obtain very thin single filaments. To improve the mechanical properties of these elements, the "striation" phase is carried out at this point, allowing to stretch and join more fibers using heat. At this point, the filaments can be joined to form a multiple one, with greater elasticity and adaptability (Figure 10). Starting from the multiple filaments obtained, it is then possible to start the weaving process of the prostheses themselves, which can be manufactured in the woven or knitted forms (Singh et. al., 2015).

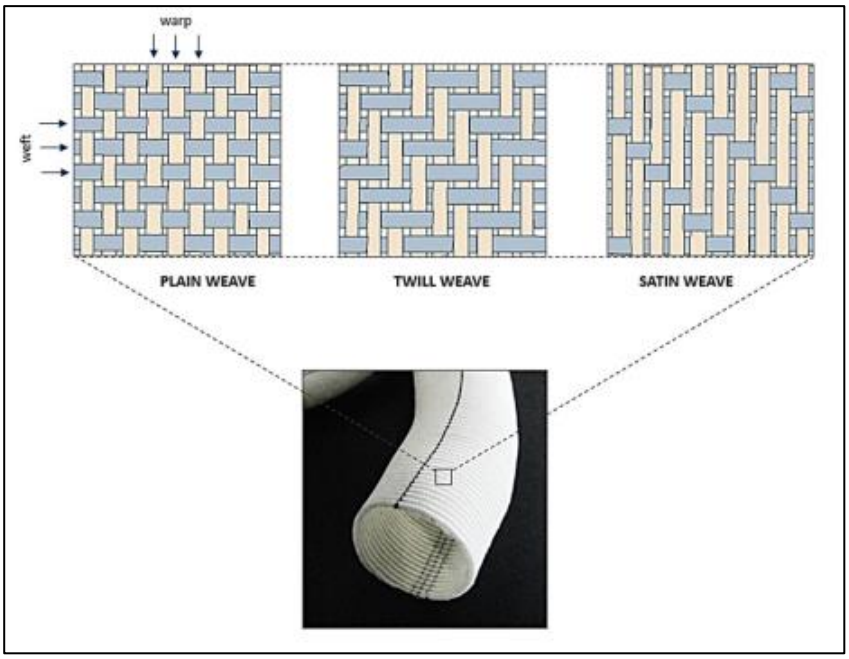

***Figure 11**: Structural patterns of a woven Dacron® graft (Singh et. al., 2015).*

Woven grafts are made by interlacing two sets of yarn (warp and weft) oriented at 90° to each other. These grafts are currently available in different types of weave designs, including plain, twill, and satin.

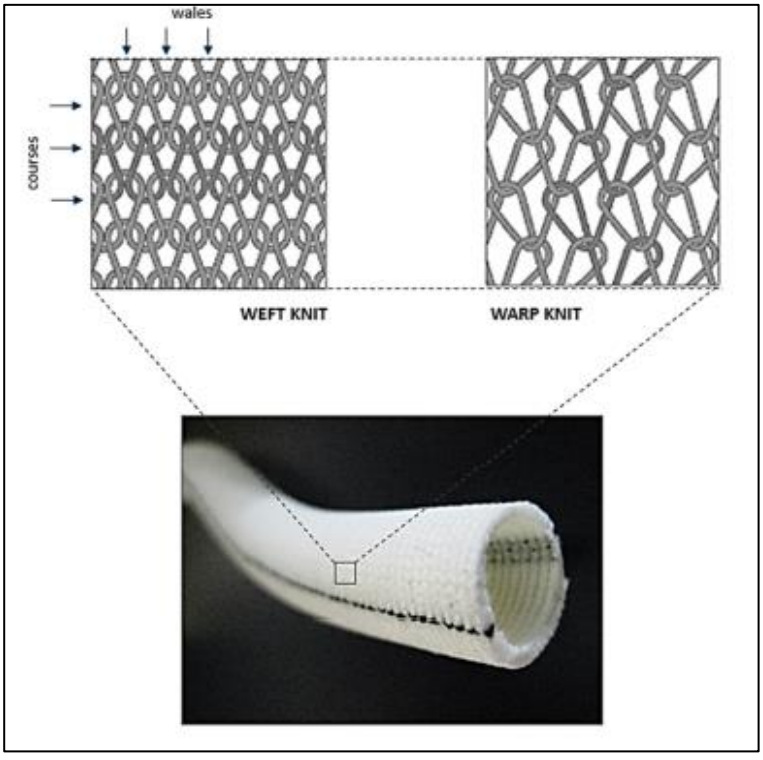

***Figure 10**: Structural design patterns of a knitted Dacron® graft (Singh et. al., 2015).*

Knitted grafts, instead, present a ring filament structure in which a continuous chain of threads is wound in a spiral around the circumference of the graft (Figure 11). Knitted structures are softer, more flexible, compliant, and they have better handling characteristics than the woven ones.

The behavior of a Dacron prosthesis is determined by the type of intertwining of the filaments, in relation to the mechanical stress to which it is subjected after the implantation. Despite the general good performance of PET prostheses, there is no lack of complications and problems. Aneurysms, vascular dilation, calcification, and mechanical failure are still considered daunting problems after years of implantations, sometimes leading to the need for additional surgery. Several studies have shown some discrepancies between the actual physical properties of the grafts and those of the native vascular tissue. This is not only at the basis of the prosthesis's mechanical failure, but also of the pathology's onset (Spadaccio et al., 2016).

Polytetrafluoroethylene (PTFE), commonly known as Teflon, is a polymer belonging to the class of perfluorocarbons (PFC), and it derives from the homopolymerization of tetrafluoroethene. It is certainly the most important and the most used material among the fluorine and carbon-based polymers (Figure 12). It is a plastic material smooth to the touch and capable of maintaining its properties unaltered up to temperatures of 250 °C.

The synthesis of Teflon consists in a chain polymerization, which is carried out by radical way in the presence of a suitable initiator (Puts et.al, 2019).

PTFE has a series of peculiar characteristics that led it to be considered a strategic material until the Seventies: it is chemically inert, completely insoluble in water and in any organic solvent, it has excellent dielectric and non-stick qualities, and it presents the lowest coefficient of friction among all the industrial materials.

PTFE prostheses were originally designed with a woven structure, which was, however, rejected because it was charged with hemorrhages and the formation of aneurysms.

The expanded form, on the other hand, is well known and widely used as a substitute for arteries. The ePTFE is made with a high temperature stretching process that generates PTFE nodules interconnected with highly oriented fibrils.

Despite the positive clinical applications, these latter prostheses also have numerous disadvantages:

- poor compliance, responsible for intimal hyperplasia and anastomosis;
- superficial bacterial colonization phenomena;
- possibility of thrombosis due to lack of flow inside the vessel.

Various attempts were employed to overcome these drawbacks, including the modification of the internal surface to make it more hydrophilic or the addition of rigid supports to increase the strength of the construct.

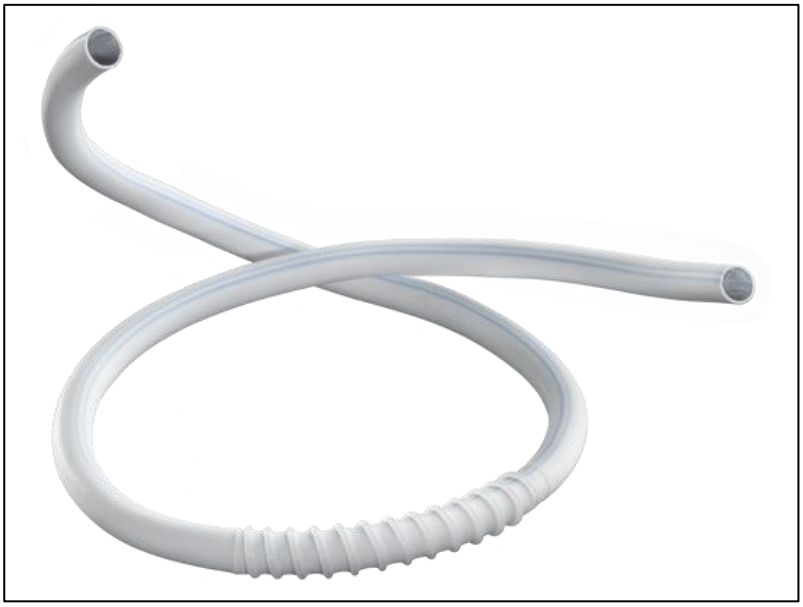

***Figure 12**: Vascular prosthesis in ePTFE*

Polyurethane (PU) include a large family of block copolymers obtained from diisocyanatos, macro glycols and chain extenders, held together by urethane bonds, whose chemical formula is NH-(CO)-O-.

Urethane polymers are widely used in the production of a great variety of materials, rigid, flexible, or semi-rigid.

In the biomedical field, linear polyurethanes are widely used in the production of implantable devices in contact with blood and soft tissues, such as cardiovascular prostheses. However, they have some limitations related to poor stability and susceptibility to calcification *in vivo*. In fact, the phenomena of hydrolysis and oxidation can compromise the success of the final plant. However, these limits can become advantages in the design of biodegradable materials that can be used in tissue engineering.

The main advantage of polyurethanes compared to other polymeric materials, for the realization of the scaffold, lies in the great versatility of this type of polymers: through an

appropriate selection of the basic reagents and their stoichiometric ratios, it is possible to obtain extremely different materials (Leoni, 2017). Polyurethanes have shown high blood compatibility, excellent abrasion resistance, exceptional mechanical properties, and very high flexural fatigue resistance. Currently, this category of polymeric materials is collecting more approvals and attentions, thanks to their great structural and processing versatility. Grafts can be built with various techniques, such as filament winding, solvent casting, spray depositions, etc.

Another feature of these materials lies in the excellent elastomeric properties that allow the construction of small-caliber tubular grafts with excellent chemical-physical properties, radial compliance, and hemocompatibility. Depending on the starting reagents, hydrophilic polyurethanes can be obtained, as well as polyurethanes grafted with specific active molecules.

A recent discovery showed that biomedical polyurethanes can undergo biological degradation according to a process known as “environmental stress cracking”, which leads to the superficial micro-cracking and consequent break of the prosthesis. Some attempts to make polyurethanes biostable include polyester reinforcement and gelatin coating.

Nowadays, the need for sustainable medical therapies is growing. The biomedical sector relies on continuous research of biomedical materials: biomaterials play a fundamental role in this field. In fact, the interaction between cells and biomaterials determines the success or failure of an implantation. Among a wide range of available biomaterials, polymers are the best choice for numerous biomedical applications.

Depending on their origin, polymeric biomaterials can be classified as natural or synthetic. Thanks to their origin, natural polymers can positively enhance material-cell interactions. However, this origin can potentially induce dangerous immune reactions. On the other hand, starting from synthetic polymers, it is possible to produce biomaterials with wide-ranging and reproducible properties through tailor-made variations of the components and synthetic processes (Rai et. al., 2012).

Synthetic polymers have long played an important role in the medical therapy, finding uses in areas regarding the wound healing modulation, implantable medical devices and artificial organs, prosthetics, ophthalmology, dentistry, bone repair, and drug delivery systems. Polymeric biomaterials are relatively easy to manufacture into products with various shapes, at reasonable cost, and with desirable mechanical and physical properties.

However, one of the main limiting factors in the use of these materials is their lack of biocompatibility.

The term "biocompatibility" encompasses many different material properties, including toxicity, tissue compatibility and compatibility with blood (hemocompatibility). Although a complete view of all the factor's influencing biocompatibility has not been formulated yet, some studies show determined physical and chemical aspects that can improve it.

Surface electrical charge can also have a significant effect on biocompatibility: neutral polymers and polyanions generally show less cytotoxicity than polycations. The molecular weight of the polymer is another parameter that can influence this characteristic: the low molecular weight polymer has a lower protein absorption and platelet adhesion than a higher one.

Conformational flexibility of the polymer, surface topography, and roughness are also important factors in determining the response of proteins and cells to a foreign material surface. Mathematical models can open new research opportunities, including the further study of cell-to-cell interactions, cellular material, and behaviour (Wang et. al.,2004)

Among the many synthetic polymers suitable for biomedical applications, poly(glycerol)sebacate (PGS) currently attracts attention. PGS is a transparent, almost colourless, biodegradable polymer increasingly used in a wide variety of biomedical applications. In 2002, it firstly appeared in the context of tissue engineering as a resistant biodegradable polyester synthesized., Applications of PGS were then expanded to include drug delivery, tissue adhesives, and rigid tissue (i.e., bone) regeneration materials.

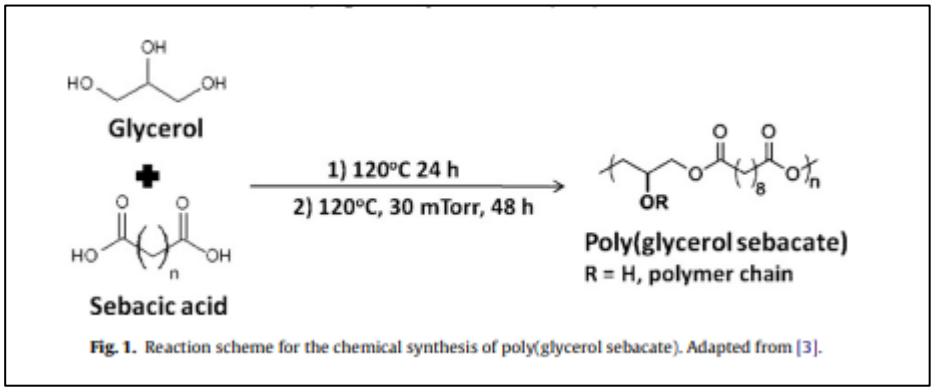

Fig. 1. Reaction scheme for the chemical synthesis of poly(glycerol sebacate). Adapted from [3].

***Figure 13**: Synthesis of PGS*
(Rai et. al., 2012).

The synthesis of PGS is based on a two-step polymerization of glycerol and sebacic acid, which can be performed under varying conditions of temperature and reaction time (Figure 13). Typically, a straight-chain PGS pre-polymer is firstly synthesised via pre-polycondensation. Crosslinking then takes place to form the PGS elastomer based on a covalently three-dimensional (3D) network. The resulting PGS is a strong and flexible elastomer with a non-linear stress-strain behaviour, for which the polymer can recover from large strains. Such mechanical properties can be attributed to the crosslinking interactions and the hydrogen bonding between the hydroxyl groups on the backbone, making PGS particularly attractive for soft tissue engineering (Sha et.al., 2021).

Unlike other polymeric elastomers, PGS is bioabsorbable in the human physiological environment, undergoing surface erosion during degradation. This indicates a slow loss of mechanical strength, thus making PGS stable after implantation. Furthermore, both precursors used in the synthesis of PGS can be directly found in the human metabolism process, and they were approved by the US Food and Drug Administration (FDA). Due to these positive attributes, PGS was explored for numerous biomedical applications, ranging from soft and hard tissue engineering to drug delivery and sensing devices.

Another polymer that has attracted a lot of interest is poly (ε-caprolactone) (PCL). It is a biodegradable aliphatic polyester, widely used as biomaterial. Its slow rate of degradation and its chemical structure make it suitable for various applications, including the biomedical field. Among its good properties, there are a low melting temperature, a variable viscosity, and an overall versatility. They make it particularly suitable for processing by injection moulding, melt extrusion, 3D printing, and electrospinning. PCL can be synthesised from the cyclic ester ε -caprolactone (CL) through a ring-opening polymerization, catalysed by metal alkoxides, metal carboxylates, or ionic initiators, at elevated temperatures (> 120 ° C). Alternatively, the polycondensation of 6-hydroxyhexanoic acid can be pursued, although a lower quality product is generally obtained (Figure 14).

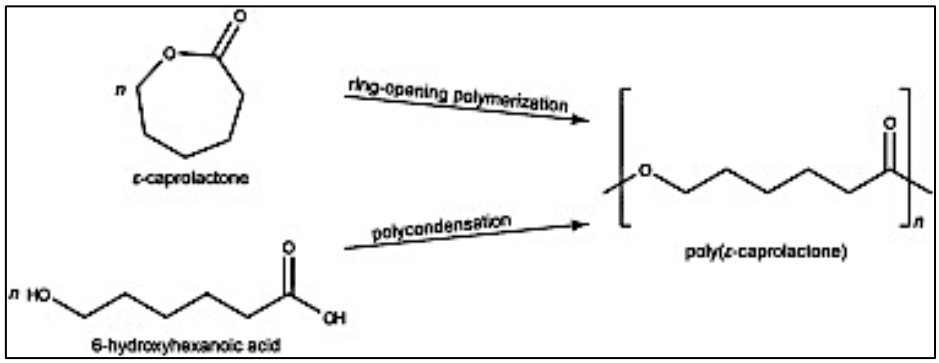

***Figure 14**: Synthesis of PCL*

PCL is soluble in many solvents at room temperature, including toluene, benzene, chloroform, cyclohexanone, carbon tetrachloride, tetrahydrofuran (THF), dimethyl carbonate (DMC), dioxane, 2-nitropropane, and dichloromethane (DCM). It is partially soluble in acetone, ethyl acetate, dimethylformamide (DMF), 2-butanone, and acetonitrile. It is insoluble in water, alcohols, diethyl ether, and petroleum ether. It is also miscible with other polymers, and it can form mechanically compatible composites. These properties allowed the researchers to customise the mechanical properties, degradation rates, and, occasionally, the bioactivity of the polymer (Bartnikowski et. al., 2019).

Rai et al. investigated the incorporation of PCL (18–33% total polymer blend) to a PGS-based solution increased the viscosity of the blend to a level suitable for electrospinning. PGS and PCL were dissolved at different weight ratios (5: 1, 3: 1, 2: 1 and 0: 1, respectively) in an anhydrous mixture of chloroform: ethanol (9: 1) and electrophilated at 12.5, 15, 17.5 and 20 kV. A further increase in tension caused the fibres to melt. Likewise, higher PGS concentrations in the polymer resulted in a significant increase in fibre diameter. The mechanical properties of PGS: PCL scaffolds were comparable to heat-cross-linked or light-cross-linked polymer sheets, although no cross-linking method was used. At the same time, PGS-PCL scaffolds did not result in a decrease of mechanical properties, compared to PCL-only scaffolds. Therefore, these studies demonstrated that simple PGS prepolymer blends with PCL can be used to fabricate microfibrotic scaffolds with mechanical properties in the range of a human aortic valve flap (Rai et. al., 2012).

1.6 Processes to produce scaffolds

1.6.1 Electrospinning

The electrospinning is an electrohydrodynamic process by which it is possible to obtain continuous fibers with a less than one micron diameter. The starting material can consist of a binary polymer-solvent solution ("solution electrospinning") or a melt polymer ("melt electrospinning") (Bhushani et. al.,2014).

The typical configuration of the electrospinning system consists of the following components (Figure 15):

• a high voltage generator;

• a syringe pump;

• a metal injection needle;

• a grounding collector.

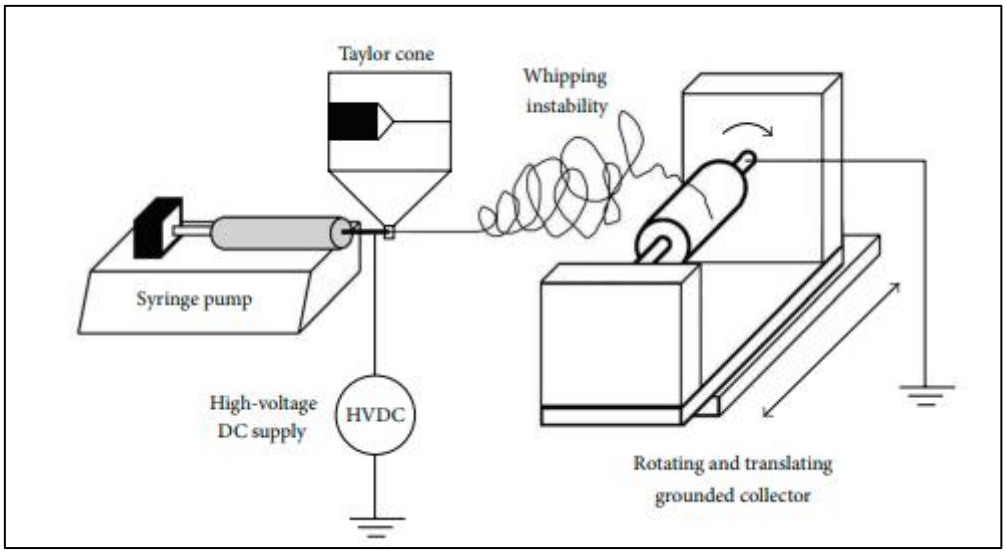

Figure 15*:Typical configuration and operating principle of the system for electrospinning with rotating collector*
(Liu et.al.,2013)

The polymeric material to be spun is dissolved in a solvent and fed to a needle via a dosing syringe, while a high potential electric field (1-30kV) is applied between the tip of the injection needle and the manifold. The volume of the fluid that flows out of the needle tip thus acquires a charge, overcoming the surface tension and assuming a particular conformation, known as Taylor's cone (Kumar et. al., 2019). The charged jet thus created tends to follow the direction of the external electric field. While the jet is pushed towards the collector, the solvent evaporates and the polymer chains intertwining are randomly

deposited on the collection area, where they are picked up and, subsequently, arranged in the desired shapes. The collector can have different shapes: it can be a flat plate, or a rotating cylinder and it commonly consists of metal supports, aluminum foil, paper, or conductive fabrics.

The parameters governing the electrospinning process can be classified into three groups.

- **Process parameters**

  They include voltage, flow rate, needle and manifold size and shape characteristics, as well as the distance at which they are located.

  The *voltage* applied to the process directly affects the fibers of the electrospun scaffold. As the voltage of the electric field increases, there is a decrease in the diameter of the fibers and a reduction in the evaporation rate of the solvent.

  The *flow rate* value determines the amount of solution available per unit of time. As the flow rate increases the diameter of the fibers also rise, if the speed with which the jet of solution passes from needle to collector remains constant. At high flow rates, however, the total evaporation time of the solvent decreases. Therefore, it is usually preferred to work at lower flow rates.

  The *distance between the tip of the needle and the collector* is a parameter that has repercussions both on the time taken by the jet to reach the collector and on the intensity of the electric field. As the distance decreases, the space the jet will have to travel will be smaller, the electric field will increase as well as the acceleration of the jet. This distance also affects the morphology of the fibers. If the two charged bodies are too close, the electric field will grow and lead to the formation of an unstable jet with possible formation of droplets along the fibers. By increasing the distance, however, the jet will take a longer time to reach the collector and the fibers will therefore have a smaller diameter. These are both extreme cases with which good results are not obtained. Once the electric field has been fixed, it will therefore be necessary to find the appropriate distance that allows to maximize the elongation of the fibers, reduce their diameter to a minimum and obtain complete evaporation of the solvent (Tan et. al.,2022)

- **Solution parameters**

  This group includes the parameters relating to the polymer solution. They are connected to the characteristics of the polymers and solvent used and include

concentration, molecular weight, viscosity, surface tension, material volatility, conductivity, and density (Bhardwaj et. al.,2010).

Viscosity is certainly one of the most important values. It is essential because the fiber must have a sufficiently high viscosity to be able to form continuously and without defects. If this does not happen, problems such as the breaking of the jet, the appearance of drops or the formation of fibers sprinkled with beads can occur. To ensure adequate viscosities, a high molecular weight polymer is used. Another parameter with which the viscosity of the solution can be adjusted is the concentration of the polymer.

For the electrospinning process to begin, the solution charged by the effect of the electric field must be able to overcome the *surface tension*. Starting from solutions with low surface tension, the formation of smooth fibers will be favored.

As regards parameters related to the solvent used, the value of the *electrical conductivity* is fundamental. The higher it is, the greater will be the accumulation of charges on the solution, facilitating the elongation of the fibers with a consequent decrease in their diameter. In addition, problems of discontinuity linked to the formation of beads are avoided. To reach suitable conductivity values, a polar solvent can be chosen or a small quantity of ionic compounds, such as salt for example, can be added to the solution.

The surface tension of the solvent, on the other hand, acts in the opposite way. To avoid the formation of droplets it is advisable to work with solvents with low values, possibly introducing surfactants to the solution.

The *nature of the solvent* is another equally relevant parameter. If you use solvents with a high dielectric constant, you will have a greater deposition area and you will get smooth fibers with a reduced diameter.

- **Environmental conditions**

To ensure that the process takes place in an optimal manner, the atmosphere should be controlled in terms of relative *humidity* and *temperature*.

The first parameter directly affects the volatility of the solvent and therefore its evaporation rate. As mentioned above, these aspects affected the morphology of the electrospun fibers. If the ambient humidity is too high, pores may form. For too low values, on the other hand, the evaporation rate of the solvent can be even

greater than the speed with which the polymer solution leaves the needle and in this case the needle quickly clogs up.

As for the temperature, its increase leads on the one hand to a faster evaporation of the solvent. On the other hand, it decreases the viscosity of the solution and therefore the stretching of the jet. The fibers produced will therefore have a smaller diameter (Haider et. al.,2018).

There is a wide range of polymers that through this technique can form nanofibers, which are widely applied in various technologically advanced sectors, including that of biomedical engineering. Natural materials are generally less suitable than synthetic ones, therefore, for the former, the optimization of polymer and solvent concentrations must be carefully considered (Torres-Giner et.al., 2016).

With electrospinning it is possible to combine the advantages of synthetic materials with natural ones and for this reason it is considered such an innovative process, especially for vascular graft of engineered tissue (TEGV), where a high mechanical durability is required in terms of breaking strength. It is possible to monitor the composition, size and alignment of the fibers that have an impact on the porosity, the distribution of pores and the architecture of the scaffolds. The most used polymeric blends for electrospinning require the use of preferably volatile solvents. In the field of tissue engineering, the bioabsorbable polymers that have shown the best performances are poly(ε-caprolactone) (PCL), polyglycerolsebacate (PGS), polylacticacid (PLA), polyglycolicacid (PGA) and their copolymers.

Overall, electrospinning is an innovative, simple, versatile, and economical process, which can be applied to all polymeric materials returned to the viscous fluid state. Electrospun nanofibers, compared to fibers obtained with conventional methods, offer several advantages (Thangadurai et. al., 2022): high surface-volume ratio, improved porosity, intertwined structure and high elastic modulus, characteristics that positively affect the mechanical performance and surface functionality of the constructs.

1.7 Engineering materials

1.7.1 Quercetin

Quercetin, or 3,3 ', 4', 5,7-pentahydroxyflavone, is a natural organic compound belonging to the class of flavonoids, which are categorized as polyphenolic compounds (Figure 16). Quercetin, with the chemical formula $C_{15}H_{12}O_7$, is widely spread in the plant world: it is found in some plants including *Ginko biloba*, *Hypericum perforatum*, *Sambucus canadensis* and it enriches various foods, such as capers, broccoli, asparagus, tomatoes, grapes, citrus fruits, tea, and coffee. (https://www.artoi.it/quercitina-e-bioflavonoidi/)

Quercetin is a photosensitive compound that has a cedar yellow crystalline form, insoluble in water and partially soluble in lipids and alcohols (Ilja Gasan Osojnik Cˇ rnivec et al., 2021).

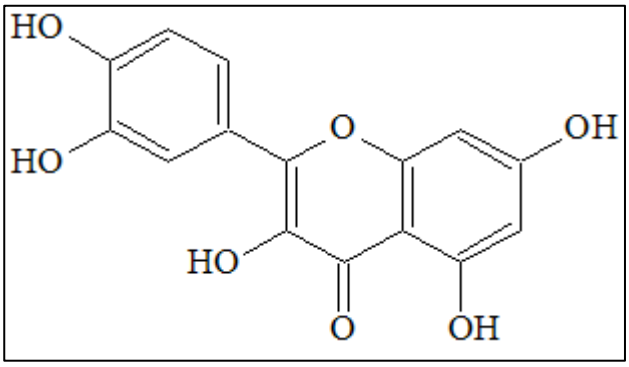

***Figure 16**: Chemical structure of quercetin (https://www.artoi.it/quercitina-e-bioflavonoidi/)*

Quercetin frequently shows up in the form of a glycoside, such as rutin, in which the hydrogen of the hydroxyl group R-4 is replaced by a disaccharide (Lamson et. al., 2000). Quercetin is currently one of the most studied flavonoids, being known for its good pharmacological qualities: it appears to have anti-inflammatory, antimicrobial, anticancer, and antithrombotic properties (Katia Rubini et. al., 2020).
In addition, the chemical structure rich in phenolic groups allows the compound to work as a powerful antioxidant:

- It can transform radical species, such as oxygen and nitrogen, into non-toxic compounds.

- It increases the expression of various antioxidant enzymes, including catalase, PON2, and glutathione peroxidase (Li et al.,2016), It can slow the production of nitric oxide. (Lamson et al., 2000)

Thanks to its high bioavailability, quercetin revealed to be a good candidate for biomedical applications. It can inhibit the proliferation of some types of cancerous cells (Caltagirone et al., 2000), preventing the formation of enzymes that produce inflammation, and ensuring an effective antioxidant activity (Haizhou Wu et al., 2022).

1.7.2 Gelatin

Gelatin is a natural biopolymer resulting from the partially acid or alkaline hydrolysis reaction of collagen present in the skin, bones, and tendons of animals. It is a high molecular weight polypeptide. The name gelatin came into common use in 1700, and it derived from the Latin 'gelatus', meaning firm or frozen. Although the term gelatin is sometimes used to refer to other gel formers, it is properly applied only to collagen-derived protein materials.

The main areas in which gelatin is used, are food industry (confectionery, meat products, dairy products, etc.), pharmaceuticals (capsules, etc.), photography, and technical applications.

In the food industry, gelatin is one of the hydrocolloids or water-soluble polymers that can be used as a gelling, thickening, or stabilising agent. It differs from other hydrocolloids because most of them are polysaccharides, such as carrageenan and pectins, whereas gelatin is a totally digestible protein, containing all the essential amino acids, except tryptophan.

At present, the world production of gelatin is estimated to be 140000-160000 tonnes per year and there is a 3% average annual increase in the use of gelatin in the food area, mainly for confectionery and low-calorie spreads (Poppe, 1992).

Gelatin has long been used in different fields, due to its exceptional characteristics:

• Commercially available at low cost and readily available;

• It is a biodegradable and biocompatible;

• It exhibits low antigenicity;

• It does not produce harmful by-products upon enzymatic degradation;

• It contains motifs, such as Arginine-Glycine-Aspartic acid sequences that modulate the cell adhesion;

• It presents a high number of accessible functional groups for modification (e.g., crosslinking) and targeting ligands (e.g., drug delivery vehicles) (Hoque et al., 2015).

1.8 Bioreactors

A bioreactor can be defined as a system that simulates strictly monitored physiological environments for the creation, the physical conditioning and the testing of cells, tissues, precursors, and organs in vitro (Figure 17) (Barron et al.,2003),(Plunkett et al.,2011).

A bioreactor should be able to perform one of the following functions:

- Establish a uniform distribution of cells on a three-dimensional scaffold;
- Maintaining the desired concentration of gasses and nutrients in the culture medium;
- Provide efficient mass transfer to the growing tissue;
- Expose the developing tissue to physical stimuli;
- Provide information on the formation process of 3D tissues, which come from isolated cells.

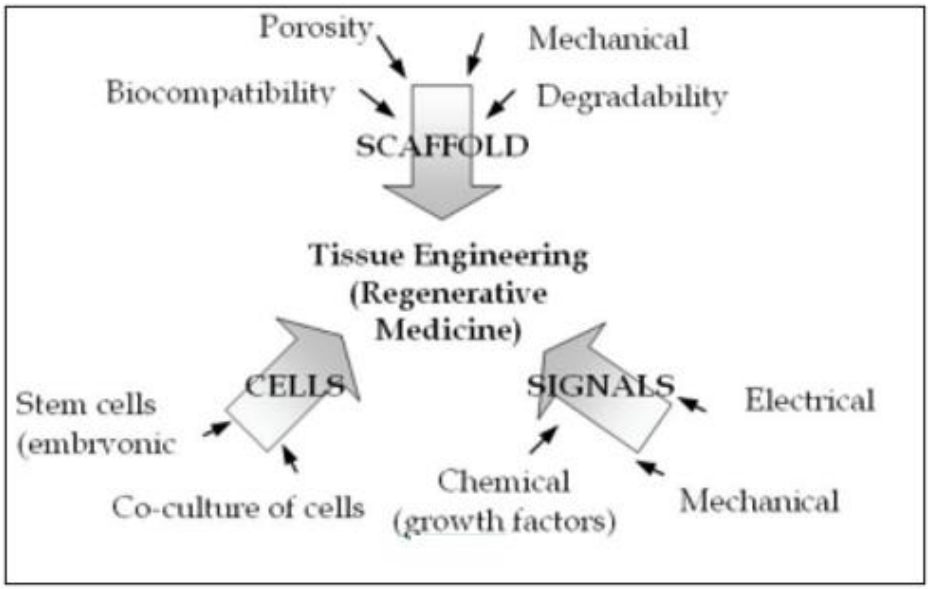

***Figure 17**: Tissue engineering*

There are some general principles that must be followed when developing a bioreactor, as well as specific requirements for each fabric and/or application.

Material selection is very important as it is critical to ensure that the materials used to create the bioreactor do not elicit any adverse reactions from the cultured tissue. Any material in contact with the media must be biocompatible or bioinert. Furthermore, it's important to consider that such simulations could require a set temperature of 37°C, a humid atmosphere, and sterilized conditions. In general, transparent, or opaque materials and flexible or rigid materials are chosen depending on their function. For example, transparent materials can be useful in enabling the monitoring of the construct in the bioreactor, while hoses can help with the assembly.

The specific application of the bioreactor must be kept in mind during the design process to ensure a good compliance with all the design constraints. If various parameters, such as pH, nutrient concentration, or oxygen levels, must be monitored, different sensors would have to be incorporated into the design. Furthermore, the forces required for the cell stimulation are very small; therefore, in this case, it is important to ensure that the pump/motor can apply small forces with great precision. Finally, it's important to design reliable sealing systems, to minimize fluid leaks.

1.8.1 Types of bioreactors

There are different types of bioreactors, defined depending on the conditions necessary for the survival of the cells, to the functional and mechanical requirements and those of the final user. The functional specifications are represented by the flow, controlled in composition, pressure and temperature, eventual heat forces, pulsatile forces, shear forces, pressure forces, the frequency of stress, and the flow rate.
The main components of a bioreactor are (Figure 18):

- a reservoir;
- mechanical valve;
- pump;
- filter;
- a resistance;
- chamber where the scaffold resides.

In particular, the term "reservoir" refers to the chamber containing the growth medium that is spread through the pump. Given the different generalities of bioreactors, these are divided into: static systems, dynamic systems, and biomimetic systems (Barron et al.,2003).

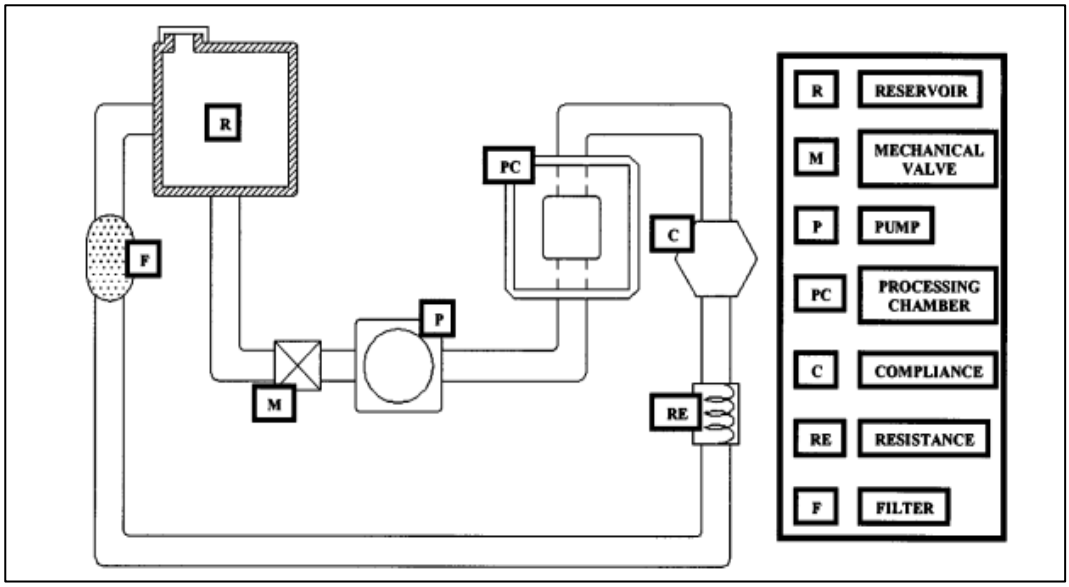

***Figure 18**: Schematic diagram of a model pulsatile flow system*

Static system

The static system is the simplest type of biological reactor.

Optimal gas exchange and mass transfer conditions are extremely important for the growth of a tissue. In the static system the gas aeration is provided by the surface aeration of the culture medium, while the mass transfer occurs by molecular diffusion, since there is no fluid flow on the surface of the tissue constructs. In a static system with mechanical agitation, instead, the transfer occurs by turbulent convection. In this case, the tissues are subjected to turbulent flow at the surface, which can lead to structurally non-uniform fabric constructs, generally inadequate.

In general, during the development of these engineered constructs, there are some critical issues, such as providing efficient mass transfer from the medium to the tissue surface, as well as a low-stress environment, and exposing the tissue to physical stimuli. Since it was demonstrated that physical stimuli can modulate the tissue development, the focus was shifted to the design of a bioreactor capable of exposing the growing tissues to mechanical forces and thus the static system was abandoned.

Dynamic system

The dynamic system is composed by rotating wall vessels, fluid-filled culture vessel. The initial rotational speed can be adjusted so that the culture medium and cells rotate synchronously with the vessel, providing an efficient mass transfer in a low shear environment, since fluid flow is laminar. These bioreactors were the first systems designed to simultaneously integrate cocultivation, low shear, high mass transfer, and three-dimensional growth, without sacrificing any other parameters.
Furthermore, it was demonstrated that engineered cardiac tissues grown in rotating vessels are structurally and functionally more superior to constructs grown in static or mixed flasks (Barron et al.,2003).

The "spinner flask" was one of the first systems used for 3D culture under dynamic conditions (Figure 19). It induces mixing of oxygen and nutrients throughout the medium and reduces the concentration boundary layer at the construct surface. In this case, a magnet is positioned inside the bioreactor, and its rotation is induced by an external magnetic field. The flow across the scaffolds surface results in turbulent instabilities called eddies, which are associated with transitional and turbulent flow. In this way, the fluid transport to the centre of the scaffold is enhanced. This system is very promising also because it solves the problem of sterility, avoiding the use of joints or the presence of internal mechanical organs managed externally (Partap et al, 2011).

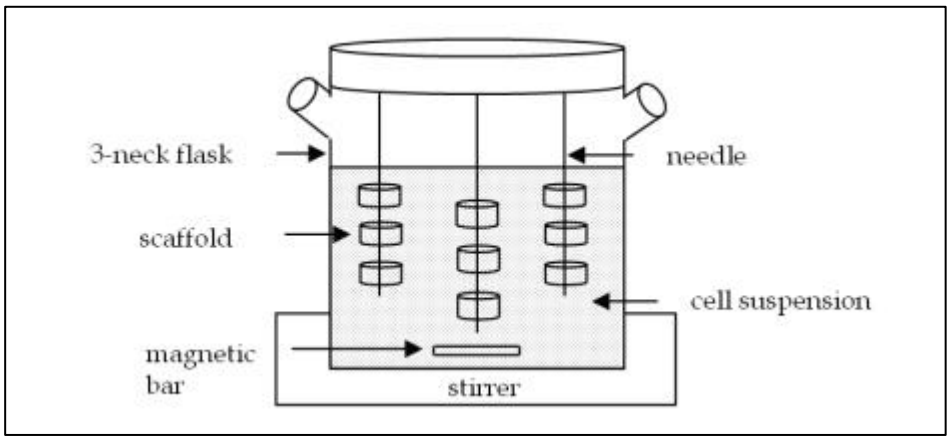

***Figure 19**:A spinner flask bioreactor*

Biomimetic system

Recently, several systems, miming the cardiovascular conditions in vitro, were developed (Figure 20). They allow the tissue growth and survival, and the reproduction of mechanical stimuli. Known as biomimetic systems, they are the most innovative and functional apparatuses, compared to the previous ones.

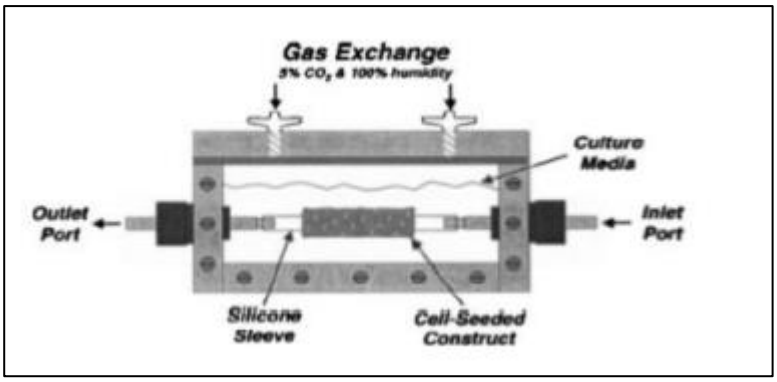

Figure 20*:Seliktar biomimetic bioreactor*

Many research works studied these reactor types in the field of cardiovascular prostheses. Wolfinbarger, for instance, created a device for developing tissue development on a devitalized and decellularized graft from humans or animals. Moreover, Hoerstrup studied both heart valve bioreactors and small diameter vascular ducts (Barron et al.,2003). Another example is the bioreactor designed by Seliktar.

This system subjected the tubular constructs to cyclic stresses. A silicone tube was placed in contact with the culture medium and the seeded scaffold was placed on it. The mechanical stresses were due to a compressed air mechanism, connected to the silicone tube, which allowed the duct to inflate and deflate. The system was maintained at 37 ° C in a CO2 incubator. The tubular structures were exposed to dynamic mechanical conditioning by inflation and deflation of the ducts at a frequency of 1 Hz for periods of 4 and 8 days (Black et al.,2000).

In another study, Niklason developed a bioreactor to closely mimic in vivo conditions, this perfusion system provided intraluminal pressure and pulsatile flow to four bioreactors, each of which contained one tissue-engineered vessel. Gas exchange was provided via a reservoir bag, and the pressure was monitored constantly.

The bioreactor was incubated and maintained in a controlled atmosphere with 10% CO2 and 100% humidity, at 37 °C. The purpose of this research was to create small-gauge arterial vascular implants and it was carried out starting from analogous vascular cells, seeded on a biodegradable polymer scaffold. Subsequently, the graft was placed in a bioreactor that mimicked the physiological conditions in which the graft was then found in vivo. In addition to the bioreactor, the system was composed of a tank, in which the culture medium was contained, a pulsatile pump, a compliance chamber and three other bioreactors, connected in parallel. Within these four bioreactors in total, the scaffolds were positioned and filled with the culture medium and other substances, including ascorbic acid, proline, alanine, glycine, and 20% fetal bovine serum. The bioreactor was placed on a stir plate and mixed continuously. A silicone tube was inserted inside the scaffolds which, thanks to its elasticity, allowed the medium to pass into the vessel lumen, avoiding flaking of the graft itself. The compliance chamber, located between the pump and the bioreactors, avoided the transmission of high frequency vibrations to the bioreactors. The pump made the flow coming from the reservoir pulsatile to simulate the blood flow and it exerted a certain pressure. After a certain period, approximately two months, the silicone tube present in the scaffolds was removed so that the flow could come into direct contact with the lumen of the implant. In this way, the presence of tangential forces on the graft was also verified: they increased as the flow of the medium increased (Niklason et al.,1997).

1.9 Mathematical modeling

Fluid dynamics is the branch of physics that deals with the behavior of moving fluids. In the common sense, a fluid means a particular state of matter that includes liquids and gases. At a macroscopic level, a fluid, unlike a solid, does not have its own shape but takes on that of the container in which it is contained. This behavior is due to properties that regulate matter at the microscopic level: the molecules of a solid make only small oscillations around fixed positions, while those of a fluid can freely change their location.

Referring to the concepts of normal and tangential stress, however, we can give a more rigorous definition: "by saying fluid we mean a substance capable of deforming continuously and indefinitely when subjected to an external tangential stress"(Zuccher , 2022).

While in solids stresses generated as a function of a shear deformation depends on the deformation itself, in fluids the stresses are proportional to the deformation rate.

The description of a fluid (at rest or in motion) from a macroscopic point of view consists in the representation of the properties of the fluid, including speed, pressure, density, and temperature, through functions that depend on both space and time.

$$f(x,t) \tag{1}$$

This type of definition makes it possible to refer to continuous bodies, governed by laws of motion formulated through suitable partial differential equations.

At the basis of the macroscopic description, however, there is the consideration of the mechanical properties of the individual molecules. The two levels, macroscopic and microscopic, are joined by a statistical or probabilistic link.

For any isolated mechanical system, the conservation laws of microscopic mechanical quantities are valid: mass, momentum, and energy. These are the so-called "additive mechanical invariants", which remain constant among a given isolated volume. In a not-isolated system these quantities will vary the more slowly the greater the number of particles from which the system itself is composed.
A variation of a size is necessarily attributed to an interaction with the outside:

- locally through the surface (flow);
- at a distance due to the intervention of force fields (gravity, electric field) (Batchelor, 2020).

It is possible to write balance equations, which link the temporal variations of the mechanical invariants in an arbitrary volume V to their flow through the surface ∂V that delimits the volume itself. Let us consider a volume, isolated as a whole and not subject to force fields, divided into two parts by a separating surface. Since each of the two parts taken separately is not isolated, its mass, energy and momentum will be free to vary but, for the total quantities to be constant, the increase on one side must be compensated by an equal decrease from the other. This creates a flow, that is a vector

quantity determining the volume of fluid that crosses a surface in the unit of time. It is possible to distinguish the flow into two types: stationary and not stationary.

The fundamental laws of fluid dynamics are peculiar cases of balance equations. These constitute the Navier-Stokes equations, which is a system of not-linear partial differential equations. This differential system, in its not-simplified form, does not present a general solution in closed form and to solve them it is necessary to rely on the methodology of computational fluid dynamics (CFD), using computer numerical methods.

1.9.1 Steady state: Flow of Poiseuille

For the steady state it is necessary to consider the laminar, axial symmetric and stationary flow of a fluid through a tube of constant circular section and radius R.
Considering the geometry of the problem, it is useful to use the cylindrical coordinates (r, θ, z),
where v_r is the radial velocity, v_θ the angular velocity and v_z is the axial speed. It is assumed that $v_r = v_\theta = 0$, being only v_z the non-zero velocity component (Figure 21).

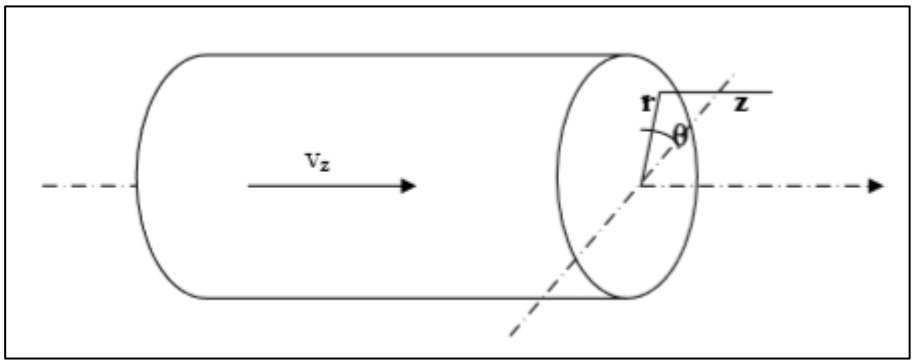

***Figure 21**: Representation of cylindrical coordinates*

For simplicity the Navier-Stokes equations and the continuity equation are reported in cylindrical coordinates. As far as continuity is concerned, it is obtained that:

$$\frac{\partial v_z}{\partial z} = 0 \tag{2}$$

Furthermore, for axial symmetry and stationarity:

$$\frac{\partial v_z}{\partial t} = \frac{\partial v_z}{\partial \theta} = 0$$

(3)

This means that v_z is only a function of r: $v_z = (r)$. The equations of N-S reported in cylindrical coordinates, are the following (we denote by g_r, g_θ and g_z are the components of the gravity vector in the three directions of the reference system).

Along r:

$$\rho\left(\frac{\partial v_r}{\partial t} + v_r\frac{\partial v_r}{\partial r} + \frac{v_\theta}{r}\frac{\partial v_r}{\partial \theta} - \frac{v_\theta^2}{r} + v_z\frac{\partial v_r}{\partial z}\right) =$$
$$-\frac{\partial P}{\partial r} + \rho g_r + \mu\left[\frac{1}{r}\frac{\partial}{\partial r}\left(r\frac{\partial v_r}{\partial r}\right) - \frac{v_r^2}{r} + \frac{1}{r^2}\frac{\partial^2 v_r}{\partial \theta^2} - \frac{2}{r^2}\frac{\partial v_\theta}{\partial \theta} + \frac{\partial^2 v_r}{\partial z^2}\right]$$

(4)

Along θ:

$$\rho\left(\frac{\partial v_\theta}{\partial t} + v_r\frac{\partial v_\theta}{\partial r} + \frac{v_\theta}{r}\frac{\partial v_\theta}{\partial \theta} - \frac{v_\theta v_r}{r} + v_z\frac{\partial v_\theta}{\partial z}\right) =$$
$$-\frac{1}{r}\frac{\partial P}{\partial \theta} + \rho g_\theta + \mu\left[\frac{1}{r}\frac{\partial}{\partial r}\left(r\frac{\partial v_\theta}{\partial r}\right) - \frac{v_\theta^2}{r} + \frac{1}{r^2}\frac{\partial^2 v_\theta}{\partial \theta^2} - \frac{2}{r^2}\frac{\partial v_r}{\partial \theta} + \frac{\partial^2 v_\theta}{\partial z^2}\right]$$

(5)

Along z:

$$\rho\left(\frac{\partial v_z}{\partial t} + v_r\frac{\partial v_z}{\partial r} + \frac{v_\theta}{r}\frac{\partial v_z}{\partial \theta} + v_z\frac{\partial v_z}{\partial z}\right) =$$
$$-\frac{\partial P}{\partial z} + \rho g_z + \mu\left[\frac{1}{r}\frac{\partial}{\partial r}\left(r\frac{\partial v_z}{\partial r}\right) + \frac{1}{r^2}\frac{\partial^2 v_z}{\partial \theta^2} + \frac{\partial^2 v_z}{\partial z^2}\right]$$

(6)

Through these simplifications, the following final system is obtained:

$$\begin{cases} -\dfrac{\partial P}{\partial z} + \mu\left[\dfrac{1}{r}\dfrac{\partial}{\partial r}\left(r\dfrac{\partial v_z}{\partial r}\right)\right] = 0 \\ -\dfrac{1}{r}\dfrac{\partial P}{\partial \theta} - g\rho\cos\theta = 0 \\ -\dfrac{\partial P}{\partial r} - g\rho\sin\theta = 0 \end{cases}$$

(7)

By integrating the last two equations it is obtained:

$$P = -g\rho r sen\theta + f_1(z) \tag{8}$$

Or

$$P = -g\rho y + f_1(z) \tag{9}$$

Fixed z, the expression indicates that the pressure is distributed hydrostatically along the vertical direction and that $\frac{\partial P}{\partial z}$ does not depend on either r or θ. Taking these assumptions into account, equation (8) can be further integrated as follows:

$$\frac{1}{r}\frac{\partial}{\partial r}\left(r\frac{\partial v_z}{\partial r}\right) = \frac{1}{\mu}\frac{\partial P}{\partial z} \tag{10}$$

$$r\frac{\partial v_z}{\partial r} = \frac{1}{2\mu}\frac{\partial P}{\partial z}r^2 + C_1 \tag{11}$$

$$v_z(r) = \frac{1}{4\mu}\frac{\partial P}{\partial z}r^2 + C_1 \ln r + C_2 \tag{12}$$

This last equation is elaborated by applying the following boundary conditions:

1- for r = 0 (on the z axis) the speed must be a finite value. The only way to make it happen
   is that $C_1 = 0$;
2- Along the wall (r = R) the speed must be zero, therefore:

$$C_2 = -\frac{1}{4\mu}\frac{\partial P}{\partial z}R^2 \tag{13}$$

The constants are so made explicit, and the relation becomes:

$$v_Z(r) = \frac{1}{4\mu}\frac{\partial P}{\partial z}(r^2 - R^2)$$

(14)

In each cross section, the profile is thus parabolic. To obtain the flow rate in terms of volume Q, v_z must be integrated as follows:

$$Q = \int_0^R v(z)2\pi r dr = 2\pi \int_0^R \frac{1}{4\mu}\frac{\partial P}{\partial z}(r^2 - R^2)rdr = -\frac{\pi R^4}{8\mu}(\frac{\partial P}{\partial z})$$

(15)

The flow is positive as the term $\frac{\partial P}{\partial z} < 0$. It is very important to note the dependence of Q on R^4.

It is crucial to consider linear pressure drops along x to express the pressure gradient along a distance ΔL using the following expression:

$$\frac{\Delta P}{\Delta L} = -\frac{\partial P}{\partial z}$$

(16)

Going to replace this equality within the expression of scope the Hagen-Poisuille law is obtained:

$$Q = \frac{\pi R^4}{8\mu}\frac{\Delta P}{\Delta L}$$

(17)

At this point, the average speed can be obtained by dividing this flow rate by the area:

$$U = \frac{Q}{\pi R^2} = \frac{R^2}{8\mu}\frac{\Delta P}{\Delta L}$$

(18)

Furthermore, the maximum speed is obtained instead on the axis of the tube, so for r = 0 and it will be:

$$v_{z\,max} = \frac{R^2}{4\mu}\frac{\Delta P}{\Delta L} = 2U$$

(19)

The following expression is taken in dimensionless form, to normalize the speed v_z with respect to $v_{z\,max}$, and the Equation (8) is obtained:

$$\frac{v_{z\,(r)}}{v_{z\,max}} = 1 - (\frac{r^2}{R^2})$$

(20)

At this point it is needed to calculate the mechanical stress due to the contact of the fluid with the

wall. Replacing Equation (18) in Equation (13), it is possible to express $v_{z\,(r)}$ in the following expression:

$$\tau_w = \mu \frac{\partial v_z(r)}{\partial r}|_{r=R} = \mu \frac{\partial}{\partial r}\left[\frac{2U}{R^2}(R^2 - r^2)\right]|_{r=R} = \mu \frac{2U}{R^2}(0 - 2r)|_{r=R} =$$
$$= \mu \frac{2U}{R^2}(-1)2R = -\mu \frac{2U}{R}$$

(21)

Where:

τw is the shear stress (Pa);

μ is the dynamic viscosity (Kg/ms);

U is the average speed (m/s);

R is the radius (m).

The minus sign in the following expression expresses the magnitude of the force itself, that represents the opposition of the effort to the flow.

In this expression the terms of viscosity and the pressure gradient no longer appear. The latter equation quantifies the resistance of motion to the fluid. A measure of this resistance is expressed by a dimensionless parameter, called the coefficient of resistance, defined by the following expression:

$$\lambda = -\frac{\left(\frac{\partial P}{\partial z}\right)}{\frac{\rho U^2}{2}} 2R = \frac{64}{Re}$$

(22)

Where Re is defined on the basis of the average speed and diameter.

The coefficient λ is also defined as the Fanning coefficient and allows a dimensionless estimation of the head losses due to friction.

As mentioned above, these considerations are valid talking about the laminar flow. From the experimental analyzes, it appears that the limit in terms of Re is about 2100. This means that beyond this limit,

after a transition phase, the law (Equation 21) can no longer be considered valid.

Based on some experimental data, relating to smooth tubes, in turbulent conditions, Blasius obtained the following expression:

$$\lambda = 0.3164\ Re^{-0,25} \tag{23}$$

In those days there was not much data available at high Re numbers; in fact, the previous equation agrees with the experimental data for values of Re <100000.

From subsequent studies, emerged some theories that still give very accurate predictions on the speed profile. In the region closest to the wall, the velocity (μ) varies linearly with the distance from the wall (y) while for greater distances (always inside the boundary layer) this relationship becomes of the logarithmic type. The wall law for the turbulent boundary layer is expressed as follows:

$$u^+ = y^+ very\ close\ to\ the\ wall$$

$$u^+ = A \log y^+\ farther\ from\ the\ wall\ (but\ always\ within\ the\ limit)$$

Where the apex (+) indicates the non-dimensional quantities with respect to wall variables:

- wall speed:

$$u_\zeta = (\frac{\tau_w}{\rho})^2 \tag{24}$$

- characteristic length:

$$l = \frac{v}{u_\tau} \tag{25}$$

and where A and B are two constants to be determined with experimental data (Figure 22).

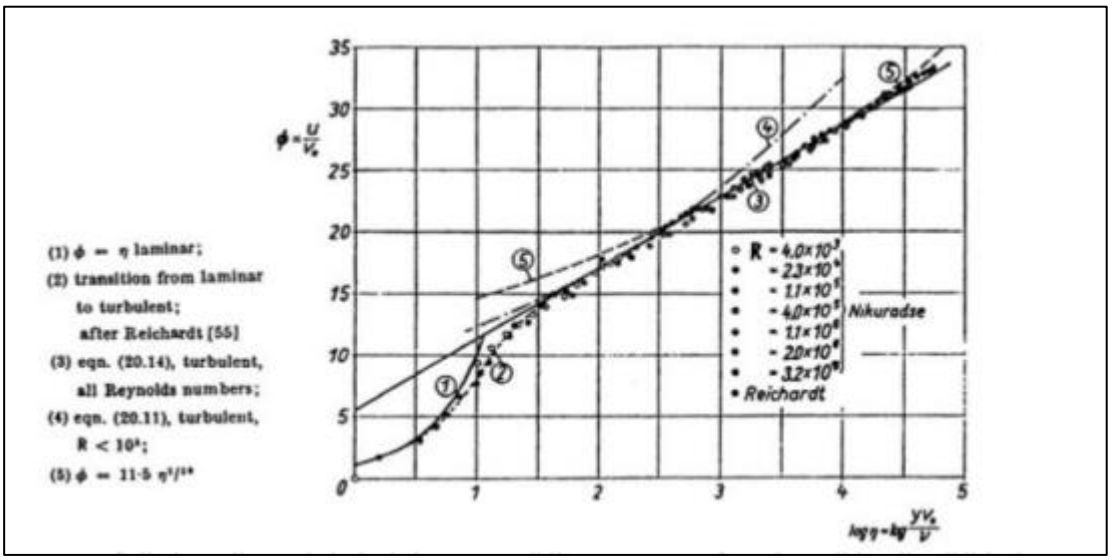

***Figure 22**: Representative diagram of the flow trend as a function of ϕ and η*

Thanks to these results it was possible to obtain a more general formula:

$$\frac{1}{\sqrt{\lambda}} = 2\log\left(Re\sqrt{\lambda}\right) - 0.8 \tag{26}$$

The following expression is defined as Prandtl's universal law, usable for any value of Re always for smooth turbulent pipes (Figure 23).

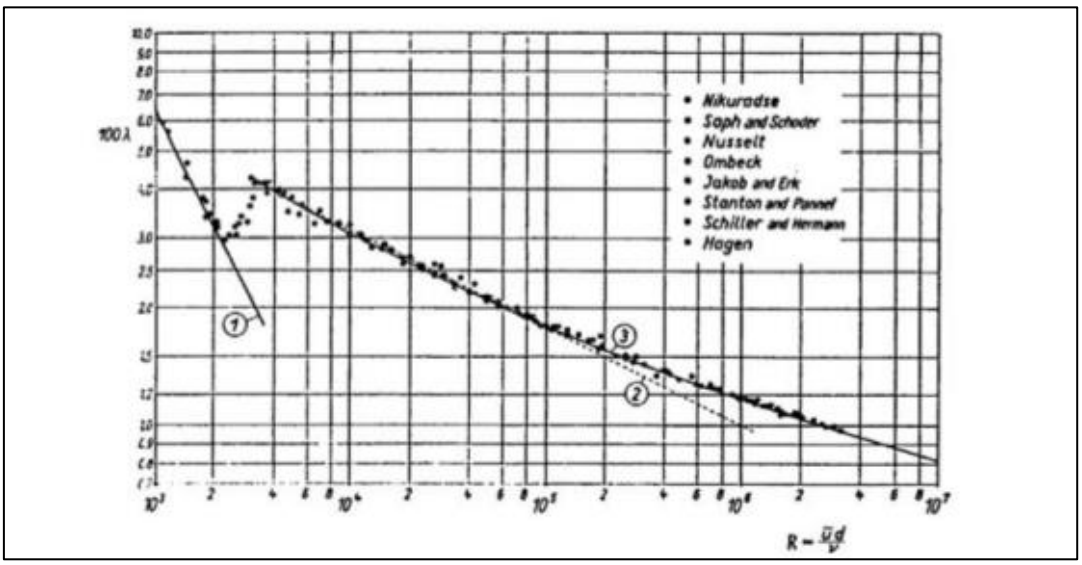

***Figure 23**:Representative diagram of the flow trend as a function of λ and R.*

The above equation can be solved through an iterative method, such as for example the Newton's method.

All this can be applied to smooth pipes. In case of wrinkled pipes instead it is necessary to introduce a new parameter, ε, which provides information on the average size of the roughness on a wall. For instance:

• ε = 0 for plastic and glass;

• ε = 0.0045 for commercial steel;

• ε = 0.18 – 1.9 for wood.

Thanks to the experimental data collected it was possible to obtain a general diagram in function of λ (Re) and ε / D defined as Moody's card or Nikuradse harp (Figure 24):

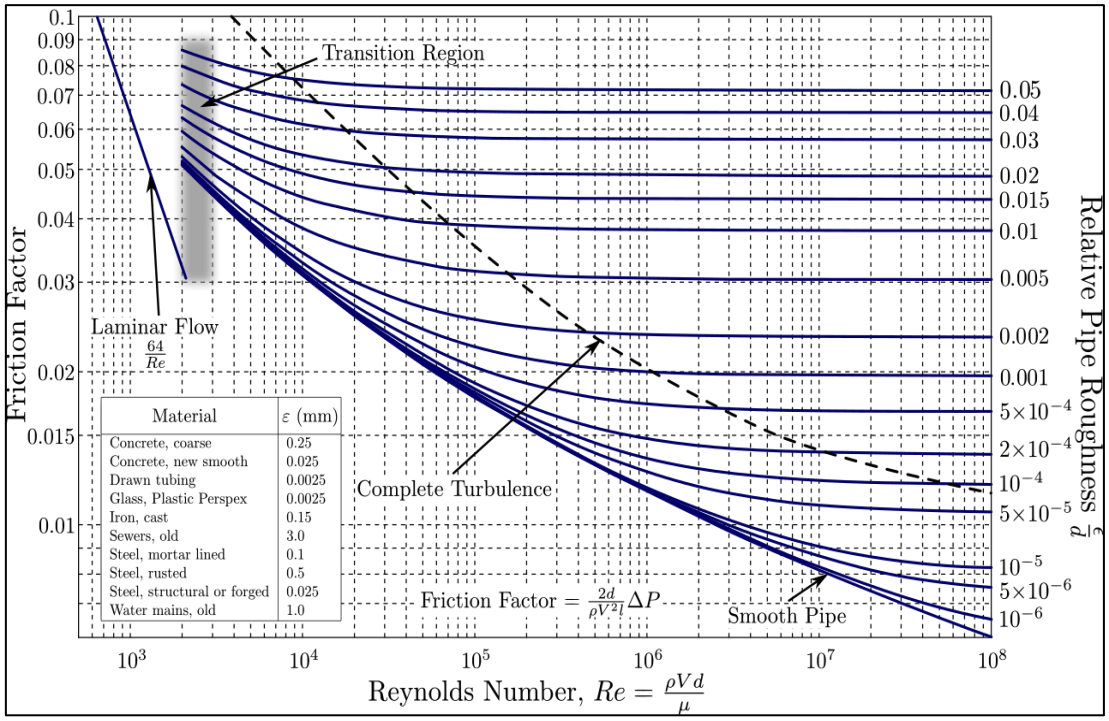

***Figure 24**: Moody diagram*

In the case of laminar flows, roughness is not a determining parameter while it becomes fundamental when it comes to turbulent flows, especially with high Re values.

This is closely related to the size of the turbulent boundary layer that, if Re grows, becomes thinner and thinner until it becomes of the same order or smaller than the size ε.

Still based on the experimental data for smooth or rough pipes, a law has been obtained

more general than Prandtl's universal law, which relates f(Re, λ, $\frac{\varepsilon}{D}$) called Colebrook's law.

In fluid dynamics, the Colebrook correlation is an equation that allows to derive the Darcy coefficient of friction λ of a generic fluid in a duct. This mathematical link arises from the combination of empirical results with flow studies about laminar and turbulent fluxes in pipes. It was developed in 1939 by C. F. Colebrook and White, and it is defined by such Equation (26) which can be described with an iterative method (Dulio et al., 1987):

$$\frac{1}{\sqrt{\lambda}} = -2\log\left(\frac{\frac{\varepsilon}{D}}{3.7} + \frac{2.51}{Re\sqrt{\lambda}}\right) \tag{27}$$

Where:

λ is the Darcy coefficient of friction;

$\frac{\varepsilon}{D}$ is the relative roughness;

Re is the Reynolds number.

The Colebrook equation is represented in the Moody diagram, which allows its graphic solution (Figure 26) as different parameters vary (Figure 25):

	Prandtl, eqn.	Blasius, eqn.
$R = \frac{\bar{u}d}{\nu}$	λ	λ
10^3	(0·0622)	(0·0567)
$2 \cdot 10^3$	(0·0494)	(0·0473)
$5 \cdot 10^3$	0·0374	0·0376
10^4	0·0309	0·0316
$2 \cdot 10^4$	0·0259	0·0266
$5 \cdot 10^4$	0·0209	0·0212
10^5	0·0180	0·0178
$2 \cdot 10^5$	0·0156	0·0150
$5 \cdot 10^5$	0·0131	—
10^6	0·0116	(0·0100)
$2 \cdot 10^6$	0·0104	—
$5 \cdot 10^6$	0·0090	—
10^7	0·0081	(0·0056)

***Figure 25**: Table containing data relating to R and λ*

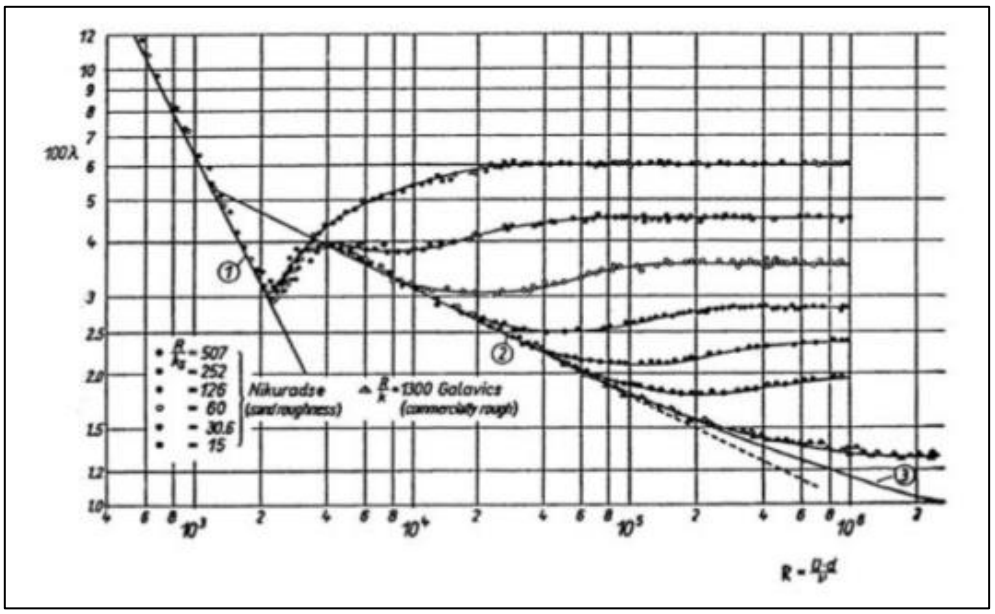

***Figure 26**:Representative diagram of the flow trend as a function of λ and R*

2. AIM OF THE STUDY

The aim of this study is to compare the behavior produced by scaffolds studied in a home-made bioreactor compared to a high performance one. In both the bioreactors, the same procedure was followed: each experiment was repeated three times to verify that the instrumentation was correct. To understand which effect is due to a particular element/polymer that it has added, experiments on "control" scaffolds (without quercetin) were carried out.

For the experiments in bioreactor, scaffolds that had already incorporated quercetin were produced. This was added to the PCL and PGS solutions before the prosthesis production phase through electrospinning. The purpose is in fact to use constructs that already contained a substance capable of performing the immune and anti-inflammatory function, removing the need to administer additional drugs after implantation in the body.

The choice was quercetin for its high bioavailability and for its multiple biological effects: it enhances the relaxation of blood vessels by increasing their dilation, and thus reducing cardiovascular risk (Li et al.,2016).

Later the scaffolds were covered with a layer of porcine gelatin to decrease the porosity given by the electrospinning process. Once the scaffolds were obtained, 5 days of test in bioreactor was performed with 5 different sampling moments.

3. MATERIALS AND METHODS

3.1 Preparation of the polymeric prostheses

Poly(ε-caprolactone) (PCL) (molecular weight = 8 x 10^4 Dalton) (Sigma-Aldrich, St. Louis, MO, USA) and poly(glycerol)sebacate (synthesized as reported in Wang et al., 2002) were used for the preparation of the polymeric prostheses. These two polymers were used to prepare two different solutions: PCL (20%) (m/v) and PGS (20%) (m/v) in ethanol, in which 0.05% (m/v) quercetin was previously dissolved, and chloroform in the ratio 1:9 (v/v). The choice of this type of solvents is due to their volatility, suitable for the electrospinning process, and the addition of quercetin is explained by its property of modulating the inflammatory response, allowing the control of the body's immune response. The obtained solutions were stirred overnight under a chemical hood and at room temperature. A blend of the PCL and PGS solutions was then prepared in a 1:1 (v/v) and it was mixed for 30/40 minutes at room temperature.

3.2 Production of prostheses by electrospinning

An electrospinning apparatus (Basic Lab Unit, Spinbow, Bologna, Italy) was used for the fabrication of the prostheses (Figure 28). The system was mainly composed by a syringe pump (KDS-100, KD Scientific, Holliston, MA, USA), a high voltage power supplier (PCM series, Spellman, NY, USA), an 18-gauge needle, corresponding to 1.27 mm of outer diameter and a cylindrical collector. The vertical and horizontal distances between the top of the needle and the centre of the collector were pre-defined. In particular, the vertical distance was 18 cm.

The PCL/PGS solution was inserted into a 5 mL glass syringe (FORTUNA® OPTIMA®, Poulten & Graf GmbH, Wertheim, Germany). The pump was set with a defined volume and flow rate. For prostheses with a diameter of 2 mm, the volume and the flow rate were configured equal to 1.5 mL and 2.2 mL/h, respectively. Regarding the 5 mm diameter prosthesis, the volume and the flow rate were 2 mL and 1.1 mL/h, respectively. The solution was directed towards the collector inside a capillary, ending with a flat-tipped needle. Because of the electric field, fibres were then deposited in a random way on the cylindrical collector (Figure 27).

***Figure 27**:Electrospinning cylindrical collector*

The generator was set to a voltage of 17.0 kV and the rotation and translation speed of the collector were set to 500 rpm and 600 mm/min, respectively (Table 1).

***Table 1**: Parameter of electrospinning*

Parameter	**Diameter (2 mm)**	**Diameter (5mm)**
V (volume)	1.5 mL	2.0 mL
R (rate)	2.20 mL/h	1.1 mL/h
D (needle-collector distance)	18 cm	18 cm
V (voltage)	17.0 kV	17.0 kV
$\mathbf{v_r}$ (rotation speed)	500 rpm	500 rpm
$\mathbf{v_t}$ (translation speed)	600 mm/min	600 mm/min
t(time)	40 min	1.50 h

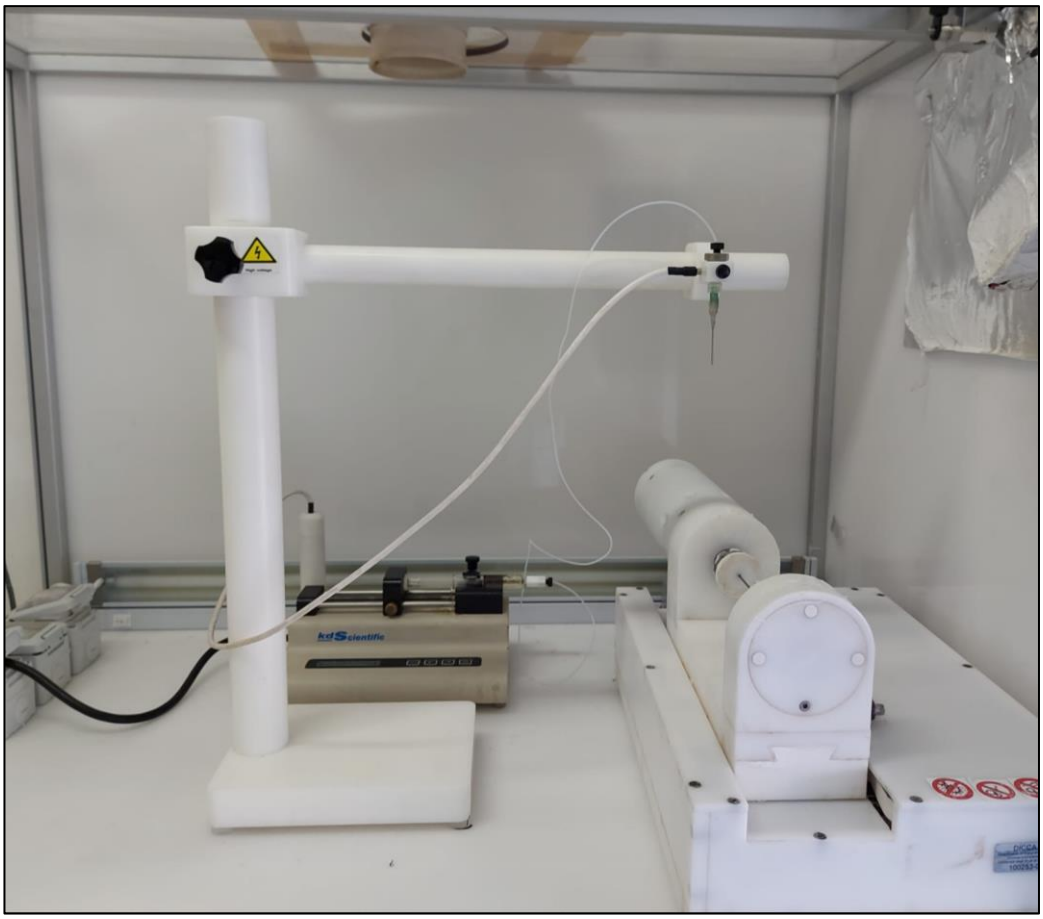

***Figure 28**: Structure of electrospinning*

3.3 Gelatin coating

After the electrospinning process, scaffolds were coated with a layer of gelatin (Sigma Aldrich, St. Louis, MO, USA), to decrease the porosity and, therefore, the permeability, given by the electrospinning process. The coating was made by dissolving 3.30 g of gelatin in 50 mL of deionized water (concentration of 67 mg/mL); the solution was left under stirring for 1 hour at 60°C. Subsequently, prostheses were soaked into the gelatin-based solution, placed on a mechanical stirrer (KIRK 510 Bicasa, Italy) (Figure 29), for 1 hour, at 37°C and with a rotation speed of 135 rpm.

***Figure 29**: Prostheses were submerged into the gelatine-based solution, placed on a mechanical stirrer*

The gelatin-coated prostheses were then sterilized under UV (FASTER, DASIT) for at least an hour in order to reduce the humidity of the sample, sterilize the scaffold and thus obtain the cross-linking of the gelatin on its surface.

At the end of this last operation, the sterilized scaffold was placed overnight in an dessicator.

3.4 Permeability test

For this test, scaffolds were connected to a pump loaded with water that increase water pressure since it achieves a physiological value. In this way, it was possible to establish the pressure at which the rupture of the scaffolds occurs. Therefore, water passed through the scaffolds and pressure was monitored versus time since the graft started to leak water; after reaching the pressure at which leakage occurred the flux was monitored constant for one minute (Figure 30).

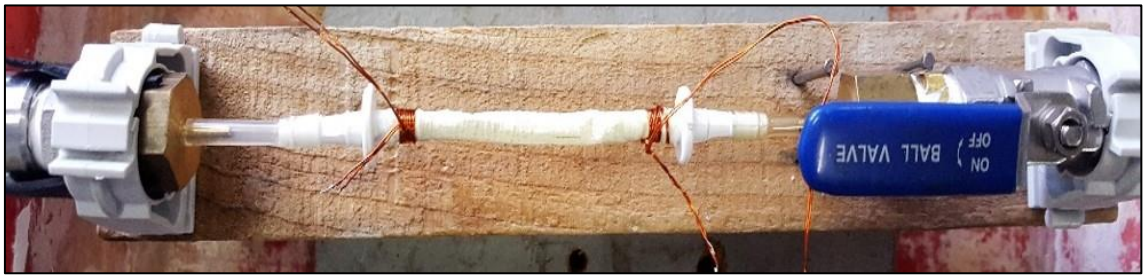

***Figure 30**: Permeability test*

As shown in the table, the presence of the gelatin coating gives the scaffold a lower water permeability, allowing the PCL:PGS 1:1 covered with gelatin to exhibit a permeability of 0% at a pressure of 0.2 bar, pressure of slightly higher than human physiological values. These data allow us to affirm the usefulness of the gelatin coating as a waterproofing agent, thereby solving the problem of the excessive permeability, initially observed, of the PCL:PGS as it was. When the applied pressure reached the value of 0.3 bar, the first drops of water appeared. This pressure value corresponds to 225 mmHg which is higher than the systolic pressure of a person without severe heart disease (Table 2). The ability of the coated sample not to be permeable at 0.2 bar can be explained by analysing the architecture of the 3D fibres. Ferrari et al (2017) showed that the porosity of the gelatin-coated samples was lower (43.49 ± 10.85%) compared to PCL:PGS 1:1 (68.19 ± 0.02%).

***Table 2**: Permeability at different pressure of scaffolds*

Sample	Pressure (mmHg)	Permeability (%)
PCL:PGS 1:1	150	100
PCL:PGS 1:1+ GQ	150	0
PCL:PGS 1:1+ GQ	225	100

3.5 Set up of the bioreactors

The electrospun scaffolds were then test in bioreactor. Processing the prostheses in an implant that simulates the conditions of the human body as much as possible is essential for predicting the activity that the constructs will have *in vivo*.

Tests were carried out at both constant and variable pressure. They were firstly performed in a home-made bioreactor and then they were transferred to a high-performance one.

3.5.1 Set up of the home-made bioreactor

Testes were firstly performed in a bioreactor built *ad hoc*, consisting of a peristaltic pump (Miniplus 2, GILSON), a reservoir, a pressure gauge (Italmanometri Cavriago DIG) and a chamber capable of hosting a single prosthesis at a time. In this case, the pressure was set manually; The prosthesis is mounted inside the chamber and mounted at both ends on tubes that allow it to be connected to the rest of the implant (Figure 31) (Table 3).

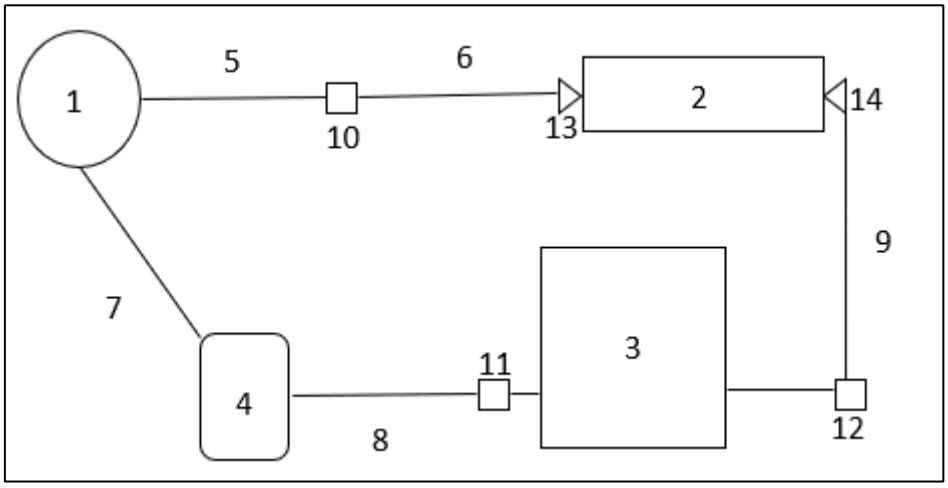

***Figure 31**: Home-made bioreactor component diagram*

***Table 3**:home-made bioreactor components*

1	manometer
2	bioreactor chamber
3	pump
4	Becher
5,6,7,8,9	tubes
10,11,12,13,14	junctions

3.5.2 Set up of the high-performance bioreactor

***Figure 32**: Above we have bioreactor with given performances positioned in an incubator at 37 ° C; and below the parameter monitoring software*

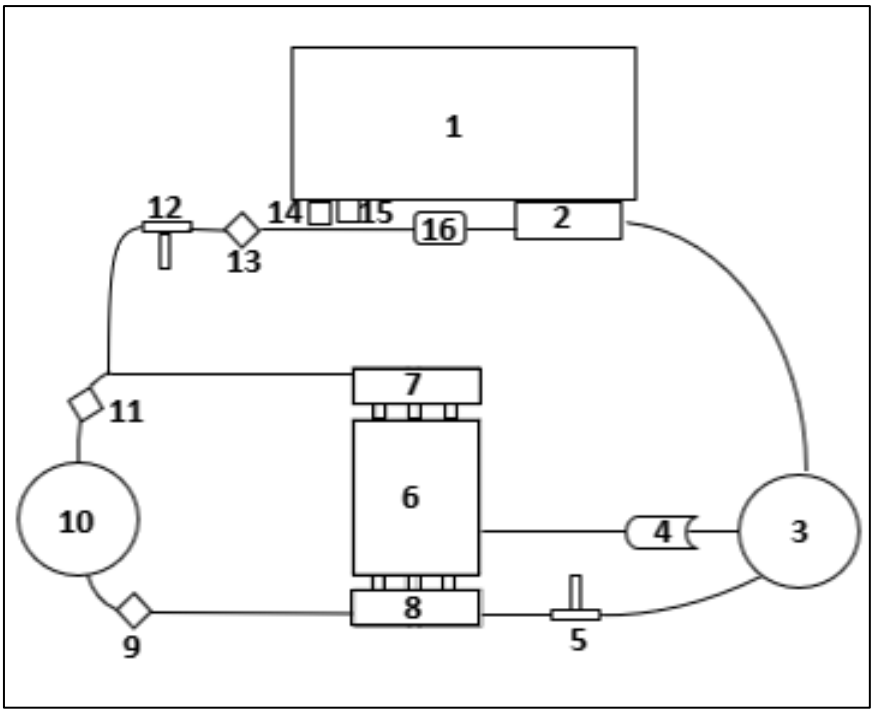

***Figure 33**: High performance bioreactor scheme with all components*

***Table 4**: High performance bioreactor components*

1	controls box
2	peristaltic pump
3	reservoir
4	flow meter
5	outer pressure & t-fitting (pressure 2)
6	vascular chamber
7	input manifold
8	output manifold
9	clamp: drops systolic pressure
10	compliance chamber
11	clamp: raises systolic pressure
12	inner pressure transducer (pressure 1)
13	clamp: raises both pressures
14	waveform generating pinch valve 1
15	waveform generating pinch valve 2
16	pulse dampener

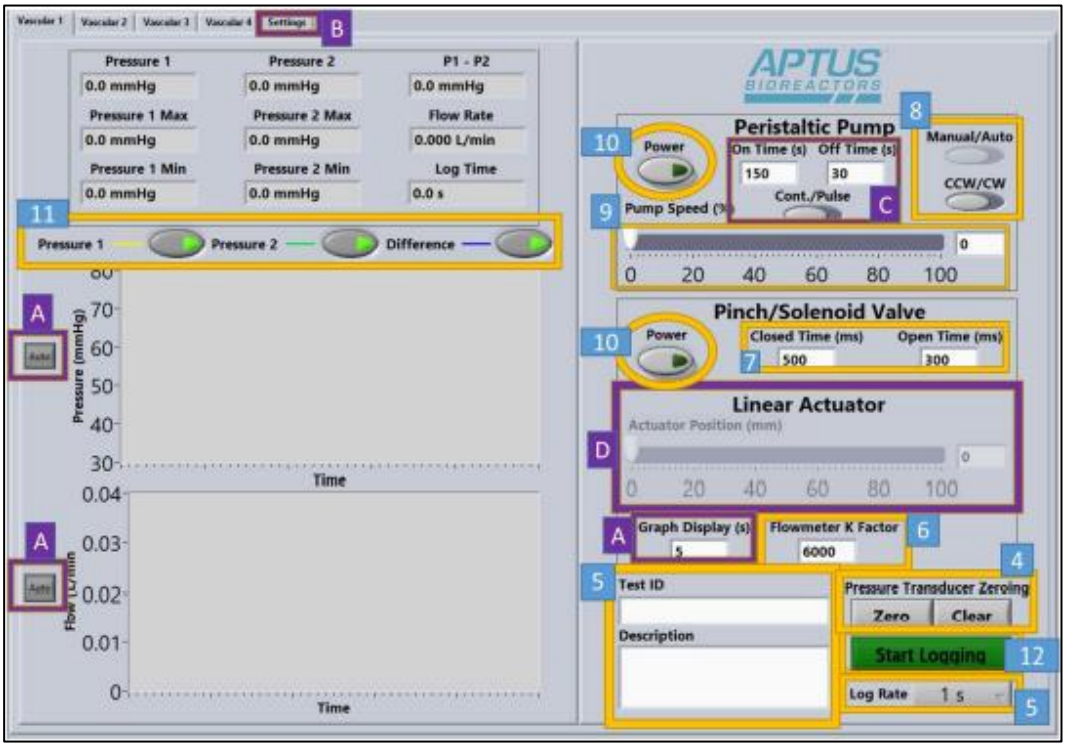

***Figure 34**: Software scheme*

***Table 5**: Software scheme*

A	auto scaling and graph display
B	advanced settings
C	continuous or pulse pinch valve settings-not available for some customers
D	linear actuator settings
4	zero pressure transducers
5	test id, description of run, and data logging rate
6	k factor
7	closed and open time
8	manual / automatic pump button
9	pump speed regulator
10	button for turning on the pump and the pinch valve
11	deactivation of certain graphically represented pressures
12	data register

Validation tests of the prostheses were then performed in a high-performance bioreactor (APTUS Bioreactors) (Figure 32). This apparatus basically consisted of some components like the previous one, but a more complex and sophisticated piping system was present. Three different vessels were installed: a compliance chamber, a pulse dampener, and a reservoir (Figure 33) (Table 4). The compliance chamber held a certain

volume of air, used to maintain back-pressure on the vessels. Increasing the volume of air, the release of pressure could be slowed down, and the diastolic pressure raised. Conversely, decreasing the volume of air, the release of pressure could be speeded up, and the diastolic pressure decreased. Regarding the dampener, it allowed to dampen the cyclical pulsations of fluid and pressure caused by the peristaltic pump functioning by containing a small volume of air. Finally, the reservoir was used to allow sterile gas exchange via a vented filter cap. As opposed to the previous home-made bioreactor, the chamber of the high-performance one allowed to process three prostheses at a time, considerably reducing the time required for the experiments. An inflow manifold and an outflow manifold distributed the flow across all three vessels.

The reactor was connected to a computer which, through a software developed *ad hoc*, allowed to observe online the trend of the systolic and diastolic pressures and the flow (Figure 34) (Table 5). Two pressure transducers, placed within the flow loop, permitted to measure the inflow and outflow pressures registered by each vessel of the main chamber. Pressures were regulated by three clamps, which allowed to drop or raise the systolic pressure, or raise both the pressures, respectively. A flowmeter measured the flow through the entire system: the turbine's rotations were measured by an infrared sensor, initially calibrated through a K-factor, equal to 4705). Furthermore, the simulation of the heartbeat was possible thanks to the activation of a pinch valve

3.5.3 Validation of the prostheses

The chamber and piping system were filled with a specified amount of Phosphate Buffered Saline (PBS) (Dulbecco, Euroclone) It is a buffer solution widely used in the biological field and consists of deionized water containing different salts:

- sodium chloride (nacl);
- potassium chloride (kcl);
- potassium dihydrogen phosphate (kh_2po_4);
- sodium hydrogen phosphate (na_2hpo_4).

PBS is therefore an isotonic solution that helps to keep the pH at a constant value of about 7.4.

The circulation of PBS in the bioreactor was operated thanks to both the pump action and the pressure effect.

All the devices were placed inside an incubator set at a temperature of 37°C, to simulate that of the human body.

The simulated pressures were 80 and 120 mmHg because they are the values of physiological pressure, and each test lasted five days.

Periodical samplings were carried out to successively perform release studies on the molecules of interest (gelatin and quercetin). In particular, the defined sampling times were: 30 minutes, 1 hour, 2 hours, 24 hours, 48 hours, 72 hours, 96 hours, and 120 hours.

Experimental validation tests were carried out at the following pressures:

- constant pressure of 80 mmHg
- constant pressure of 120 mmHg;
- alternated pressure of 80 and 120 mmHg.

During the experiments at alternated pressure, it was changed every twenty-four hours by adjusting the flow rate through a Hoffman clip and the pump.

3.5.3.1 Validation of prostheses in the home-made bioreactor

Tests with the home-made bioreactor were performed on the (2-mm) diameter gelatin-coated prostheses. Once the chamber was assembled, the reservoir was filled with PBS (60 mL) and sealed by wrapping the cap with Parafilm® to avoid PBS leakage (Figure

***Figure 35**: Prosthesis inserted in the home-made bioreactor chamber*

35). The pump was turned on, and the pressure was adjusted with the Hoffman clip to the desired one (80 mmHg or 120 mmHg). At each fixed time, 9 mL of PBS solution were collected, and new PBS was added in the same quantity. Once the test was completed, the liquid solution and the prostheses were collected for further analyses.

3.5.3.2 Validation of the prostheses in the high-performance bioreactor

***Figure 36**: Prosthesis inserted in the chamber of the high-performance bioreactor*

The high-performance reactor allowed to process three prostheses at the same time, making the analysis faster. Scaffolds of 5 mm-diameter were tested. They were inserted inside the chamber and connected to the overall system thanks to the use of specific adapters, whose sealing was guaranteed using O-rings (Figure 36) (Table 6). In this case the Volume of PBS is of 600 mL

***Table 6**: Different O-ring sizes*

Fitting size (mm)	Band size (-000)
1.5	-003
2.0	-003 or -004
2.5	-004
3.0	-004 or -005
3.5	-005 or -006
4.0	-006 or -007
4.5	-007
5.0	-007 or -008
5.5	-008
6.0	-009
6.5	-009

3.6 Release and quantification of gelatin

To study the trend of the gelatin release as a function of time, a colorimetric method, the bicinchoninic acid test (BCA), was performed in this assay, proteins react by reducing

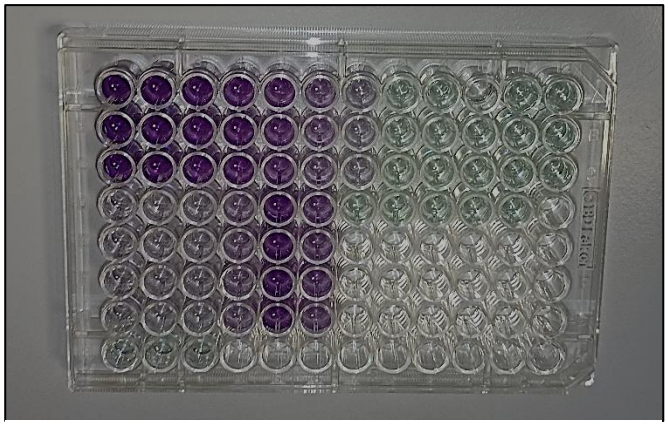

***Figure 37**: Microplate for the BCA colorimetric technique*

cupric ions Cu^{2+} (II) to cuprous ions Cu^{+} (I) in a basic environment (Figure 36); the latter reacts with bicinchoninic acid through chelation to form a purplish complex. The more the proteins are concentrated, the more the colour will go from green to purple. The complex absorbance can be measured at a wavelength of 562 nm. The kit required for this assay consists of two solutions A and B which should be mixed in a 50:1 ratio to obtain the so-called stock solution. Solution A contains Na_2CO_3, $NaHCO_3$, sodium tartrate and bicinchoninic acid, in a 0.1 M NaOH solution. Solution B is, instead, composed of a 4% solution of $CuSO_4$ copper sulphate (Euroclone BCA Protein Assay Kit, Euroclone S.p.A. Pero, Italy). The amount of each sample required for the analysis was 25 µ, whereas the working reagent required for each sample was 200 µL.

A standard solution was prepared to obtain a calibration curve, necessary for the calculation of the sample concentration. BSA (Bovine Serum Albumin) was chosen as standard protein. Starting from a stock solution in PBS, with a concentration of 1500 µg/mL, several dilutions were prepared in the range of 125-2000 µg/mL.

The analysis procedure was divided into several steps (Rogatsky, 2021):

1- 25 µL of sample (including the standards and the blank) were taken with a pipette and inserted into a well;
2- 200 µL of working solution were added to each well;
3- the plate was covered and inserted into the incubator at 37°C for 30 min;

4- the absorbance of each sample is read by a spectrophotometer (TECAN SPARK) at a wavelenght of 562 nm (Figure 38).

***Figure 38**: Spectrophotometer (TECAN SPARK)*

The spectrophotometer is an instrument able to measure the light intensity transmitted by a specific compound at various wavelengths. The system is made up of various components, schematized in the figure below (Figure 39).

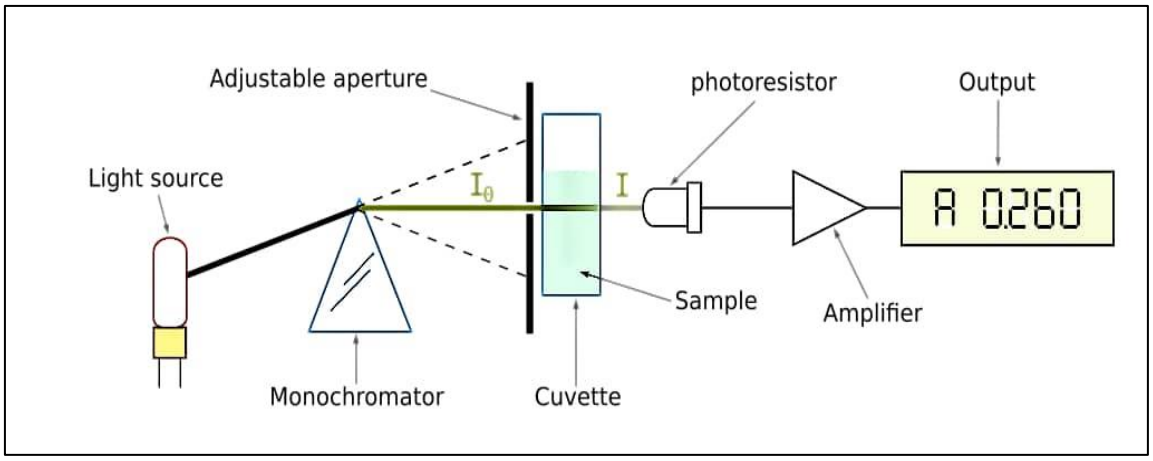

***Figure 39**: Spectrophotometer operation method (https://paramedicsworld.com/biochemistry-practicals/demonstration-of-spectrophotometer-principle-components-working-applications/medical-paramedical-studynotes*

A light beam, originating in a light source, is directed towards a monochromator at a predetermined wavelength, usually in the UV-Vis range. The beam is then directed into a cuvette, where the sample to be analysed is present. The initial light radiation (I0) is partially reflected, partially absorbed, and partially transmitted (I). The transmitted quantity is measured in a photosensor as a transmittance parameter. Once this value has been obtained, the spectrophotometer automatically calculates the absorbed light through the relationship:

$$A = -logT = -\log(\frac{I_0}{I}) \quad (1)$$

where:

A is the absorbance.

T is the transmittance;

I0 is the initial light intensity;

I is the intensity of the transmitted light.

Absorbance is also defined by the Lambert Beer's law, according to the following formula:

$$A = \varepsilon\, l\, c \quad (2)$$

where:

ε is the molar absorption coefficient ($M^{-1}cm^{-1}$);

c is the molar concentration of the sample (M);

l is the thickness of the solution contained in the cuvette and crossed by the light (cm).

The Lambert Beer's law has validity in the absorbance range between 0.1 and 1.

Data obtained at the spectrophotometer were subsequently exported to Excel, where they ware analyzed by performing the following calculations:

- The absorbance value of the blank was subtracted from the value of all the absorbances, including the standards;
- considering the validity of Lambert Beer's law, it was possible to determine the protein concentration of each unknown sample by means of the obtained calibration curve, showed in the figure below (Figure 40).

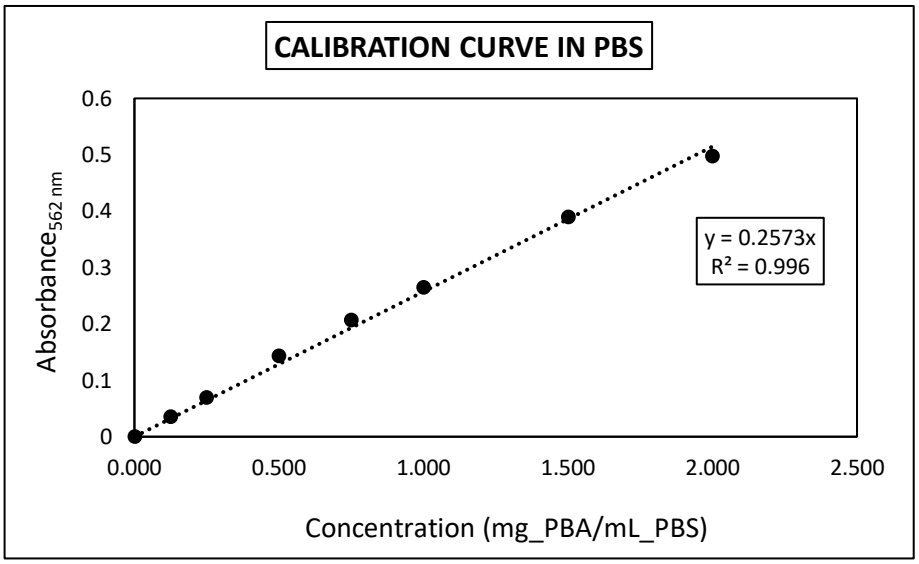

***Figure 40**: Calibration curve in PBS*

$$ABS(562\ nm) = 0.2573 \cdot C \qquad R^2 = 0.9984$$

where:

ABS_{562} is the absorbance at a wavelength of 562 nm;

C is the concentration of albumin in the solution, expressed in mg/mL.

3.7 Release and quantification of quercetin

The analysis of quercetin consisted in the absorbance lecture at the spectrophotometer previously described (TECAN SPARK), set to a specific wavelength. However, as a first step, a qualitative analysis was carried out to visualize the absorption spectrum of quercetin, expressed as the absorbance change in a function of the wavelength, in the range of 200-1000 nm.

As shown in the graph, quercetin had an absorption peak around 368-370 nm, considering that the initial trend was due to the plastic of the plate used to read the sample. In this way, the wavelength with the maximum absorbance of quercetin, 368 nm, was selected. A quantitative analysis of the samples was then carried out through the spectrophotometer and according to the Lambert-Beer law.

Since the collected samples contained a minimal amount of quercetin, not detectable at the spectrophotometer, an initial concentration step was performed using a freeze dryer.

This apparatus allows the reduction/elimination of a solvent by sublimation. It's composed by three sectors (Figure 41):

- a chamber capable of withstanding high depression values;
- a vacuum pump;
- a refrigerant system.

***Figure 41**: Freeze dryer*

The obtained lyophilized samples were then resuspended in 250 µL of ethanol, by applying a concentration factor equal to 15 to maximize quercetin solubility.

Furthermore, the concentrated samples were centrifuged at 4°C, 12000 rpm for 10 minutes, to separate the quercetin-enriched solution from the PBS salts (NaCl, KH_2PO_4, and Na_2HPO_4), whose solubility in ethanol was negligible.

At this point, 100 µL of each sample, including the blank samples and the standard solutions, were loaded into each well of a microplate for the reading at the spectrophotometer, at the wavelength of 368 nm.

Standard solutions of quercetin were prepared in known dilutions, in the range of 200 µg/mL and 2 µg/mL, to obtain a calibration curve, necessary for calculation (Figure 42).

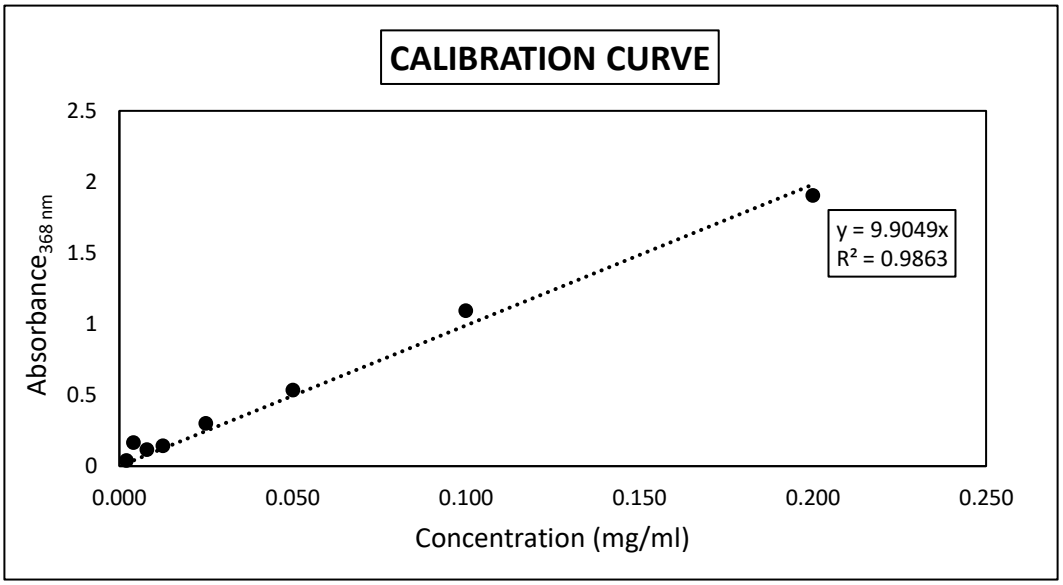

***Figure 42**: Calibration Curve*

$$ABS(368\,nm) = 9{,}9049 \cdot C \qquad R^2 = 0.9923$$

where:

$ABS_{368\,nm}$ is the absorbance at a wavelength of 368 nm;

x is the concentration of quercetin in the solution, expressed in mg / ml

Moreover, from the spectrophotometer we have also obtained the spectrum of quercetin (Figure 43).

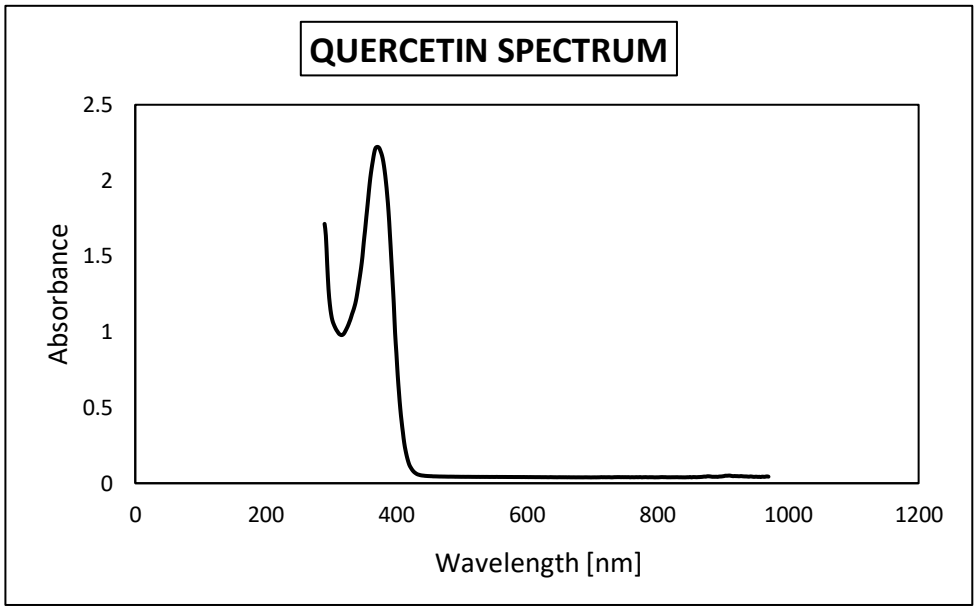

***Figure 43**: Quercetin Spectrum*

3.8 Scanning electron microscopy

Scanning electron microscopy (SEM) is a technique that uses an electron beam. Unlike the optical microscope, the SEM it was used did not use light as a source of radiation, but rather analyzes the interaction between a beam of focused primary electrons and the atoms that the sample under examination produce. Through the SEM, it is possible to analyze different types of samples, of different nature, shape, and size. The fundamental constraint is that the samples should be conductive or metallized, to avoid the production of electrostatic charges that could damage and therefore prevent detection.

The equipment used allows to generate images with very high enlargements, sometimes with a resolution at the atomic level, overcoming the limits of optical microscopy. The apparatus can be classified according to the type of source, which can be thermionic or field emission.

In the first case, the beam is generated by an electronic source, typically a tungsten filament, which emits a flow of primary electrons concentrated by a series of electromagnetic lenses and deflected by an objective lens. The latter, in addition to further refocusing the beam, imposes a controlled deflection, to allow the scanning of areas of the sample. When the beam hits the sample, secondary electrons are produced and collected by a detector; depending on where the beam hits, a different number of

secondary electrons are produced (for example, more if the surface is curved, less if it is flat) (Abedzadeh et al., 2021).

In the case of a field emission source, the operation with the various lenses is similar, but the electron beam is emitted by an electric field, and the resolution can be much better (Figure 44).

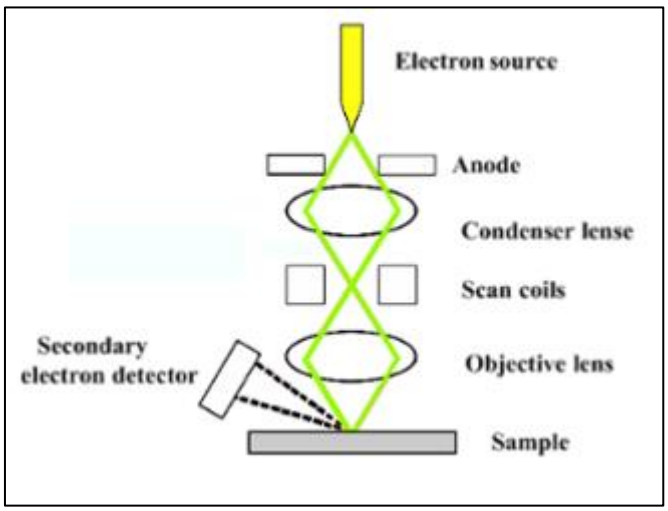

***Figure 44**: schematic representation of base compounds of SEM*

To work properly, the SEM needs a high vacuum (at least $5x10^{-4}$ mbar) since the electrons generated and accelerated would otherwise hit the gas molecules and disperse instead of arriving on the sample. Furthermore, the "mean free path" is the average distance traveled by a particle before it encounters another, it is about 1 mm per electron.

The SEM returns a virtual image starting from the signals emanating from the sample. These vary in intensity, point by point, according to the morphological, chemical, and structural anisotropies of the sample and are collected, converted into digital, processed and displayed on a cathode ray tube screen (Stopka et al., 2021).

In our experimentation, the morphology of the scaffolds has been studied using a scanning electron microscope with a very high-resolution field emission source (SEM, Zeiss CrossBeam XB 1540) at an acceleration voltage in the range 100 V-30 kV, obtaining images at different magnifications (500x, 1000x). Furthermore, the dimensional analysis of the fibers starting from the images produced by the SEM (Figure 40) was carried out using the ImageJ software (Figure 45).

***Figure 45**:Scanning Electron Microscope*

3.9 Degradation and fluid uptake

After their processing in the bioreactor, the scaffolds degradation was determined. The percentage of mass loss by the sample during in the tests in the bioreactor can be expressed by the following equation (Equation 1):

$$Degradation\ \% = \frac{m_0 - m_f}{m_0} * 100 \quad (1)$$

where:

m_0 is the mass of the gelatinized prosthesis before the bioreactor test.

m_f is the mass of the dried prosthesis after the bioreactor test.

It's important to consider the fact that this equation can give very high degradation values, between 20-30%. In fact, it considers all the mass loss by the prosthesis, including that relating to the released gelatin. The formula was, therefore, modified considering the mass loss by the polymer.

The so-called "fluid uptake" was then evaluated: it expresses the ability of the sample to absorb liquids. This value was expressed as the percentage change of the scaffold mass (Equation 2):

$$Fluid\ uptake\ \% = \frac{m_{fw} - m_{fd}}{m_{fd}} * 100$$

(2)

where:

m_{fw} is the final mass of the wet prosthesis;

m_{fd} is the final mass of the dry prosthesis.

The absorption of liquids is an important aspect, both for macroscopic and microscopic reasons. In the first case, it is essential to check that the prosthesis has a high, but not excessive absorption, to guarantee its function. Regarding the microscopic scale, it is useful to analyze the material from the point of view of porosity, that should be sufficiently high. In this way, the biocompatible polymer can be colonized by cells, which necessitate of a continuous exchange with the extracellular environment.

The values obtained are adequate. The fact that they are greater than 100% indicates a high-water absorption, mainly since the PGS used in the realization of the prostheses is a highly hydrophilic polymer.

3.10 Mechanical analysis

In order to characterize the mechanical properties of the prostheses, vertical elongation tests were carried out in the uniaxial direction, until the prosthesis breakage. The Zwick Roell BL-GRS010K 10kN apparatus was used for this purpose (Figure 46).

***Figure 46**: Zwick Roell BL-GRS010K 10kN*

Firstly, the external diameters of the constructs under examination were measured with the use of a caliper, making multiple measurements along the scaffold, and, subsequently, averaging them. The external thickness was then calculated, knowing that the internal diameter was (2mm or5mm) (Equation 1).

$$Thickness = \frac{outer\ diameter - internal\ diameter}{2} \quad (1)$$

Subsequently, the prostheses were cut both longitudinally and transversely, obtaining four minor parts from each one.

Their width was then calculated (Equation 2):

$$Length = [(internal\ diameter + thickness) * \Pi : 2] \quad (2)$$

Before inserting the scaffolds into the apparatus, they were immersed in deionized water, to simulate the surgical practice.

To lengthen the samples, the following data were set in the software:

• uniaxial velocity = 20 mm / min

• preload = 0.1 N

4. RESULTS AND DISCUSSION

4.1 Morphology

Regarding the analysis of the morphology of the electrospun scaffolds after the experimentation in bioreactors, an appropriate software was used, ImageJ. Through this software it was possible to analyze the images obtained by SEM and calculate the internal diameter of the fibers of the constructs.

For each sample, the internal and external surfaces were visualized, using two different magnifications (500 x and 100 x) for each type of sample. For each image, 70 to 100 measurements of the various fibers were then carried out, and the average value was finally calculated, which was equal to:

***Table 7**: Internal diameter of fibres*

PRESSURE	Internal diameter fibers (mm)
80 mmHg	4.589 ± 0.53
80-120 mmHg	4.572 ± 0.91
120 mmHg	4.524 ± 0.15
control	3.46 ± 0.48

The addition of gelatin and quercetin did not alter either the arrangement or the size of the fibers that make up the sample comparable to PCL:PGS (1:1). The most important difference in terms of morphology was about porosity that was drastically reduced in the gelatin-coated scaffolds. The fibers shown are randomly distributed.

The images obtained by SEM are shown below (Figure 47, 48).

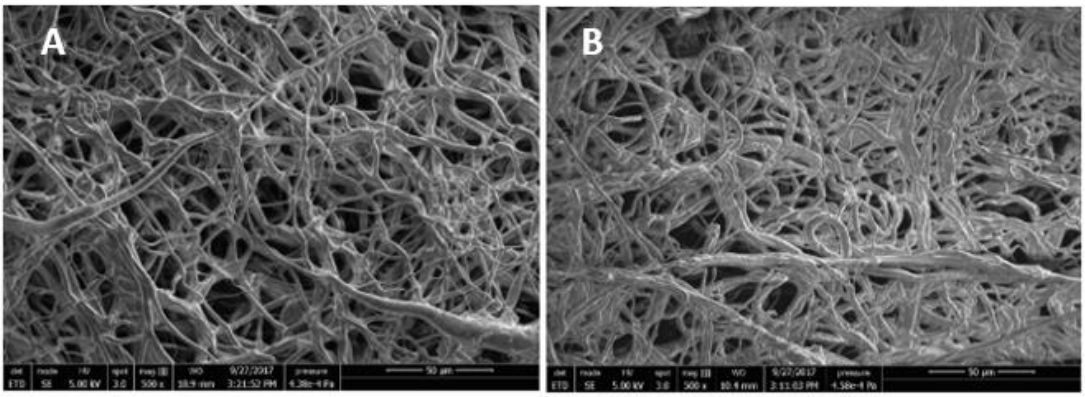

***Figure 47**: (A) Internal surface of the control sample (PCL: PGS), (B) External surface of the control sample (PCL: PGS)*

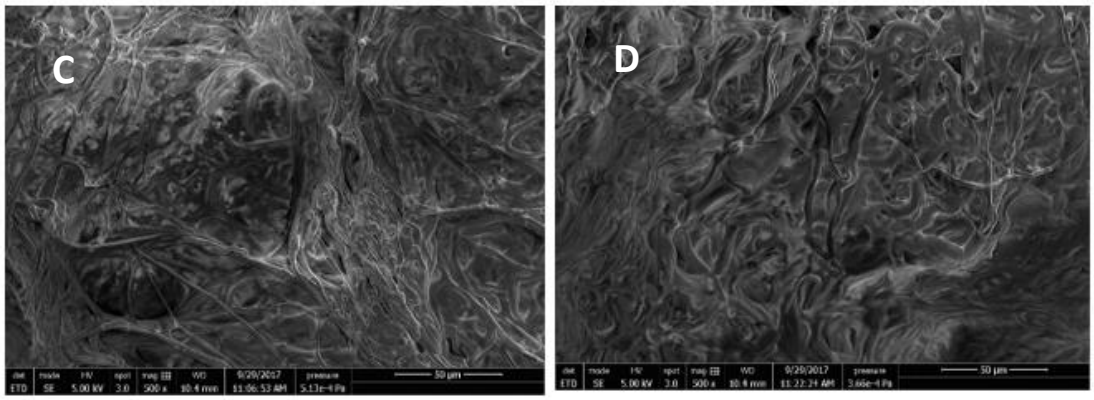

***Figure 48**: (C) Internal surface (PCL: PGS + gelatin + quercetin), (D) External surface (PCL: PGS + gelatin + quercetin)*

As far as the thickness of the electrospun constructs is concerned, it was measured using a caliber and is found to be between 0.23 and 0.44 mm in the scaffold of 2 mm and 0.075 and 0.125 for scaffold of 5 mm of diameter.

As described by Ghasemi-Mobarakeh et al. (2009) the thickness of the PCL samples influences cell proliferation by being a better substrate on which cells can adhere.

The sample containing PCL:PGS (1:1) has an intermediate thickness (0.46 ± 0.11mm) and this makes it a good substrate for cell proliferation.

4.2 Degradation and fluid uptake

The study of degradation is fundamental as this affects not only cell adhesion and proliferation, but also the structure of the new tissue being regenerated. The degradation of the biomaterial used in engineering tissue should not be too fast, otherwise it would not fulfill its task of scaffolding and would not allow the regeneration of the new tissue. The degradation of scaffolds was studied in the two different reactors used. The values have been calculated, shown in the tables below, and have been calculated as a percentage (Table 8).

The fluid uptake on biomaterials which needed to be sutured with organs has been studied because it can influence different characteristics of the grafts. For example, it can lead to an increase of the volume. This process, known as swelling, consist of the absorption of the liquid and is a parameter that can modify mechanical properties of the prosthesis, its biological response and, eventually, the drug release behavior.

***Table 8**: Degradation and fluid uptake values for each prosthesis processed in the home-made bioreactor*

Pressure	Degradation %	Fluid uptake %
80 mmHg	28.75 ± 3.18	285.45 ± 12.98
120 mmHg	29.13 ± 4.41	279.58 ± 39.85
80-120 mmHg	40.62 ± 26.11	228.68 ± 3.05

In the case of the home-made reactor, as shown in the table 5, as the pressure impressed by the peristaltic pump increases, there is a corresponding increase in the stress on the walls of the scaffold. Consequently, the mechanical stress to which the prosthesis has been subjected turns out to be greater. This could justify a greater degradation in the sample when subjected to a pressure of 120 mmHg. The high pressure exerted on the walls of the scaffold may be at the basis of the breakdown of the microscopic structure of the prosthesis tested. In the case of pulsed pressure, the degradation seems to be even greater. This could be because a variation in conditions, even if minimal, causes a greater stress on the material from which the prostheses are made (Table 9).

***Table 9**: Degradation and fluid uptake values for each prosthesis processed in the high-performance bioreactor*

Prosthesis	Degradation %	Fluid uptake %
PCL:PGS	35.00 ± 3.70	164.40 ± 41.97
PCL:PGA and quercetin	32.51 ± 2.53	274.19 ± 27.61

Table 6 shows the data relating to the high-performance bioreactor. In general, considering the percentage of degradation, the values do not seem to be very distant for the two bioreactors. Values are however higher in the case of the high-performance reactor. This could be essentially since, having a greater flow, the prostheses will necessarily be subjected to a greater effort, as will be seen in paragraph 4.5.1

4.3 Mechanical characterization

The following Table (Table 10,11) shows Young's modules, tensile strength, and the stretching percentage of the samples subjected to pressure of 80, 120 and 80-120 mmHg in home-made bioreactor, using a human artery as a control. Considering the mechanical properties possessed by the studied prostheses, as those of the human artery, we can conclude that this construct is promising for future *in vivo* experimentation.

***Table 10**: Some parameters measured in 2mm scaffolds*

	Medium outside diameter(mm)	Thickness(mm)	Length(mm)
80 mmHg	2.88	0.44	3.830
80-120 mmHg	2.88 ± 0.06	0.4425 ± 0.03	3.83 ± 0.05
120 mmHg	2.58 ± 0.1	0.292 ± 0.05	3.583 ± 0.07

***Table 11**: Mechanical properties in 2 mm diameter scaffolds*

Sample	Young's modules (MPa)	Tensile strength (MPa)	Strain (%)	A_0 (mm^2)	Tensile strength (N)
80 mmHg	2.11 ± 1.60	1.01 ± 0.29	87.55 ± 28.52	1.69	1.70 ± 0.49
80-120 mmHg	2.86 ± 1.30	1.36 ± 0.39	154.88 ± 50.70	1.70	2.29 ± 0.47
120 mmHg	4.02 ± 0.32	1.22 ± 0.29	89.44 ± 16.52	1.06	1.24 ± 0.08
Human artery	2.58 ± 0.34	1.13 ± 0.06	46.54 ± 11.31	-	-

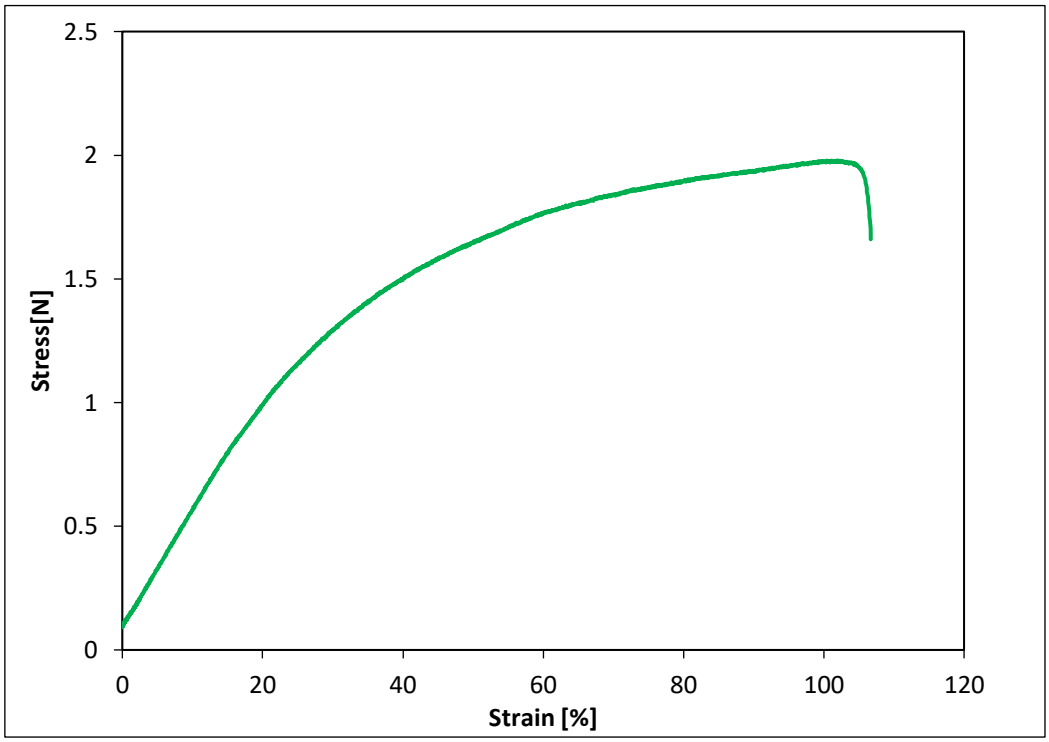

***Figure 49**: Stress- strain graph at 80 -120 mmHg*

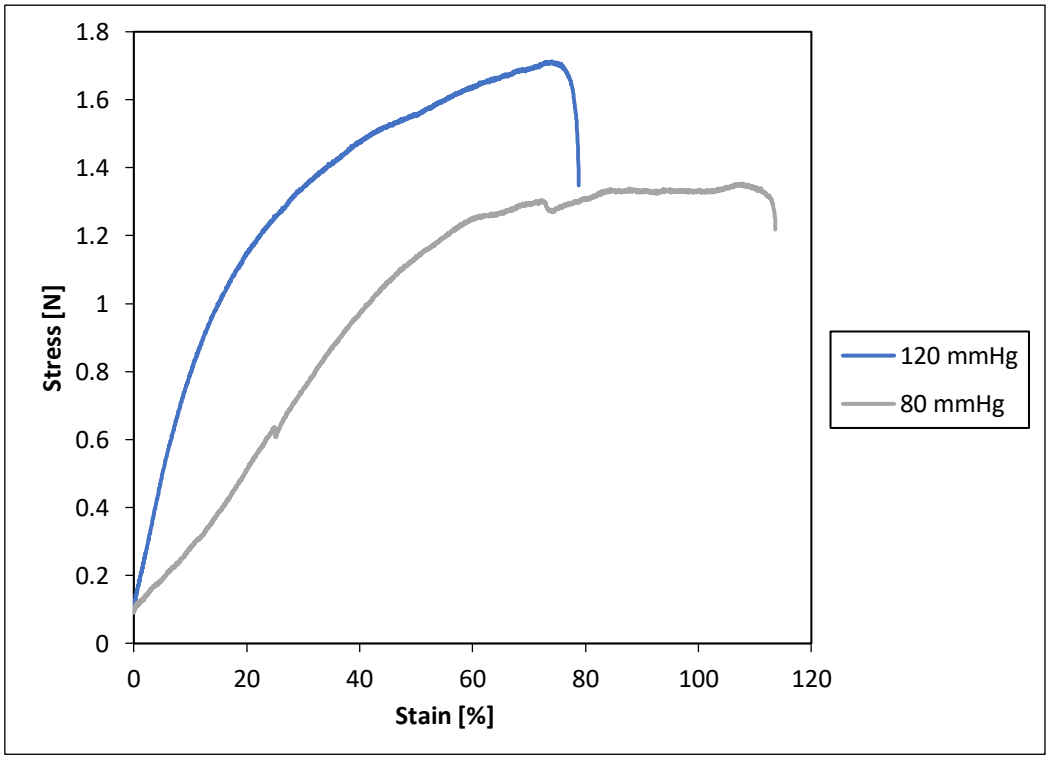

***Figure 50**:Stress-strain graph at 80 mmHg and 120 mmHg*

Sample	Young's modules (MPa)	Tensile strength (MPa)	Strain (%)	A_0 (mm^2)	Tensile strength (N)
80-120 mmHg	6.58 ± 3.13	2.11 ± 1.24	50.54 ± 23.26	1.18	1.86 ± 0.64
Human artery	258 ± 0.34	1.13 ± 0.06	46.54 ± 11.31	-	-

***Table 12**: Some parameters measured in 5mm scaffolds without quercetin and control*

	Medium outside diameter(mm)	Thickness(mm)	Length(mm)
80-120 mmHg	5.29 ± 0.2	0.145 ± 0.1	8.077 ± 0.16

***Table 13**: Some parameters measured in 5mm scaffolds with quercetin and control*

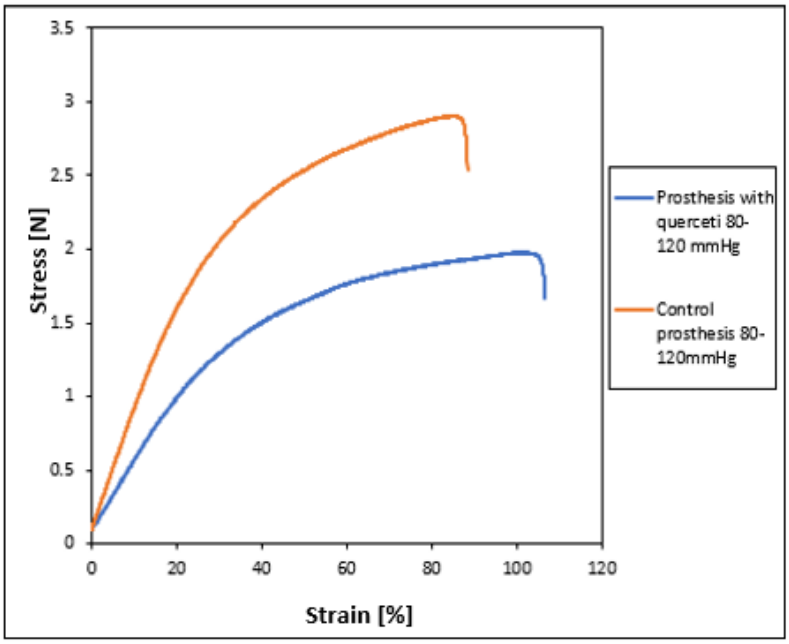

***Figure 51**:Standard force trend and deformation at pressure of 80-120 mmHg*

4.4 Release of gelatin and quercetin from the prosthesis

4.4.1 Release of gelatin

The release of gelatin from the prostheses has been calculated at the three different pressure conditions. The graphs of the releases were made in two ways: by expressing the cumulative release rate of the biomolecule considered on the ordinate axis, or by showing the cumulative mass expressed in mg. Both parameters were plotted as a function of time on the abscissa.

Figure 52 and figure 53 show the trend of gelatin release in the home-made reactor, compared to the two fixed pressure cases studied.

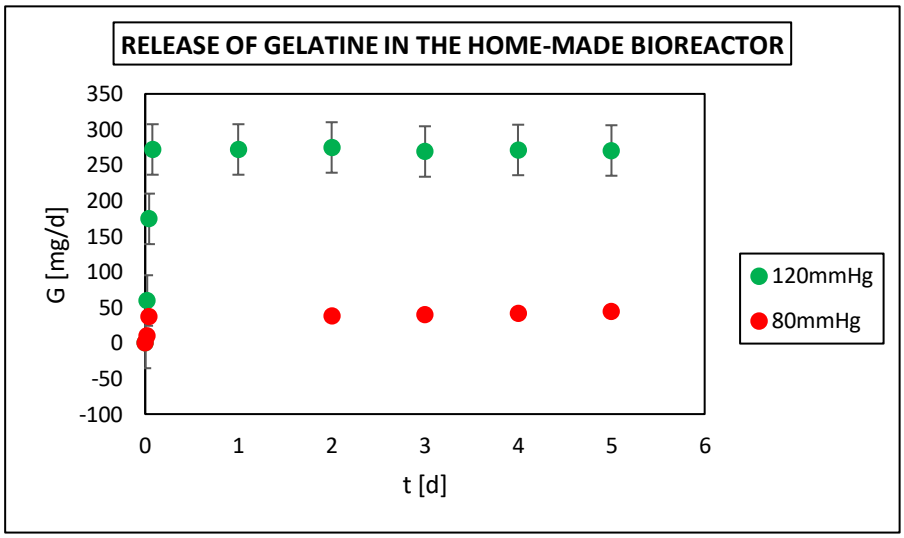

***Figure 52**: Cumulative gelatin release rate as a function of time with fixed pressure*

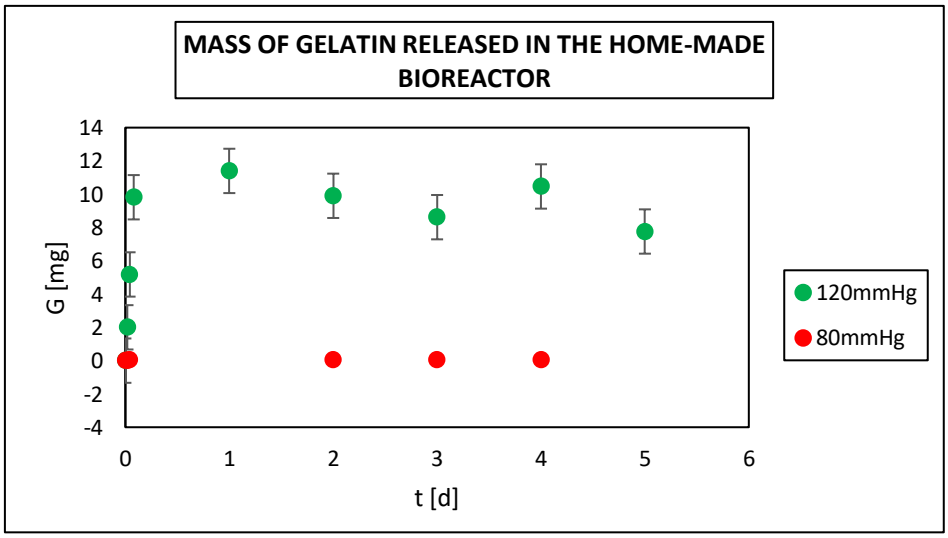

***Figure 53**: Mass of gelatin released as a function of time with fixed pressure*

As can be seen from the graphs, higher pressures lead to a greater release of material. In the case of the prosthesis subjected to 80 mmHg, the gelatin is released into constant manner until the fifth day. For prostheses maintained at 120 mmHg the gelatin released in the first hours varies drastically depending on the pressure exerted. In fact, gelatin is largely released during the first samplings, reaching the maximum value after the first day. Subsequently the trend become slightly fluctuating and would probably stabilize after "n" days of experimentation. This is because gelatin is highly soluble in water and that it consists of the outermost material layer of the scaffold, which is then removed immediately.

Regarding the 80-120 mmHg pulsed pressure, the variation was performed in the following way: the test was started at a pressure of 120 mmHg. After the 24h sampling, the pressure was changed manually and set to the value of 80 mmHg. This process was performed every day.

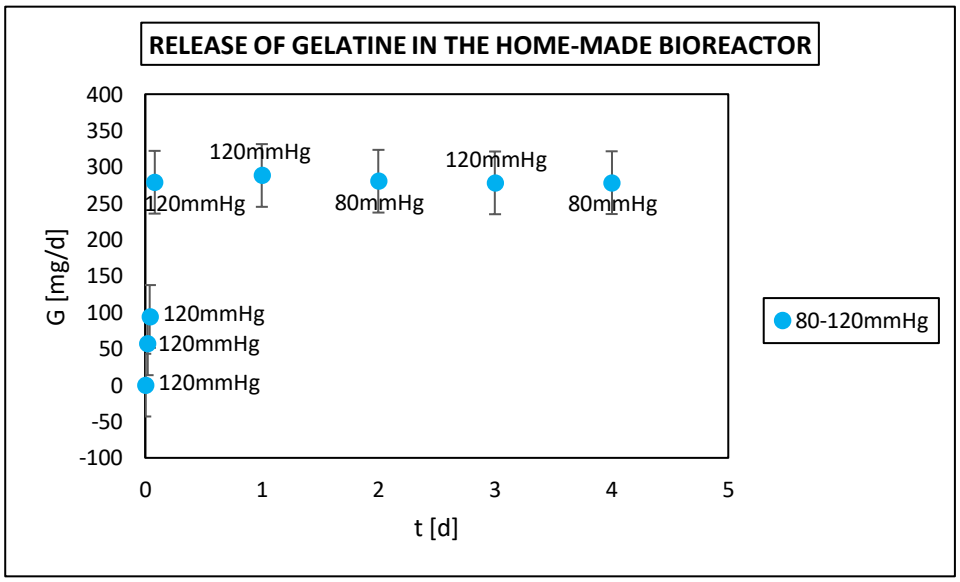

***Figure 54**: Cumulative gelatin release rate as a function of time with pulsed pressure*

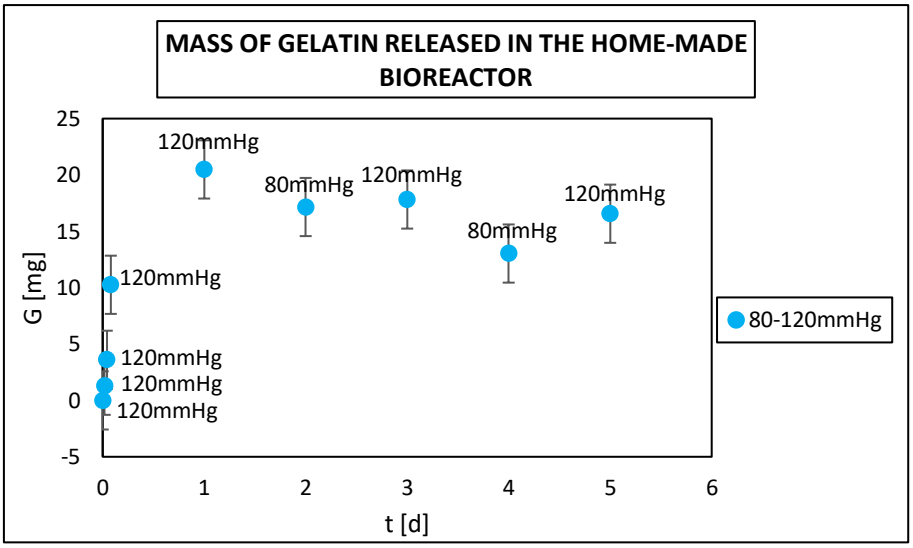

***Figure 55**: Mass of gelatin released as a function of time with pulsed pressure*

Figure 54 and figure 55 show that also for prostheses maintained at 80-120 mmHg the gelatin released in the first hours varies drastically. After a day the pulsed pressure release appears almost constant, contrary to what one would expect. This could be because the flow value is almost constant. In reality it can be seen that the releases decrease for low pressure values, even if slightly, while they increase for high pressure values.

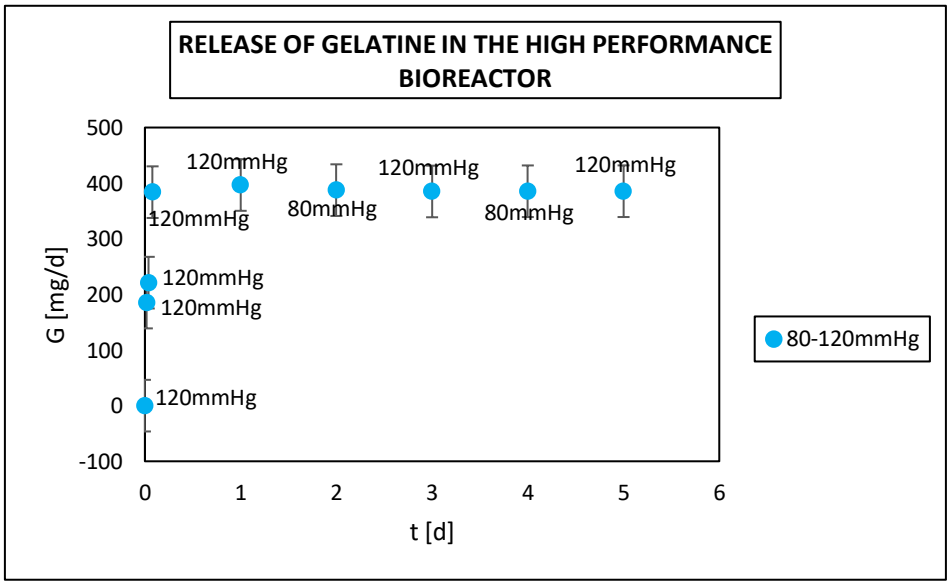

***Figure 56**: Cumulative release of gelatin in the high-performance bioreactor*

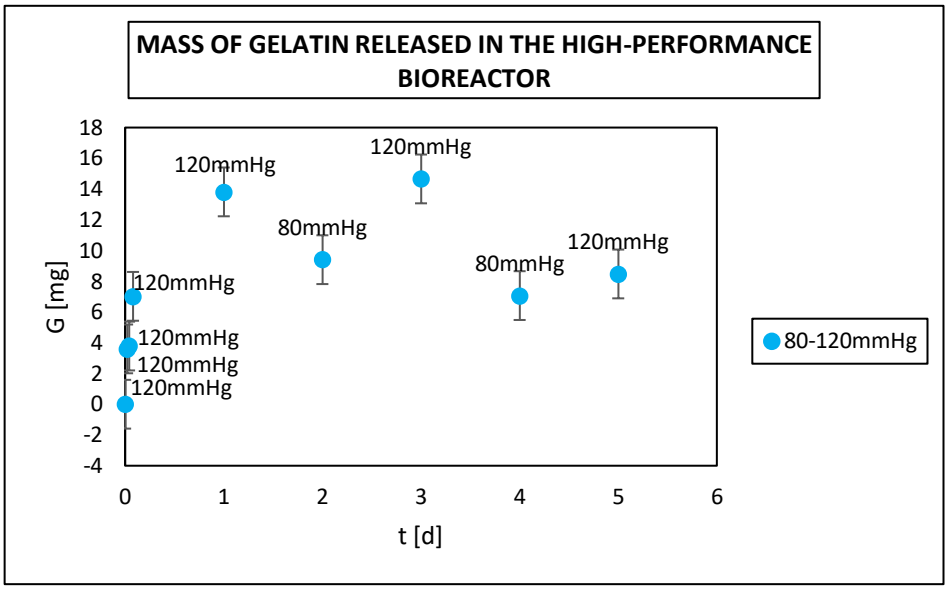

***Figure 57**: Mass of gelatin released as a function of time in the high-performance bioreactor*

In the case of the high-performance reactor, we only carried out the pulsed pressure test. The general trend of gelatin release does not differ from that seen for the home-made reactor. Also in this case, after 24h the cumulative release rate seems to be about constant. In general, the fact that substances are taken away from the prosthesis depends on the value of the stress on the wall, which is a function of the load capacity of the scaffolds. For the high-performance bioreactor the value of the flow at the two pressures deviates only to the third decimal number.

Viewing the graph of the derivative in function of the time allows to evaluate the slope of the release curve and then make a forecast of the possible behaviour of the trend over time, even after five days of experimentation.

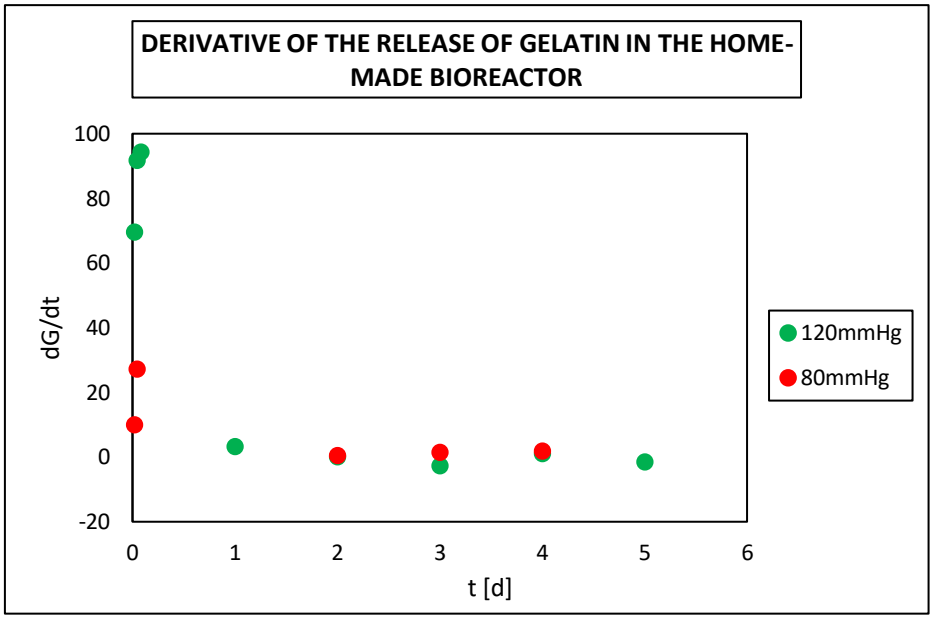

***Figure 58**: Derivative of the cumulative release of gelatin as a function of time in the home-made bioreactor with fixed pressure*

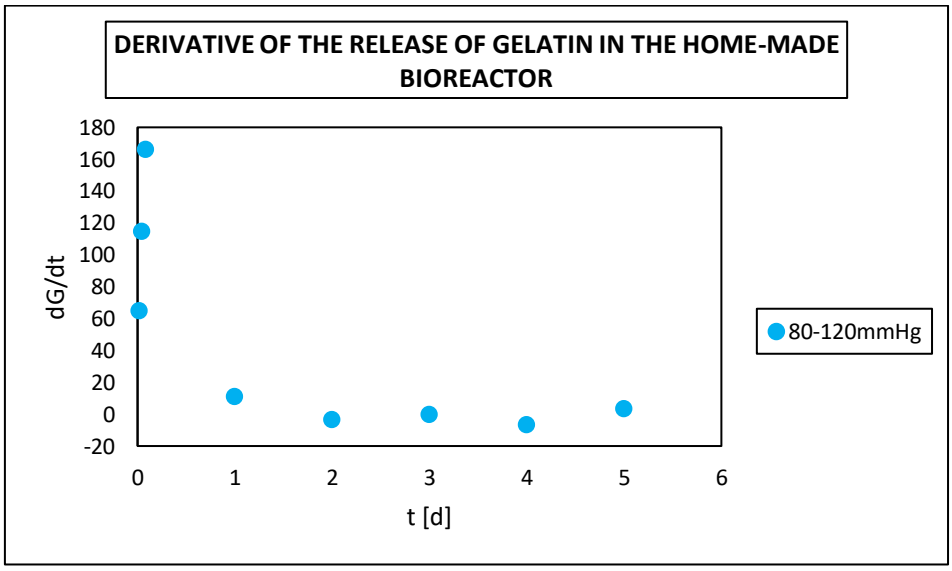

***Figure 59**: Derivative of the cumulative release of gelatin as a function of time in the home-made bioreactor with pulsed pressure*

From figure 58 can be seen that, with a constant pressure of 80 mmHg, the derivative becomes zero after 48h. In the case of fixed pressure at 120 mmHg (figure 58) or pulsed 80-120 mmHg (figure 59) the derivative, on the other hand, decreases already after the first day of experimentation. The same happens in the high-performance bioreactor (figure 60).

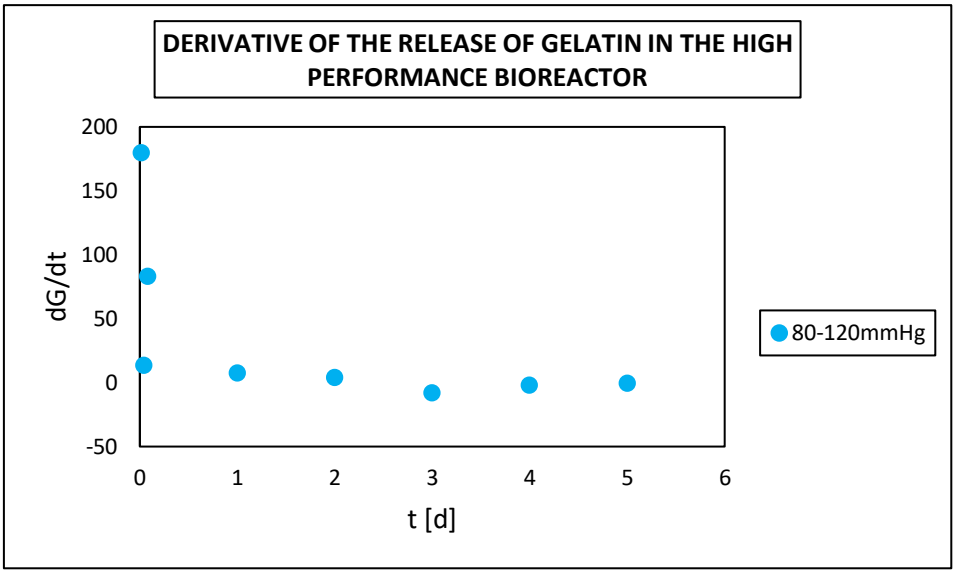

***Figure 60**: Derivative of the release of gelatin as a function of time in the high-performance bioreactor*

4.4.2 Release of quercetin

The same graphs were made for the release of quercetin. While in the case of gelatin an external coating was made on the prosthesis, quercetin is a component of the material used during the electrospinning process. Moreover, quercetin is not very soluble in water, unlike gelatin. Confirming this, quercetin values released are extremely low. On the other hand, the temporal trend appears to be similar to that shown for gelatin. The release of quercetin is more sustained during the first hours, and then stabilizes over the first 2 days in all three cases studied. Quercetin released in the early hours varies drastically depending on the pressure exerted.

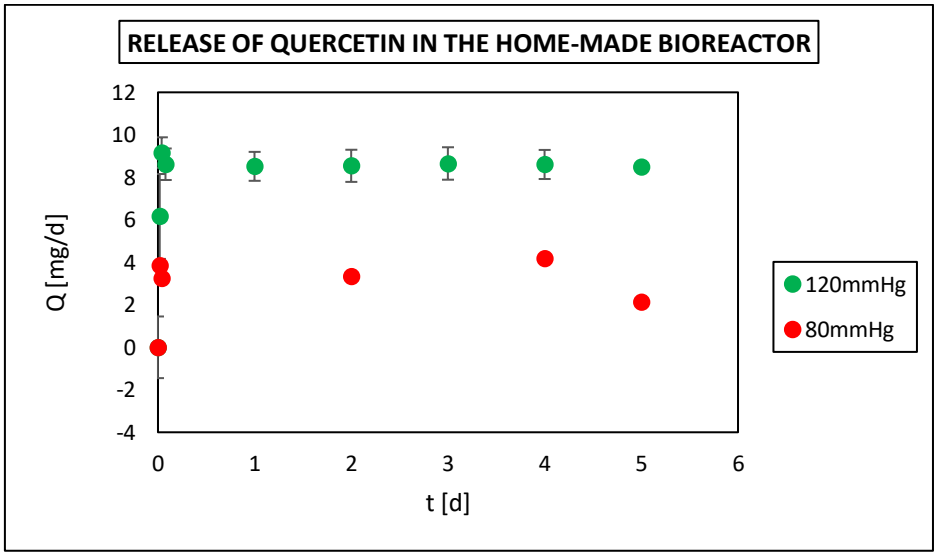

***Figure 61**: Cumulative quercetin release rate as a function of time with fixed pressure*

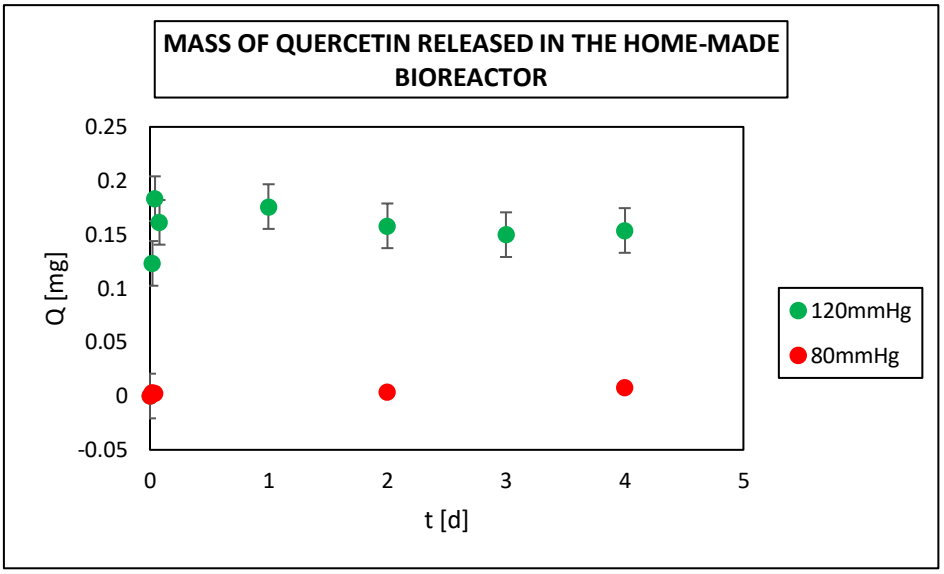

***Figure 62**: Mass of quercetin released as a function of time with fixed pressure*

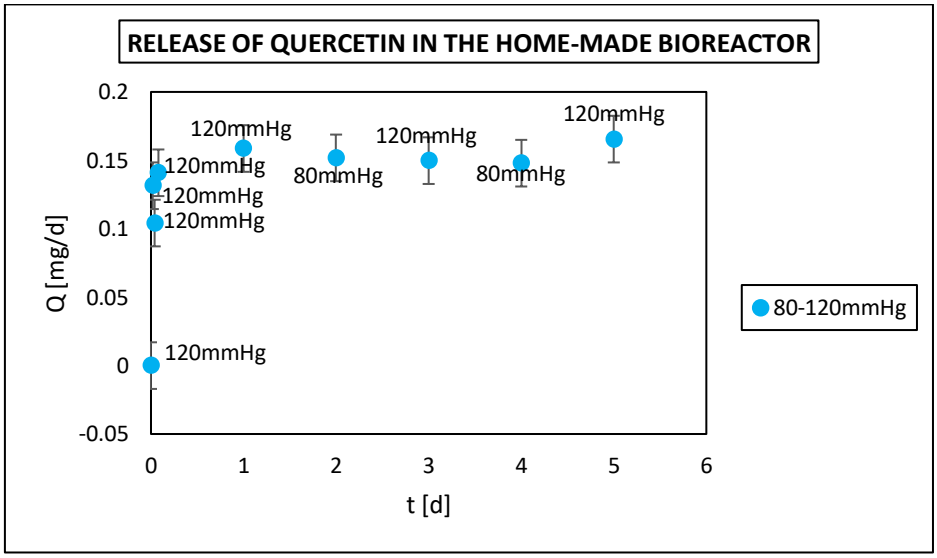

***Figure 63**: Cumulative quercetin release rate as a function of time with pulsed pressure*

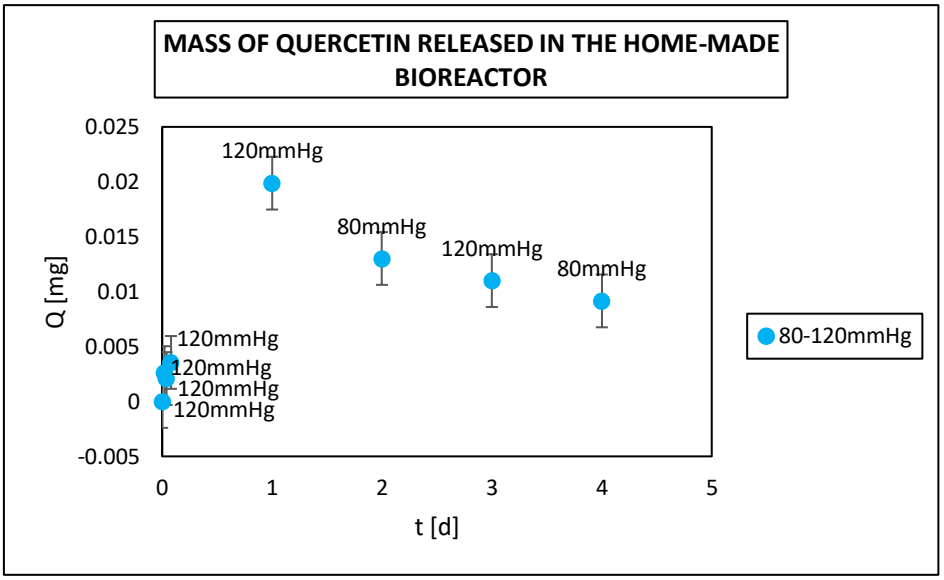

***Figure 64**: Mass of quercetin released as a function of time with pulsed pressure*

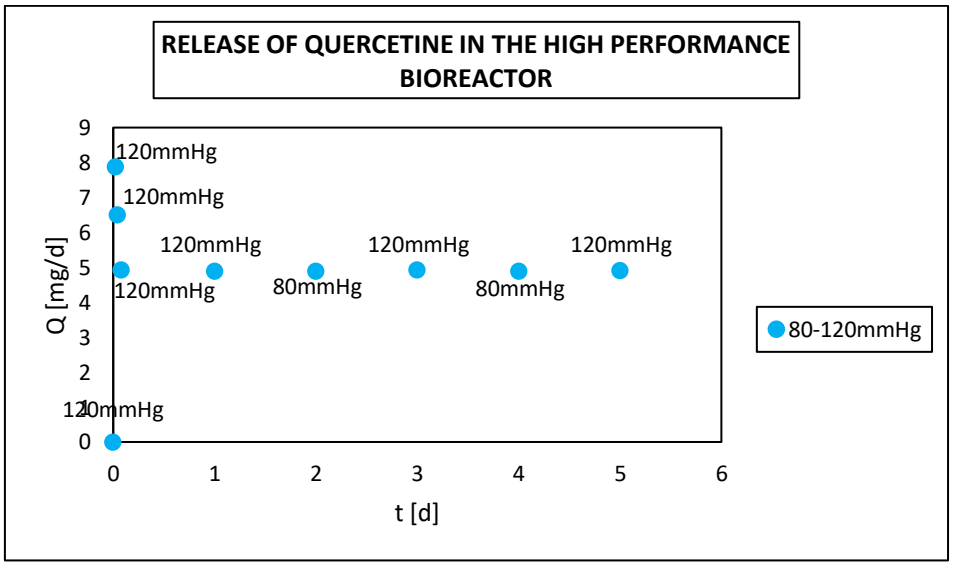

***Figure 65**: Cumulative release of quercetin as a function of time in the high-performance bioreactor*

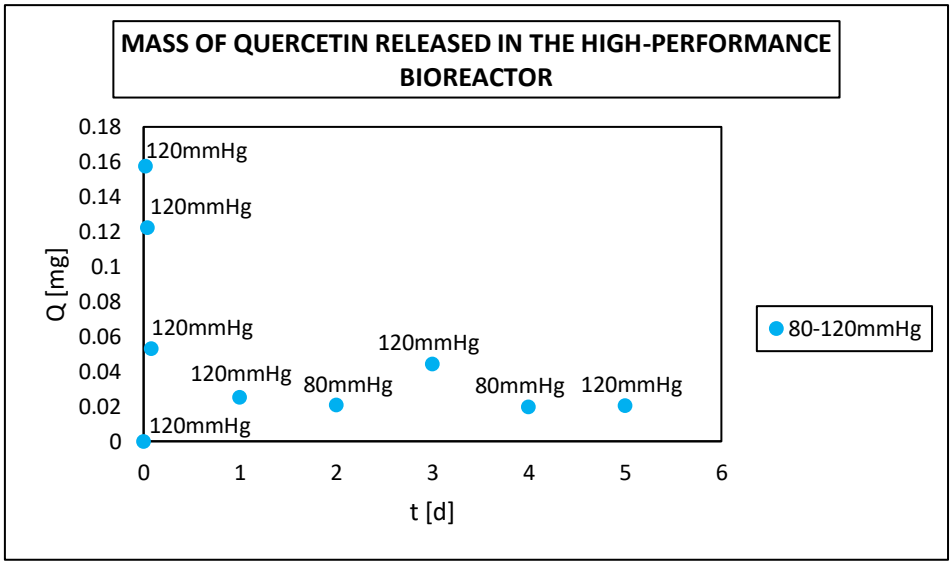

***Figure 66**: Mass of quercetin released in the high-performance bioreactor*

Viewing the graph of the derivative in function of the time allows to evaluate the slope of the release curve and then make a forecast of the possible behaviour of the trend over time, even after five days of experimentation.

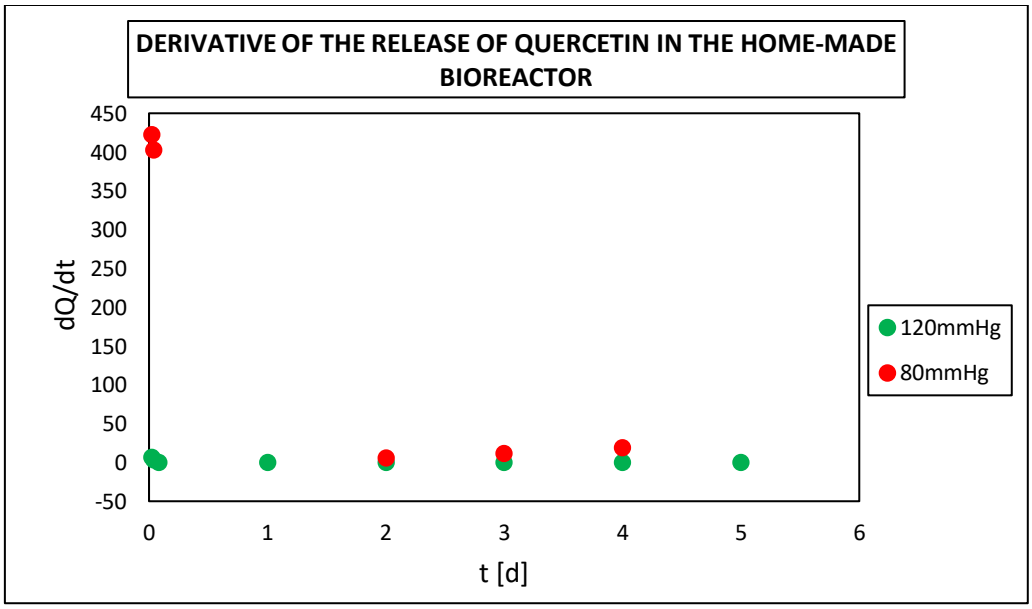

***Figure 67**: Derivative of the cumulative release of quercetin as a function of time in the home-made bioreactor with fixed pressure*

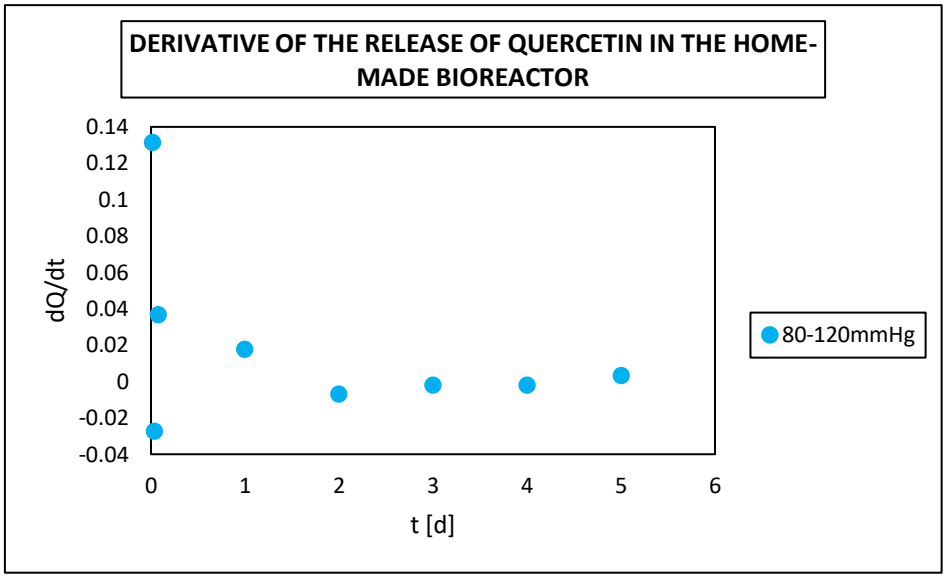

***Figure 68**: Derivative of the cumulative release of quercetin as a function of time in the home-made bioreactor with pulsed pressure*

From figure 67 can be seen that, with a constant pressure of 80 mmHg, the derivative becomes zero after 48h, as in the case of pulsed pressure 80-120mmHg (figure 68). In the case of fixed pressure at 120 mmHg (figure 67) the derivative, on the other hand, decreases already after the first day of experimentation. The same happens in the high-performance bioreactor (figure 69).

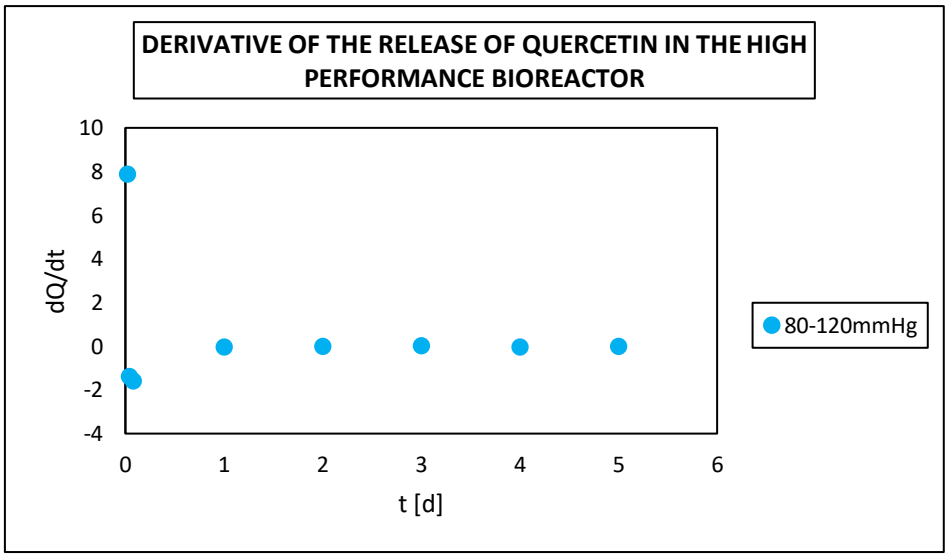

***Figure 69**: Derivative of the release of quercetin as a function of time in the high-performance bioreactor*

4.5 Fluid dynamic properties

4.5.1 Steady state

Approximating our scaffolds to tubes of constant circular section and radius R, for the stationary case we have considered a laminar, axial symmetric and stationary flux of a fluid through the tube itself.

At each preset pressure, it was obtained a constant flow, a situation described as stationary case. The goal is to calculate the mechanical stress made by the fluid on the prosthesis wall, and then observe its trend with pressure (Equation 1).

$$\tau_w = -\mu \frac{4U}{R} \tag{1}$$

Where:

τ_w is the shear stress applied by the fluid on the scaffold wall (Pa);

μ is the dynamic viscosity (Kg/ms);

U is the average speed (m/s);

R is the radius of the prosthesis (m).

In the chapter 1.9.1 the theoretical passage through which we arrive at the formula (1) has been reported. Before calculating the effort, however, we evaluated the Reynolds number. Being Re < 2000, we can consider having a laminar flow, and therefore use the expression for the stress on the walls shown above.

The minus sign in the following formula expresses the magnitude of the force itself, that represents the opposition of the effort to the flow (Table 14).

To calculate the average speed, the volumetric flow value should be used (Equation 2):

$$U = \frac{Q}{A} \tag{3}$$

Where:

Q is the volumetric flow (m^3/s);

A is the surface crossed by the flow (m^2)

In our case, the surface consists of the basic circular area and can be expressed as (Equation 3):

$$A = \Pi\ R^2 \tag{3}$$

***Table 14**: Some parameters of the scaffolds*

Symbol	Description	Value
R (m)	Radius of the scaffold	R=2.5mm=0.0025m
μ (Kg/ms)	Dynamic viscosity of the fluid in the reactor (like water) at T = 37 ° C	μ=6.91×10^{-4} Kg/ms
Q (m^3/s)	Volumetric flow that varies with pressure	Q(80 mmHg) = 1.88×10^{-6} m^3/s Q(120 mmHg) =1.95×10^{-6} m^3/s

Calculation of the tube cross section:

$$A = 1.96 \times 10^{-5}\ m^2$$

Calculation of the mean velocity U for P = 80 mmHg and for P = 120 mmHg:

$$U_{80} = 0.096\ m/s$$
$$U_{120} = 0.099\ m/s$$

The shear stress for the two pressures is therefore:

$$\tau_w\ (80)\ =\ 0.106\ Pa$$

$$\tau_w\ (120)\ = 0.109\ Pa$$

To make a graph of the shear stress in relation to operating pressures and flow, the modulus of the vector was considered, as can be seen from the following representations (Figure 70,71):

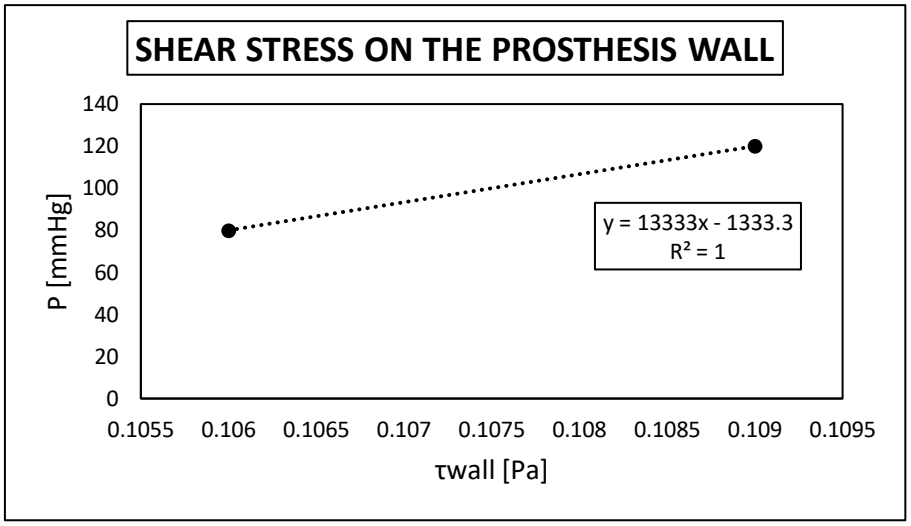

Figure 70: Representation of the shear stress as a function of pressure.

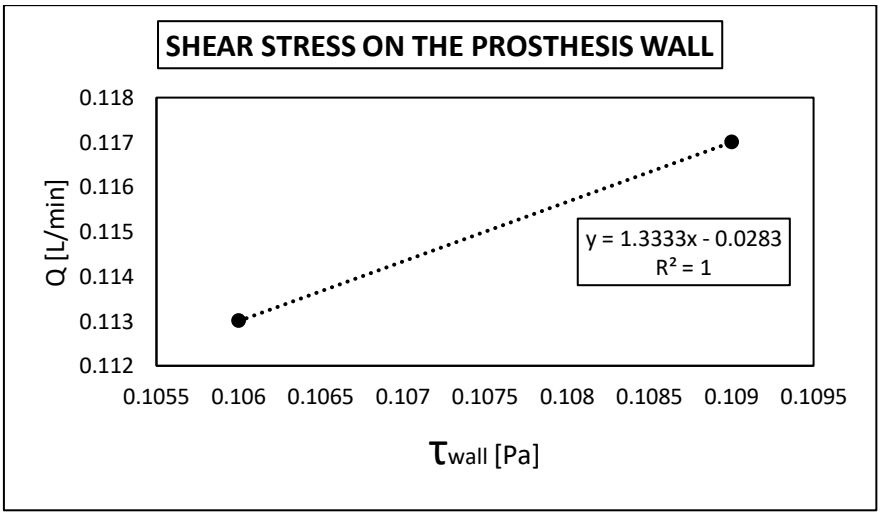

Figure 71: Representation of the shear stress as a function of flow rate

The flow at the lower pressure (80 mmHg) turns out to be lower than the flow at the highest pressure (120 mmHg), even if only slightly. This reflects the phenomenon on a theoretical level. Since the diameter of the prosthesis is the same, the average velocity (U) in the case of the pressure of 80 mmHg will also be lower. The only free parameter in the formula for calculating the effort on the walls is the average speed, so the effort in the case of low pressure will be lower than in the case of high pressure. Physically this is correct.

In our case, as the pressure changes, the flow remains almost constant. In fact, as previously assessed, the value of the flow at the two pressures deviates only to the third decimal number, which corresponds to a minimum variation, less than 1%.

5. COMPARISONS BETWEEN THE TWO STUDIED BIOREACTORS

The advantages in using the APTUS bioreactor compared to the home-made bioreactor are many.

First, the possibility of working on three scaffolds at the same time instead of one at a time; this considerably reduces the work periods as it is possible to perform 5 days of sampling directly on three different prostheses. Another positive side is to be able to control the variation of the parameters directly from a software from which you can also modify some values manually. also, this feature allows to optimize the times and control in detail the variation of the parameters unlike what happens in the home-made reactor in which the pressure can be displayed by a simple manometer. Therefore, the operator finds it easier to use the high-performance bioreactor. Another example is in the assembly of the prosthesis in the chamber: through special applicators and O-rings, in the high-performance bioreactor, it is possible to easily fix the scaffold to the tubes, unlike those home made in which the anchorage is less solid and tight.

To make this bioreactor very performing is also the possibility of getting very close to the behaviour *in vivo*; this can be seen in the use of the pinch which simulates the heartbeat at various speeds allowing the prosthesis to undergo in the most likely way, all the oscillations that would occur *in vivo*.

The releases that the prostheses have during their permanence in the bioreactor depend strictly on the effort that the flow places on the scaffolds themselves.
In the case of the home-made bioreactor, it was taken into consideration the value of the flow calculated in a previous work of the research group (Table 15).

***Table 15**: Experimental data*

Operating pressure (mmHg)	**60**	**80**	**100**
Surface	$3.14x10^{-6}$	$3.14x10^{-6}$	$3.14x10^{-6}$
Average speed (m/s)	$3.33x10^{-3}$	$7.72x10^{-3}$	$1.04x10^{-2}$
Reynold number (-)	6.55	15.16	20.43
Shear stress on the prosthesis wall (N/m^2)	0.013	0.030	0.042

For a pressure of 80 mmHg, the calculated flow was 0.0015 L/min, against the 0.113 L/min of the high-performance reactor. Considering this data valid, the stress on the walls was also evaluated for the home-made bioreactor, remember that the prostheses processed had a diameter of 2 mm.

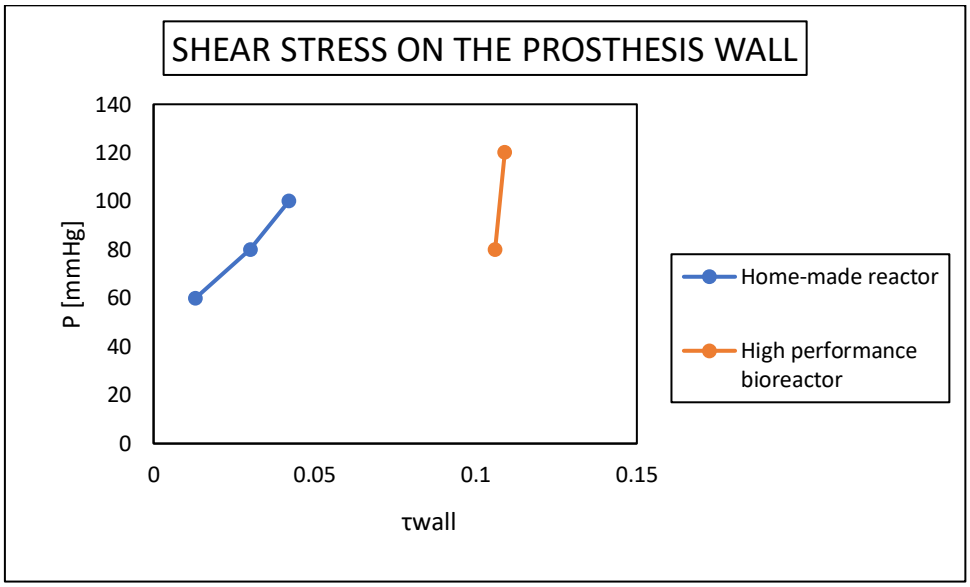

***Figure 72**: Comparison of the shear stress on the prosthesis wall between the two reactors*

Making a comparison, the flow in the case of the home-made reactor is evidently lower than the flow of the high-performance reactor, of about two orders of magnitude. This happens because probably in the new apparatus there are much less pressure drops, at the same pressure. Low flows are in fact an indication of the presence of resistances in the system, which make the circulation of the physiological solution more difficult. Since the flow is smaller, the effort exerted on the walls of the prosthesis will also be less relevant.

6. CONCLUSIONS

In the last decade, there has been a growing demand for prostheses to be used as substitutes for small caliber vessels for the treatment of cardiac ischemia and diseases related to peripheral circulation. The great limitations associated with the use of autologous vessels to solve these pathologies forced research towards the creation of small biocompatible prostheses. Electrospinning which allows to obtain biomaterials that, with the fibers from which they are made, mimic the extracellular matrix in the best possible way, is a good option to obtain biomaterials for vascular tissue engineering. Starting from these considerations, this experimental thesis focused on the fabrication of tubular prostheses with an internal diameter of 2 mm and 5 mm, made up of PGS and PCL in a ratio of 1:1, (v/v), engineered with quercetin to modulate the inflammatory process due to the implant, and coated with gelatin to reduce the permeability of the construct, preventing possible blood leakage. In these constructs, the size, the orientation of the fibers, the process of degradation and the release of gelatin and quercetin play a leading role in best simulating the properties and behavior of prostheses in a living organism, in the presence of a blood flow. In detail, the prostheses were characterized from a morphological point of view through the acquisition of images using a scanning electron, chemical-physical and mechanical properties. The images obtained by SEM analysis show how the micrometric-sized fibers are electrospun randomly.

A fundamental aspect of tissue engineering is represented by the degradation kinetics: when degradation is too fast, only a partial reconstruction of the damaged organ can occur, while a too slow a degradation can cause the formation of excess tissue that damages the functionality of the new organ. The degradation obtained is consistent with the behavior that the prosthesis should have once implanted.

The central part of this study focused on experimenting the same analyzes in two different bioreactors: one home made and one high performance. In both cases the results obtained have almost similar trends, in the same order of magnitude but in the realization of the experiments many differences have been seen. Using the high-performance bioreactor made it possible to optimize the processes, making them simpler for the operator and more likely to be applied *in vivo*. In fact, it was possible to process 3 scaffolds at the same time instead of just one; this led to achieving the same results in much shorter times. Furthermore, it was much easier for the operator to control the various parameters in the

high-performance bioreactor for the use of software rather than univocally from a pressure gauge. Compared to the use of the simple home-made bioreactor, the high performance one could also make the simulation more likely; this was made possible by adding the pinch that simulates the systolic and diastolic pressure impressed by the heart muscle. What has taken place to date is the construction of a bioreactor that simulates the body's blood flow and monitoring the properties of the prosthesis over time.

In the future, the simulation conducted up to now under dynamic conditions will be detailed. The subsequent steps to this study are represented using a non-Newtonian fluid that can simulate blood, such as aqueous xanthan gum/glycerin. This will allow to obtain an overview as close as possible to the real case.

7. REFERENCES

A. Haider, S. Haider, I. Kang, A comprehensive review summarizing the effect of electrospinning parameters and potential applications of nanofibers in biomedical and biotechnology, Arabian Journal of Chemistry 11 (2018)

Anwarul Hasan, Adnan Memic, Nasim Annabi, Monowar Hossain, Arghya Paul, Mehmet R. Dokmeci, Fariba Dehghani, Ali Khademhosseini, Electrospun scaffolds for tissue engineering of vascular grafts, Acta Biomaterialia 10 (2014)

Batchelor, K.K., An introduction to fluid dynamics, Cambridge University Press (2000)

Belcaro G., Agus Gb, Spartera C., Cao Pg, Pierangeli A., Donati A., Di Bartolomeo R., Nicolaides, Chirurgia cardiaca vascolare e angiologica (2000)

C. Dulio, G. Noseda, Idraulica, Ambrosiana (1987)

Charanpreet Singh, Cynthia S. Wong, Xungai Wang, Medical Textiles as Vascular Implants and Their Success to Mimic Natural Arteries, Journal of Functional Biomaterials (2015)

Cristiano Spadaccio, Francesco Nappi, Nawwar Al-Attar, Fraser W. Sutherland, Christophe Acar, Antonio Nenna, Marcella Trombetta, Massimo Chello, Alberto Rainer, Old Myths, New Concerns: the Long-Term Effects of Ascending Aorta Replacement with Dacron Grafts. Not All That Glitters Is Gold, Journal of Cardiovascular Translational Research (2016)

Davis W. Lamson, Matthew S. Brignall, Antioxidants and Cancer III: Quercetin, Alternative Medicine Review (2000)

Di Steven G. Friedman, MD 2005, A History of Vascular Surgery

Dominique Tremblay, Tiffany Zigras, Raymond Cartier, Louis Leduc, Jagdish Butany, Rosaire Mongrain, Richard L. Leask, A Comparison of Mechanical Properties of Materials Used in Aortic Arch Reconstruction, The Society of Thoracic Surgeons (2009)

Dongyong Sha, Zihan Wu, Jingjing Zhang, Yifan Ma, Zhaogang Yang, Yuan Yuan, Development of modified and multifunctional poly(glycerol sebacate) (PGS)-based biomaterials for biomedical applications, European Polymer Journal, Volume 161 (2021)

Dror Seliktar, Richard A. Black, Raymond P. Vito, And Robert M. Nerem, Dynamic Mechanical Conditioning Of Collagen-Gel Blood Vessel Constructs Induces Remodeling In Vitro (2000)

Eduard Rogatsky, Pandora box of BCA assay. Investigation of the accuracy and linearity of the microplate bicinchoninic protein assay: Analytical challenges and method modifications to minimize systematic errors, Analytical Biochemistry, Volume 631 (2021)

Erling Falk JACC Journals Vol. 47 No. 8 suppement Pathogenesis of Atherosclerosis 2006 c7-c12i

Frits Hess, History of (micro) vascular surgery and prostheses, Microsurgery (1985)

Gerard J. Puts, Philip Crouse, and Bruno M. Ameduri, Polytetrafluoroethylene: Synthesis and Characterization of the Original Extreme Polymer 1763–1805 (2019)

H. Liu, X. Ding, G. Zhou, P. Li, X. Wei, Y. Fan, Electrospinning of Nanofibers for Tissue Engineering Applications, Journal of Nanomaterials (2013)

Haizhou Wu, Jie Yin, Shulan Xiao, Jianhao Zhang, Mark P. Richards, Quercetin as an inhibitor of hemoglobin-mediated lipid oxidation: Mechanisms of action and use of molecular docking, Food Chemistry 384 (2022)

Ilja Gasan Osojnik Cˇrnivec, Mihaela Skrt, Danijela Šeremet, Meta Sterniša, David Farcˇnik, Erna Štrumbelj, Aleš Poljanšek, Nika Cebin, Lea Pogacˇnik, Sonja Smole Mozˇina, Miha Humar, Drazˇenka Komes, Nataša Poklar Ulrih, Waste streams in onion production: Bioactive compounds, quercetin, and use of antimicrobial and antioxidative properties, Waste Management 126 (2021)

J. A. Bhushani, C. Anandharamakrishnan, Electrospinning and electrospraying techniques: Potential food-based applications, Trends in Food Technology 38 (2014)

J. Stopka, W. Zuidema, P. Kruit, Trajectory displacement in a multi beam scanning electron microscope, Ultramicroscopy 223 (2021)

Katia Rubini, Elisa Boanini, Arianna Menichetti, Francesca Bonvicini, Giovanna Angela Gentilomi, Marco Montalti, Adriana Bigi, Quercetin loaded gelatin films with modulated release and tailored antioxidant, mechanical and swelling properties, Food Hydrocolloids 109 (2020)

Leoni Elisa, Schiume poliuretaniche nell'ingegneria tissutale, Fondamenti di Chimica e Biochimica (2016-1017)

M. Bartnikowski, T. R. Dargaville, S. Ivanovski, D. W. Hutmacher, Degradation mechanisms of polycaprolactone in the context of chemistry, geometry and environment, Progress in polymer science (2019)

M. Enamul Hoque, Tamrin Nuge , Tshai Kim Yeow , Norshariza Nordin and R. G. S. V. Prasad Polymers Research Journal ISSN: 1935-2530 Volume 9, Number 1 © Nova Science Publishers, Inc. GELATIN BASED SCAFFOLDS FOR TISSUE ENGINEERING – A REVIEW (2015)

M. S. Baguneid, A. M. Seifalian, H. J. Salacinski, D. Murray, G. Hamilton, M. G. Walker, Tissue engineering of blood vessels, British Journal of Surgery (2006)

M. Thangadurai, A. Ajith, H. Budharaju, S. Sethuraman, D. Sundaramurthi, Advances in electrospinning and 3D bioprinting strategies to enhance functional regeneration of skeletal muscle tissue, Journal Pre-proof (2022)

N. Abedzadeh, M.A.R. Krielaart, C. Kim, J. Simonaitis , R. Hobbs, P. Kruit, K. K. Berggren, Electrostatic electron mirror in SEM for simultaneous imaging of top and bottom surfaces of a sample, Ultramicroscopy 226 (2021)

N. Bhardwaj, S. C. Kundu, Electrospinning: A fascinating fiber fabrication technique, Biotechnology Advances 28 (2010)

Nasser K. Awad, Haitao Niu, Usman Ali, Yosry S. Morsi, Tong Lin, Electrospun Fibrous Scaffolds for Small-Diameter Blood Vessels: A Review, Membranes (2018)

Natalia G. Menzyanova, Svetlana A. Pyatina, Elena D. Nikolaeva, Alexander V. Shabanov, Ivan V. Nemtsev, Dmitry P. Stolyarov, Dmitry B. Dryganov, Eugene V. Sakhnov, Ekaterina I. Shishatskaya, Screening of biopolymeric materials for cardiovascular surgery toxicity—Evaluation of their surface relief with assessment of morphological aspects of monocyte/macrophage polarization in atherosclerosis patients, Toxicology Reports 6 (2019)

Niamh A Plunkett, Fergal J. O'Brien, Bioreactors in tissue engineering, Technology, and health care: official journal of the European Society for Engineering and Medicine 19 (2011)

Niklason, L. E., and R. S. Langer. Advances in tissue engineering of blood vessels and other tissues. Transpl Immunol. 5~4!:303–306, 1997

Pengju Wang, Yazhou Sun, Xiaoquan Shi, Huixing Shen, Haohao Ning, Haitao Liu, 3D printing of tissue engineering scaffolds: a focus on vascular regeneration, Bio-Design and Manufacturing (2021)

Peter libby, The changing landscape of atherosclerosis Nature volume 592, pages524–533 (2021)

Poppe, JGelatin. In: Imeson, A. (eds) Thickening and Gelling Agents for Food. Springer (1992)

Raja Jayendiran, Bakr Nour, Annie Ruimi, A fluid–structure interaction analysis of anisotropic Dacron fabric used for aortic replacement, Journal of Fluids and Structures 97 (2020)

Ranjana Rai, Marwa Tallawi, Alexandra Grigore, Aldo R. Boccaccini, Synthesis, properties, and biomedical applications of poly(glycerol sebacate) (PGS): A review, Progress in Polymer Science 37 (2012)

S. M. Tan, X. Yi Teoh, J. Le Hwang, Z. P. Khong, R. Sejare, A. Q. Almashhadani, R. A. Assi, S. Y. Chan, Electrospinning and its potential in fabricating pharmaceutical dosage form, Journal of Drug Delivery Science and Technology 76 (2022)

S. Torres-Giner, R. Perez-Masi a, J. M. Lagaron, A Review on Electrospun Polymer Nanostructures as Advanced Bioactive Platforms, Polymer Engineering & Science (2016)

Sara Caltagirone, Cosmo Rossi, Andreina Poggi, Franco O. Ranelletti, Pier Giorgio Natali, Mauro Brunett, Francesca B. Aiello, Mauro Piantelli, Flavonoids apigenin and quercetin inhibit melanoma growth and metastatic potential, International Journal of Cancer 87 (2000)

Simone Zuccher, Note di Fluidodinamica (2022)

T. S. M. Kumar, K. S. Kumar, N. Rajini, S. Siengchin, N. Ayrilmis, A. V. Rajulu, A comprehensive review of electrospun nanofibers: Food and packaging perspective, Composites Part B 175 (2019)

Timothy J. Keane, Stephen F. Badylak, Biomaterials for tissue engineering applications, Seminars in Pediatric Surgery 23, (Biomaterials for tissue engineering) (2014)

Vivek A. Kumar, Luke P. Brewster, Jeffrey M. Caves, And Elliot L. Chaikof, Tissue Engineering of Blood Vessels: Functional Requirements, Progress, and Future Challenges, Cardiovascular Engineering and Technology, Vol. 2, No. 3 (2011)

V. Barron, E. Lyons, C. Stenson-Cox, P. E. Mchugh, And A. Pandit, Bioreactors for Cardiovascular Cell, and Tissue Growth: A Review, Annals of Biomedical Engineering 31 (2003)

Yao Li ,Jiaying Yao,Chunyan Han ,Jiaxin Yang ,Maria Tabassum Chaudhry,Shengnan Wang ,Hongnan Liu , Yulong Yin , Quercetin, Inflammation, and Immunity (2016)

You-Xiong Wang, John L. Robertson,William B. Spillman, Jr., and Richard O. Claus, Effects of the Chemical Structure and the Surface Properties of Polymeric Biomaterials on Their Biocompatibility, Pharmaceutical Research, Vol. 21, No. 8 (2004)

SITOGRAFY

https://www.who.int/

https://www.diabete.com/il-danno-dei-piccoli-vasi-periferici/

http://superagatoide.altervista.org/vasi-sanguigni.html

https://facellitate.com/it/the-endothelium-an-interface-between-blood-tissue-andlymph/

https://connective-tissue-proper-cells-diagram/

https://www.riccardoquasidoc.it/il-tessuto-muscolare/

http://www.panvascular.com/pagine/info/pazienti/Varie/aterosclerosi.html

https://www.emd112.it/blog/news/morti-per-malattie-cardiovascolari-nel-mondo-ed incidenza-globale/

https://www.artoi.it/quercitina-e-bioflavonoidi/

https://paramedicsworld.com/biochemistry-practicals/demonstration-of-spectrophotometer-principle-components-working-applications/medical-paramedical-studynotes

https://www.medicalexpo.it/fabbricante-medico/protesi-vascolare-13924.html

RINGRAZIAMENTI

Ringraziamo il Prof. Pier Francesco Ferrari per aver reso possibile la realizzazione di questo lavoro di tesi e per averci trasmesso la passione per questo campo. Un grazie, inoltre, a Maria per averci seguito durante tutta l'esperienza e per essere stata presente per ogni dubbio. Ringraziamo infine il prof. Jan Oscar Pralits e la Prof.ssa Perego che hanno contribuito alla realizzazione di quest'opera.